EFFECTS OF CONSOLIDATION CHARACTERISTICS ON CPT CONE RESISTANCE AND LIQUEFACTION RESISTANCE IN SILTY SOILS

A Thesis Submitted to the
the Graduate School of Engineering and Sciences of
İzmir Institute of Technology
in Partial Fulfillment of the Requirements for the Degree of

MASTER OF SCIENCE

in Civil Engineering

by
Mustafa KARAMAN

December 2013
İZMİR

We approve the thesis of **Mustafa KARAMAN**

Examining Committee Members:

Assist. Prof.Dr. Nurhan ECEMİŞ
Department of Civil Engineering, İzmir Institute of Technology

Assoc. Prof. Dr. İsfendiyar EGELİ
Department of Civil Engineering, İzmir Institute of Technology

Assoc. Prof. Dr. Selim ALTUN
Department of Civil Engineering, Ege University

19 December 2013

Assist. Prof.Dr. Nurhan ECEMİŞ
Supervisor,
Department of Civil Engineering
İzmir Institute of Technology

Prof.Dr. Gökmen TAYFUR
Head of the Department of
Civil Engineering

Prof.Dr. R.Tuğrul SENGER
Dean of the Graduate School of
Engineering and Sciences

ACKNOWLEDGMENTS

First of all, I would like to express my gratitude to my supervisor Assist. Prof. Dr. Nurhan Ecemiş for her invaluable supervision, guidance and care throughout this thesis, as well as for her scientific support, encouragement and patient during this study.

I would like express my special thanks to the jury members; Assoc. Prof. Dr. İsfendiyar Egeli and Assoc. Prof. Dr. Selim Altun for their attendance at my thesis defence seminar and for their valuable suggestions to this study.

This work herein was supported financially by European Union 7th framework program Marie Curie fellowship (Grant number: PIRG05-GA-2009-248218) and the scientific and technological research council of Turkey, TUBITAK (Grant number: 110M602). These supports are gratefully acknowledged.

I would like to thank the members of technical team and the employees of the MSC Engineering Company and Soil Tecnologies Center Company for their technical support during the field experiment stage of this study. Also my special thanks are for my friend Geological Engineer Onur Solak for his help and support during field experiments.

My special thanks to my friend İrem Kahraman for her help, support and friendship, working on same projects and share an office with her is invaluable for me and my special thanks to Research Assistants at IZTECH and my colleagues, Emre Demirci and Paulina Backunowicz for their encouragement during this study. Furthermore, my special thanks to my special friend Hasret Güneş for her endless patient encouragement during this study.

Finally, I would like to express my special thanks to my family for their endless love and patient throughout my life and especially my parents who made me to overcome all the difficulties with her encouragement, support and love. This thesis dedicated to them.

ABSTRACT

EFFECTS OF CONSOLIDATION CHARACTERISTICS ON CPT CONE RESISTANCE AND LIQUEFACTION RESISTANCE IN SILTY SOILS

One of the most important reasons of the life and property losses caused by earthquakes is liquefaction during or after the earthquakes. Many researches focused on liquefaction after the earthquakes have revealed that liquefaction occurs mostly in silty soils. Empirical relationships between normalized cone penetration resistance (q_{c1N}), cyclic resistance ratio (CRR), magnitude of earthquake (M_w), and silt content (FC), derived from field observations, are currently used for liquefaction potential assessment of loose saturated sands and silty sands. However, the effects of fine content on liquefaction resistance and penetration resistance are not defined clearly in these researches. For this reason, it is aimed to investigate the effects of fine content on consolidation characteristics and the effects of coefficient of consolidation on liquefaction resistance and cone penetration resistance.

In this study, a number of field and laboratory studies were carried out to investigate the existing relationships. According to the results of experimental studies, first, the effects of the fines content on coefficient of consolidation and drainage characteristics of soils for different soil density ranges are examined and it is established that, both the fines content and the relative density effect the coefficient of consolidation of the sands and silty sands. Second, the changes in cone penetration resistance are investigated for different range of fines content and the relative density which have significant influence on coefficient of consolidation. It has been realized that the coefficient of consolidation indicates a significant influence on the measured penetration resistance during penetration of the CPT cone to the soil having different relative density, and it is figured out that for stiff-dense to medium dense soil, the decrease of normalized cone resistance is observed due to the change in drainage characteristics of fines or coefficient of consolidation. On the other hand, for loose soils only the relative density indicates a significant influence on the measured CPT penetration resistance around the probe. Finally, the contribution of the relative density on the liquefaction resistance of soils is observed at different fines content and compared with the available method in the literature.

ÖZET

SİLTLİ ZEMİNLERDE KONSOLİDASYON KARAKTERLERİNİN CPT KONİ DİRENCİNE VE SIVILAŞMA DİRENCİNE ETKİSİ

Dünyada depremlerin oluşturduğu büyük can ve mal kayıplarının bir önemli sebebi de deprem sırasında ve sonrasında oluşan sıvılaşma olayıdır. Tarihte oluşan birçok büyük deprem ve bu depremdeki sıvılaşma gözlemleri üzerine yapılan birçok çalışma sıvılaşmanın siltli zeminlerde oluştuğunu ortaya koymuştur (ör. Idriss ve Boulanger, 2006; Bray ve Sancio, 2006). Suya doygun gevşek kumlarda ve siltli kumlarda mevcut sıvılaşma potansiyeli araştırması normalleştirilmiş koni penetrasyon direnci (q_{c1N}), çevrimli direnç oranı (CRR), deprem büyüklüğü (M_w) ve silt muhtevası (FC) arasındaki ampirik bağıntılara ve depremlerde gözlenen arazi performansları değerlendirmelerine dayanmaktadır. Ancak, bu çalışmalarda silt muhtevasının sıvılaşma direnci ve penetrasyon direncine etkisi net olarak ortaya konulamamaktadır. Bu sebeple bu çalışmada, silt muhtevasının konsolidasyon karakterlerine etkisinin ve konsolidasyon katsayısının sıvılaşma direncine, koni penetrasyon direncine etkisinin incelenmesi amaçlanmıştır.

Bu çalışmada, söz konusu ilişkilerin incelenmesi için gereken bir dizi arazi ve laboratuar çalışması yapılmıştır. Çalışmalar sonucunda ilk olarak silt muhtevasının farklı zemin sıkılık durumlarında konsolidasyon katsayısına ve drenaj koşullarına etkisi araştırılmıştır ve her iki parametrenin de kum ve siltli kumlarda konsolidasyon katsayısının değişiminde oldukça etkili olduğu saptanmıştır. İkinci olarak, zeminin konsolidasyon karakterlerinde belirleyici etkisi olan farklı relaftif sıkılık ve silt muhtevaları için koni penetrasyon direnci değişimleri incelenmiştir ve sıkı ve orta sıkı zeminlerde normalleştirilmiş koni direncindeki azalmanın siltlerin drenaj karakterlerine ve zeminin konsolidasyon katsayısına bağlı olduğu gözlemlenmiştir. Buna karşın, gevşek siltli kumlarda sadece relaltif sıkılık CPT koni penetrasyon direnci değişiminde önemli bir rol oynamaktadır. Son olarak, zeminin relatif sıkılıklarının sıvılaşma direncine etkisi gözlemlenmiş, elde edilen bulgular, literatürde bilinen eğilimler ile karşılaştırılmıştır.

TABLE OF CONTENTS

LIST OF FIGURES

Figure **Page**

LIST OF TABLES

Table **Page**

LIST OF SYMBOLS

A_c = Area of the cone

A_s = Surface area of the friction sleeve

C_c =Coefficient of gradation

C_u = Uniformity coefficient

d = Diameter

D_{10} = Diameter through 10% of the total soil mass passed

D_{30} = Diameter through 30% of the total soil mass passed

D_{60} = Diameter through 60% of the total soil mass passed

D_r = Relative density

e = Void ratio

e_{min} = Minimum void ratio

e_{max} = Maximum void ratio

FC = Fines Content

f_s = Sleeve friction

Fs = The total force acting on the friction sleeve

a_{max} = maximum acceleration amplitude of the applied ground acceleration

g = Acceleration due to gravity

G_s = Specific gravity

k = Permeability

LL = Liquid limit

PL = Plastic limit

PI = Plasticity Index

M_s = Weight of dry loose soil

PP = Pore water pressure

q_c = Cone tip resistance

Q_c = Total force acting on the cone

R_e = Epicentral distance

R_f = Fault distance

r = Radius

r_u = Pore pressure ratio

u = Pore water pressure

u_1 = Pore pressure on the cone

u_2 = Pore pressure behind the cone

u_3 = Pore pressure behind the cone

V = Volume

V_m = Volume of the mold

V_s = Soil volume after compaction

w = Water content

W = Weight

Δu = Excess pore pressure

$\gamma_{dry\text{-}min}$ = Density of the dry loose soil

$\gamma_{dry\text{-}max}$ = Density of the dry compact soil

γ_{sat} = Saturated unit weight

σ_{vo}' = Effective vertical stress

FS = factor of safety

CRR = cyclic resistance ratio

CSR = cyclic stress ratio

τ_{av} = the average horizontal shear stress

Nm = measured standart penetration resistance

$(N_1)_{60}$ = normalized standart penetration resistance

C_E = correction for donut hammer energy ratio of 60%

C_B = correction factor for borehole diameter

C_R = correction factor for rod length

C_S = correction for standard samplers

C_Q = correction factor for cone penetration resistance

q_{c1} = corrected cone penetration resistance

q_{c1N} = normalized cone penetration resistance

m = factor based on soil density

I_c = soil behavior index

Q = normalized and modified cone resistance

F = normalized friction ratio in percent

$(q_{c1N})_{cs}$ = normalized dimensionless tip reistance equivalent to clean sand

K_c = correction factor based on grain size characteristics.

Vs = shear wave velocity

V_{s1} = normalized shear wave velocity

CRR = cyclic resistance ratio

V_{s1c} = limiting upper value of V_{s1} for liquefaction occurrence

γ_{cyc} = cyclic shear strainis calculated by a_{max}

$G_{(\gamma cyc)}$ = shear modulus of the soil at shear strain level

r_d = stress reduction factor

Δu = change in the excess pore pressure

u_i = measured pore pressure at the depth

u_0 = quilibrium in situ pore pressure at the depth

Δu_t = excess pore pressure at any time t

u_t = total pore pressure at any time t

t_{50} = the time value for 50% dissipation of excess pore water pressure

c_h = coefficient of consolidation

G_S = specific gravity of soil

W_{WP} = weight of pycnometer with water

W_S = weight of dry soil sample

W_{SWP} = pycnometer weight filled with soil and water

k = temperature coefficient for water

ρ_{dmin} = minimum index density

ρ_{dmax} = maximum index density

ρ_W = density of water (1 g/cm^3)

m_v = compressibility of the soil

q_t = corrected total cone resistance

V = normalized penetration rate

v = penetration velocity

d = diameter of the cone.

$(CRR)_{7.5}$ = cyclic resistance ratio for the 7.5 magnitude earthquakes (M_w=7.5)

CHAPTER 1

INTRODUCTION

1.1. **Problem Statement and Scope of the Study**

Soil liqueafaction is a complex phenomenon which has been attracting engineers' concern since 1964, Niigata Earthquake. Several researchers have thougth that liquefaction was a problem for clean sands and they have focused on sandy soils for more than fourty years. However, for the last ten years, studies based on liquefaction have revealed that liquefaction can also occur in silty sands and silts. There are several in-situ tests for assessment of liquefaction for sands and silty sands. These tests are standart penetration test (SPT), cone penetration test (CPT or CPTu for piezocone penetration) and shear wave velocity tests (V_s) (Youd et al. 2001). To facilitate usage of the SPT in liquefaction analyses, Seed et al. (1985) proposed a liquefaction screening chart in form of normalized standart penetration resistance $(N_1)_{60}$ versus cyclic stress ratio (CSR) induced by the earthquakes, corrected for 7.5 magnitude (M_w). Also, CSR versus V_{s1} curves which was recommended by Andrus and Stokoe (1999), can be accepted as liquefaction potential assessment for sand and silty sand soils that are difficult to CPT and SPT soundings. However, in the last decade the most common of these tests is cone penetration test. It provides the cone penetration resistance of soils continuously through the soil profile, which is one of the most commonly used parameter for liquefaction assessment of silty sands. Numerous investigators have proposed relationships between liquefaction resistance and CPT measurements (e.g. Stark and Olson 1995, Robertson and Wride 1998). The curve prepared by Robertson and Wride (1998) has been accepted as the most recent data showing the final liquefaction screening chart created from the field liquefaction observations and CPT data since the discussions made in the 1996 NCEER and in 1998 NCEER/NSF workshops (Youd et al. 2001). This chart is in the form of normalized cone penetration resistance (q_{c1N}) versus cyclic stress ratio induced by the earthquakes, corrected for M_w=7.5 earthquake, for many sites, where liquefaction problem has been observed. The relationships between normalized cone penetration resistance, cyclic resistance ratio,

magnitude of earthquake, and silt content (FC), derived from field observations, are currently used for liquefaction potential assessment of loose saturated sands and silty sands (Robertson and Wride 1998). However, the effects of fine content on liquefaction resistance and penetration resistance are not defined clearly in these researches. Therefore, it is needed that to be knowledgeable with relationships between silt content, cone penetration resistances and liquefaction potential.

The aim of this study is to determine the effects of silt content and consolidation characteristic on liquefaction resistance and cone penetration resistance. Within this scope, five in-situ tests which are commonly used for the direct evaluation of the liquefaction potential of sandy soils and a number of laboratory tests, which are essential to gain the mechanical and geotechnical properties of soils were performed. Based on these experimental results, an approach about effects of silt content on soil consolidation characteristics and relationships between fines content, soil density, cone penetration resistance and liquefaction resistance of silty soils are defined.

1.2. **Organization of the Thesis**

The thesis consists of six chapters. The first chapter, the current chapter, presents an introduction that summarizes the scope of the entire work.

Chapter 2 presents an overview of existing study focusing on liquefaction definitions and effects of liquefaction. In this chapter, factors which influence soil liquefaction are described under the title of factors known to influence liquefaction potential. Later on, previous studies focused on liquefaction potential based on field tests are presented.

Chapter 3 presents the field tests including their materials, methods, procedures, standards. The properties of soils obtained from the field test are also explained in this chapter.

Likewise, Chapter 4 presents laboratory tests with the materials, methods, procedures and standards. The properties of the tested materials are also presented in this chapter.

Chapter 5 presents the analyses of data obtained from the field and laboratory tests to assess the liquefaction potential. In this chapter, the major terms, such as;

coefficient of consolidation, relative density, normalized penetration ratio, normalized penetration resistance and liquefaction resistance are defined. Effects of fines content on consolidation characteristics of silty soils, relationships between coefficient of consolidation, cone penetration resistance and liquefaction resistance for different fines content and soil density ranges are interpreted.

Summary and findings of this study are presented in Chapter 6. This chapter is followed by a list of references.

CHAPTER 2

LITERATURE REVIEW OF LIQUEFACTION

2.1. **Introduction**

Soil liquefaction is one of the most significant, complicated and contradictive geotechnical earthquake engineering problems (Kramer, 1996). Liquefaction has been observed to have occurred during large earthquakes or immediately after the earthquakes. Effects of the liquefaction were observed after the Alaska Earthquake (1964), Niigata Earthquake (1964), San Fernando Valley Earthquake (1971), Haicheng Earthquake (1975), Tangshan Earthquake (1976), Imperial Valley Earthquake (1979), Armenia Earthquake (1988), Loma Prieta Earthquake (1989), Kobe Earthquake (1995), and Marmara Earthquake (1999). Hence, researchers have focused on the liquefaction phenomena around the world for more than forty years.

In this chapter, an overview of available literature regarding the definition and mechanisms of the soil liquefaction is presented. As part of the discussion on soil liquefaction definition, a brief review on effects of liquefaction is presented. Also physical damages of liquefaction and factors effecting liquefaction are described in detail. Liquefaction analyses criteria are presented in two parts, which are the cyclic stress approach and cyclic strain approach. Furthermore, methods of cyclic stress approach and the in-situ tests to assess the liquefaction potential are presented.

2.2. **Definition of Liquefaction**

The term “liquefaction” has been first used by Terzaghi and Peck (1948) to describe the significant loss of shear strength of very loose sands causing flow failures due to slight disturbance. Similarly, Mogami and Kubo (1953) used the same term to define shear strength loss due to seismically-induced cyclic loading. However, its importance has not been fully understood until 1964 Niigata earthquake, during which the significant causes of structural damage were reported to be due to tilting and sinking

of the buildings founded on saturated sandy soils having significant soil liquefaction potential.

Robertson and Wride (1997) reported that as an engineering term, “liquefaction” has been used to define two mainly related but different soil responses mechanisms during earthquakes: flow liquefaction and cyclic mobility. Although both mechanisms can lead to quite similar consequences, they are rather different as discussed below. The main feature of liquefaction is the generation of excess pore water pressures for undrained conditions. If saturated cohesionless soils are induced by a rapid loading suc as an earthquake, effective stress decreases and excess pore pressure increases.

2.2.1. Flow Liquefaction

In the proceedings of the 1997 NCEER Workshop, flow liquefaction is defined as follows:

“Flow liquefaction is a phenomenon in which the equilibrium is destroyed by static or dynamic loads in a soil deposit having low residual strength. Residual strength is defined as the strength of soils under large strain levels. Static loading, for example, can be applied by new buildings on a slope that exert additional forces on the soil beneath the foundations. Earthquakes, blasting, and pile driving are all example of dynamic loads that could trigger flow liquefaction. Once triggered, the strength of a soil susceptible to flow liquefaction is no longer sufficient to withstand the static stresses that were acting on the soil before the disturbance. Failures caused by flow liquefaction are often characterized by large and rapid movements, which can lead to disastrous consequences.”

In the proceedings of the 1997 NCEER Workshop, flow liquefaction is defined as follows:

The main characteristics of flow liquefaction are that:

i) it applies to strain softening soils only, under undrained loading,

ii) it requires in-situ shear stresses to be greater than the ultimate or minimum soil undrained shear strength,

iii) it can be triggered by either monotonic or cyclic loading,

iv) for failure of soil structure to occur, such as in a slope failure, a sufficient volume of soil must strain soften. The resulting failure type can be a slide or a flow, depending on the material properties and ground geometry, and

v) it can occur in any meta-stable structured soil, such as loose granular deposits, very sensitive clays, and silt deposits.

Flow liquefaction occurs once original conditions coincide with shaded zone in Figure 2.1(c), if undrained disturbance brings the effective stress path goes from the point that describes original conditions to the Flow Liquefaction State (FLS). If the original stress conditions are near the FLS zone, similar to under drained conditions an element of soil is subjected to large shear stresses, small excess pore pressures sets off flow liquefaction (Kramer & Seed, 1988). If the initial stress conditions are farther from the FLS zone, the liquefaction resistance will be greater (Kramer, 1996). In addition, Figure 2.1(a) demonstrates the mechanism of flow liquaefaction in terms of shear stress versus shear strain, whilst Figure 2.1(b) demonstrates the mechanism of flow liquefaction in terms of shear stress versus effective stress for monotonic and cycling loading at the same time.

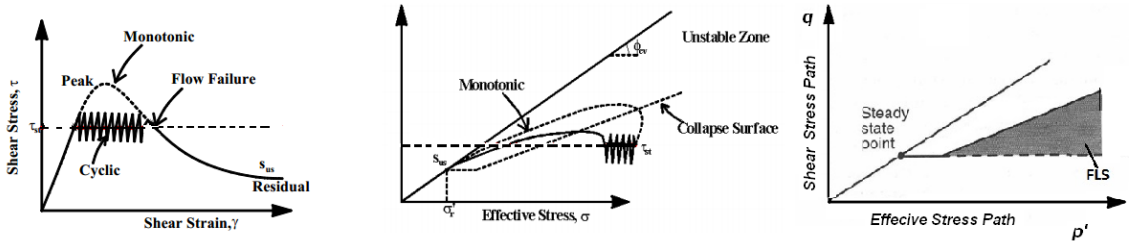

(a) (b) (c)

Figure 2.1. (a) Flow liquefaction mechanisms in terms of shear stress versus shear strain and (b) in terms of shear stress versus effective stress for both monotonic and cycling loading (c) shear stress path zone of susceptibility to flow liquefaction (Source: Kramer, 1996)

2.2.2. Cyclic Softening

Similarly, cyclic softening definitions and mechanisms, consistent with 1997 NCEER Workshop proceedings are summarized below:

"Cyclic softening is another phenomenon, triggered by cyclic loading, occurring in soil deposits with static shear stresses lower than the soil's shear strength. Deformations due to cyclic softening develop incrementally, because of static and dynamic stresses that exist during an earthquake. Two main engineering terms can be used to define the cyclic softening phenomenon, which applies to both strain softening and strain hardening materials."

2.2.2.1 Cyclic Mobility

Cyclic mobility can be identified by the facts that:

i) it requires undrained cyclic loading, during which shear stresses are always greater than zero; i.e. no shear stress reversals develop,
ii) zero effective stress will not develop,
iii) deformations during cyclic loading will stabilize, unless the soil is very loose and flow liquefaction is triggered,
iv) it can occur in almost any sand provided that the cyclic loading is sufficiently large in size and duration, but no shear stress reversals occurs,
v) clayey soils can experience cyclic mobility, but deformations are usually controlled by rate effects (creep).

Cyclic mobility mechanism is illustrated as shown in Figure 2. 2. Figure 2. 2 (a) shows the variation of shear stress during cyclic loading and Figure 2. 2 (b) shows the development of the shear strain during cyclic loading. As this figure implies, no zero effective stress develop during cyclic loading. Cyclic mobility can occur, when initial conditions plot to stay within the shaded zone. The shaded zone, in Figure 2. 2.(c) is susceptible to cyclic mobility. The shaded zone extends from very low to very high effective confining pressures, because cyclic mobility can occur both in loose and dense soils (Kramer, 1996).

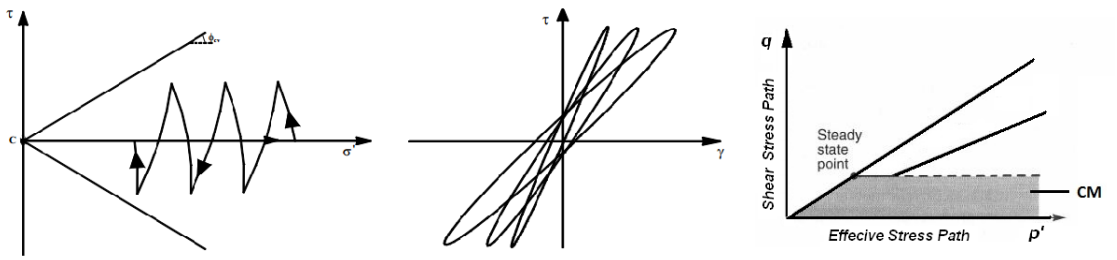

Figure 2. 2. (a) variation of shear stress during cyclic loading, (b) development of the shear strain during cyclic loading (c) stress path zone of susceptibility to cyclic mobility (Source: Kramer, 1996)

2.2.2.2. Cycling Liquefaction

Cyclic liquefaction can be identified by the facts that:

i) It requires undrained cyclic loading during which shear stress reversals occur or zero shear stress can develop; i.e. occurs when in-situ static shear stresses are low compared to cyclic shear stresses,

ii) It requires sufficient undrained cyclic loading to allow effective stress to reach essentially zero,

iii) At the point of zero effective stress no shear stress exists. When shear stress is applied, pore water pressure drops as the material tends to dilate, but a very soft initial stress strain response can develop resulting in large deformations,

iv) Deformations during cyclic loading can reach to large values, but generally stabilize when cyclic loading stops,

v) It can occur in almost all sands provided that the cyclic loading is sufficiently large in size and duration, and

vi) Clayey soils can experience cyclic liquefaction, but deformations are generally small due to cohesive strength at zero effective stress.

2.3. **Effects of Liquefaction**

During an earthquake, significant damage can result, due to instability of the soil in the area affected by internal seismic waves. The soil response depends on the mechanical characteristics of the soil layers, the depth of the water table and the intensities and duration of the ground shaking. If the soil consists of deposits of loose granular materials it may be compacted by the ground vibrations induced by the earthquake, resulting in large settlement and differential settlements of the ground surface. This compaction of the soil may result in the development of excess hydrostatic pore water pressures of sufficient magnitude to cause liquefaction of the soil, resulting in settlement, tilting and rupture of structures.

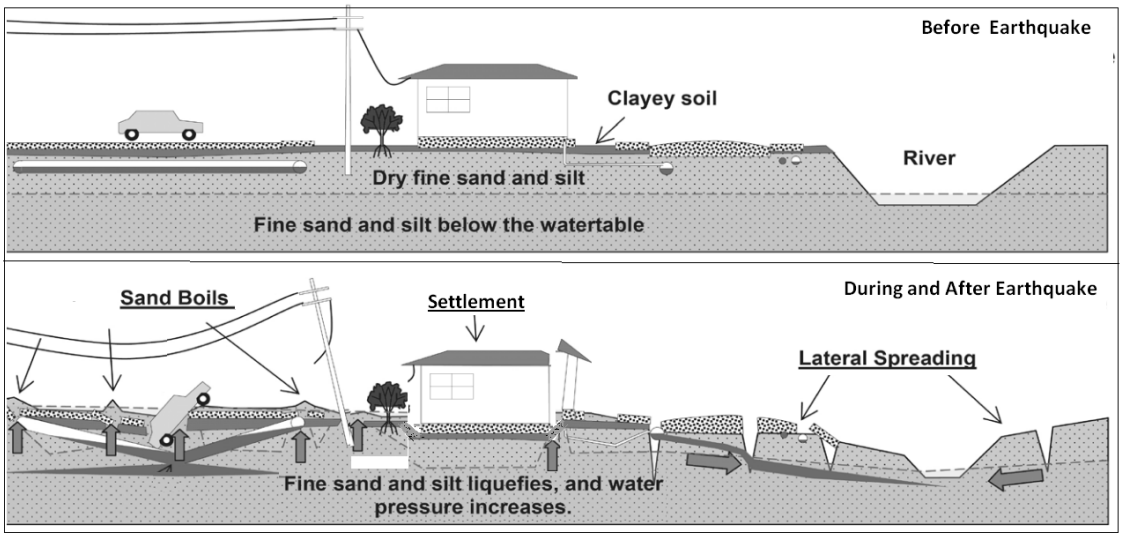

Figure 2.3. A schematic represantation of damages on ground surfce due to effects of liquefaction (Source:The Institution of Professional Engineers New Zealand)

Results of liquefaction effects can be seen in five groups of soil failures; 1) alteration of ground surface, 2) sand boils, 3) settlement, 4) instability and 5) bearing capacity. Figure 2.3 illustrates a schematic represantation of liquefaction damages such as damages on buildings, roads, piles and other facilities caused by some settelement, lateral spreading or sand boils.

2.3.1. Alteration of Ground Surface

Positive excess pore water pressure during an earthquake shaking causes in a decrease in soil stiffness. Despite a deposit of liquefiable soil is comparatively stiff at the starting phase of the earthquake shaking, the stiffness may decrease at the end of the shaking. The degree of the stiffness may vary by intensity and frequency of the surface motion.

As an outstanding case, once the layer is lower than a certain level, high frequency components of a bedrock motion cannot be transmitted with the ground surface.

Surface acceleration amplitudes decrease in correlation to the increase of pore pressure. Potential damage however, is not decreased by this situation, since low acceleration amplitudes at low frequencies may produce large displacements. These displacements may be seen in to buried structures as failures in utilities and structures supported on pile foundations that extend through liquefied soils. Liquefied soils can be decoupled from the surficial soils, when liquefaction occurs at depth beneath a flat ground surface, as earthquake produces large transient time dependent ground oscillations.

Fissures divide the surficial soils into blocks. These fissures may possibly open and / or close during shaking. Observation is based on ground waves with depths of up to several meters during ground oscillation. However generally permanent displacements are rather small.

Figure 2. 4. After 1999 Marmara Earthquake, The buildings settled and the sidewalk heaved and lifted up as part of the asphalt pavement is damaged in Adapazari (Source: Turkey-US Geotechnical Reconnaissance Team Report,1999)

Considering buildings embedded into the ground and failed by earthquake shaking and high numbers of oscillation cycles, sidewalks are lifted up, due to the ejection of soil materials during shaking Marmara Earthquake (August 17, 1999) constitutes an example to the alteration of ground surface. Figure 2. 4 illustrates the buildings settled and the sidewalk heaved and lifted up as part of the asphalt pavement damaged.

2.3.2. Sand Boils

A sand boil is sand and water that come out onto the ground surface during an earthquake as a result of liquefaction that has occurred at shallow depth. When earthquakes occur, pore pressures are produced due to multiple cycles of shaking. This may cause the liquefied sand and excess water to force its way to the ground surface from several meters below the ground are observed as sand boils at the surface. Sand boils are produced by both liquefied sand below the ground surface moving upward, as well as non-liquefied sand above it due to buoyancy.

Development of sand boils depends on the magnitude of the excess pore water pressure, the thickness, density and depth of the zone of excess pore water pressure and the thickness, permeability and intactness of any soil layers that overlay the zone of high excess pore water pressure (Kramer, 1996). Figure 2. 5 (a) illustrates a schematic explanation of sand boil mechanism and Figure 2.5 (b) shows a small sand boils example from the Chi-Chi Earthquake, 1999.

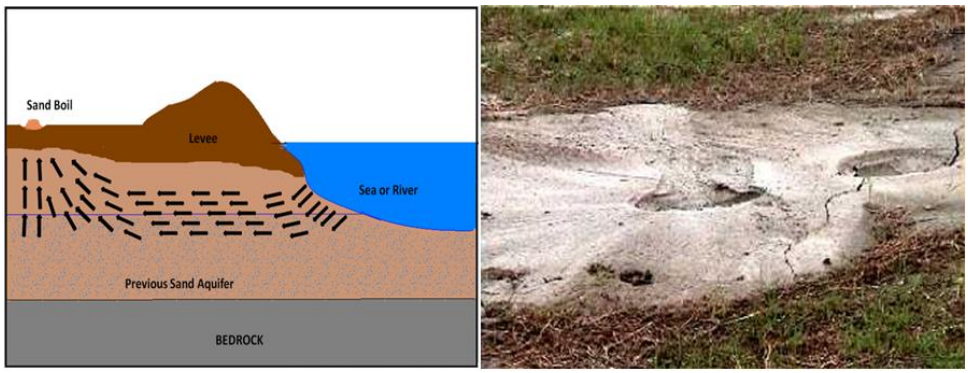

Figure 2. 5. (a) Shematic representation of sand boil mechanism and (b) Small Sand Boils from the Chi-Chi Earthquake,1999
(Source:http://nisee.berkeley.edu/taiwan/geotech/yuanlin)

2.3.4. Settlement

As known, sand has a tendency against densification when it is subjected to earthquake shaking. The densification accuring in subsurface is demonstrated at the ground surface in the pattern of ground surface settlement. Settlement is often results in as distress to structures supported by shallow foundations, seen along with damage to utilities that serve pile supported structures and in lifelines that are mainly buried at fordable depths.

Dry sand completes its densification rapidly. Hence settlement of a dry sand is often brought to a final by the end of an earthquake. Under earthquake loading, main conditions dry sand densification depends on the density of the sand in addition to the amplitude and number of cyclic shear strains applied (Silver & Seed, 1971).

Similar to dry sand behaviour, the settlement of saturated sands occurs bu requires a longer period of time. In this regard, damaging settlements can occur only as the weldments of the earthquake pore pressure dissipate. Permeability and compressibility of the soil, along with the length of the drainage path determines the duration required for this settlement. There are three factors that influence the density of post earthquake saturated sand; the density of sand, the maximum shear strain induced and the amount if pore pressure generated by the earthquake.

(a) (b)

Figure 2. 6. Examples of Settlement of Buildings after Marmara Earthquake, 1999 (Source: Report of the Turkey-US Geotechnical Reconnaissance Team,1999)

Figure 2. 6 (a) illustrates the building, which settled and shifted laterally and opening a gap between the sidewalk. Figure 2. 6 (b) presents the tilted building, because of the differential settlement. The heaving of sidewalks and settlement of buildings were common.

2.3.5. Instability

Among all the earthquake hazards seen, instabilities induced by liquefaction are the most damaging phenomena. Through the entire world, flow slides lateral spreads, retaining wall failures and foundation failures are observed to occur due to earthquakes. Instability failures are encountered to occur at times when the shear stresses are higher than shear strength of the liquefied soil. Deformation of the soil continues until a stage where shear stresses are a bit higher than the shear strength. Undisturbed sampling and laboratory testing may be used in evaluating the shear strength of liquefied soil, in addition to the comparison through in situ test parameters and back calculated strengths derived from the liquefaction case histories.

Flow failures due to liquefaction are encountered at times the shear stresses required for static equilibrium are greater than the shear strength of the liquefied soil. This result may emerge during and / or after an earthquake. Flow liquefaction arises very rapidly and causes large soil movements. Collapse of earth dams and other slopes and the failure of foundations have been observed because of flow failures during past earthquakes.

2.4. **Factors Known to Influence Liquefaction Potential**

There are lots of significant factors controlling liquefaction. These are; (1) soil type, (2) relative density and/or void ratio, (3) ground water level, (4) earthquake intensity, (5) earthquake duration, (6) historical background, (7) grain size distribution, (8) grain shape, (9) depositional environment, (10) age of deposits, (11) initial confining pressure, (12) drainage conditions and (13) soil profile. These concepts are summarized below.

2.4.1. Soil Type

It is known that soil liquefaction during earthquakes usually occurs in clean sands with few fines. However in some cases, liquefaction has occurred in gravelly soils are also encountered (Ishihara, 1985). It is controversial and complex process to determine the liquefaction potential of silty soils and also of coarser and gravelly soils and rock fills. The cyclic behavior of sandy soils is different from the cyclic behavior of coarse and gravelly soils. Sandy soils can be much more pervious than finer sandy soils, as they can rapidly dissipate cyclically generated pore pressures. Because of the great mass of larger sized particles present in coarse and gravelly soils, gravelly soils are deposited seldomly and gently. Thus, cyclic pore pressure generation and liquefaction may not occur in their very loose states, compared to sandy soils (R. B. Seed et al., 2001).

Following definitons were applied to cohesionless soils by Ishihara in 1996;

"For loose sand, the liquefaction is the state of softening in which large deformation is produced suddenly with complete loss of strength during or immediately after pore water pressure develops."

"For medium-dense to dense sand the state of softening, produced with the 100% pore water pressure build-up but the deformation does not grow indefinitely large and complete loss of strength does not take place."

"In silty sands or sandy silts, the plasticity of fines has a determining role in liquefaction potential. Silty soils with non-plastic fines are as susceptible to liquefaction as clean sands. Cohesive fines generally increase the cyclic resistance of silty soils."

"For clayey cohesive soils, if their plasticity index and liquid limit values are greater than a certain threshold limit and if they are saturated, then they may not lose their (effective) strength. Their undrained (effective) strength is generally higher than static strength under dynamic loading. Under cyclic loading, the behavior of clayey materials is defined by the decline of strength with the number of cycles and with the corresponding accumulated strain. The clayey material is easily liquefiable, if the natural water content is higher than 70% of the liquid limit."

2.4.2. Relative Density or Void Ratio

Casagrande (1936) proposed a method to determine the critical void ratio. This method helps to decide, if sand in the field would liquefy or not. According to this Eq 2.1, if the sand deposits have a void ratio smaller than the critical void ratio, then the sand deposits will not liquefy in undrained condition.

$$e_{cr} = e_{min} + (e_{max} - e_{min}) e^{(-0.75 a_{max}/g)} \quad (2.1)$$

where; e = void ratio, e_{min} = minimum void ratio, e_{max}= maximum void ratio, a_{max} = maximum acceleration amplitude of the applied ground acceleration, g = acceleration due to gravity.

Relative density or/and void ratio are significant factors to determine the liquefaction potential of soils. Seed and Idriss (1971) said that; loose sand may liquefy but the same material in a denser contition may not in any given earthquake and proposed acorrelation between the liquefaction potential of soil deposits and their relative density, depending on magnitude of earthquake acceleration. Table 2. 1 illustrates liquefaction potential with respect to relative density of fine sands.

Table 2. 1. Liquefaction potential with respect to relative density of fine sands (Source: Tezcan & Özdemir, 2004)

Maximum Surface Acceleration	Liquefaction Risk			
	Very High	High	Moderate	Low
0.10g	Dr < 17%	17% ≤ Dr < 33%	33% ≤ Dr < 54%	Dr > 54%
0.15g	Dr < 22%	22% ≤ Dr < 48%	48% ≤ Dr < 73%	Dr > 73%
0.20g	Dr < 28%	28% ≤ Dr < 60%	60% ≤ Dr < 85%	Dr > 85%
0.25g	Dr < 37%	37% ≤ Dr < 70%	70% ≤ Dr < 92%	Dr > 92%

Relative density value can be determined from laboratory tests as follows;

$$D_r = \frac{e_{max} - e}{e_{max} - e_{min}} \quad (2.2)$$

where; e = void ratio, e_{min} = minimum void ratio, e_{max}= maximum void ratio.

However for last several decades, in-situ cone penetration tests data have became more common method to determine the relative density and researchers presented equations between cone penetration resistance, pore water pressure parameters and relative density (Schmertmann 1976, Jamiolkowski 1985, Robertson and Powell 1997 etc.). The most recent and popular method is suggested by Robertson, Powell and Lune in 1997 as follows;

$$D_r = -98+66 \text{ x } \log_{10} \frac{q_c}{(\sigma_{v0}')^{0.5}} (\%) \qquad (2.3)$$

Where; D_r is the relative density in percentage, q_c is cone penetration resistance and σ_{vo}' is the effective vertical stress in the same units as, q_c.

2.4.3. Ground Water Level

Liquefaction occurs only in saturated soils, so the depth to groundwater level influences liquefaction potential. The liquefaction effects are usually observed in areas with shallow groundwater depths. In Kocaeli 1999 earthquake, most of the ground failures and loose of bearing capacity cases occour in areas where the ground water depths are about 1.5m to 2.0m. That's why; in this study the testing locations are chosen to be in North coast of the İzmir Gulf, within about 1m to 2m below the ground surface.

2.4.4 Earthquake Magnitude and Distances

The liquefaction potential during an earthquake depends on the magnitude of the stresses or strains induced by the earthquake, which is related to the intensity of ground shaking (H. B. Seed & Idriss, 1971).

Kuribayashi and Tatsuoka (1975) proposed the "line b" which can be defined by log R_e = 0.77M -3.6 in Figure 2.7a. But liquefaction case histories had shown that this line does not provide a safer boundry, Ambraseys (1988) collected the data which is related to shallow earthquakes where liquefaction was not observed at different magnitudes and estimated the limiting epicentral distance (R_e) and fault distance (R_f). Curve was generated according to the post-earthquake field investigations. Figure 2.7 a shows relationship between epicentral distance R_e and moment magnitude with line a by

Ambraseys 1988 and with line b by Kuribayashi and Tatsuoka (1975) suggestions. Figure 2.7 b shows a plot of R_f which is the closest distance from a shallow seismic source of the furthest point of liquefaction as a function of magnitude M_w.

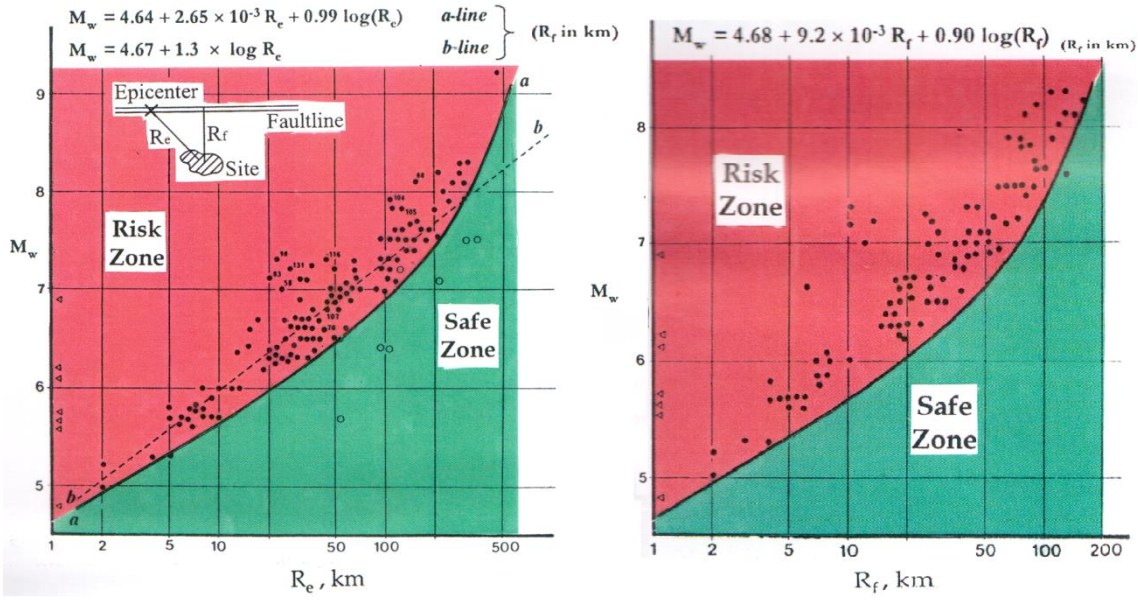

Figure 2.7. Relationship between epicentral distance R_e and moment magnitude, (b) relationship between fault distance R_f and moment magnitude.
(Source: Tezcan and Özdemir, Liquefaction Risk Analysis Book)

2.4.5. Earthquake Duration

The numbers of significant stress or strain cycles are determined during the duration of the earthquake shaking. Therefore, the duration of the earthquake shaking is another significant factor in order to determine the liqueafaction potential A number of case studies had been observed about the relationship between the effects of liquefaction and shaking duration however neither a quantative relationship nor a reliable method for predicting the duration of earthquakes established so far.

2.4.6. Historical Evidence

Post earthquake field investigations help to get useful information related to liquefaction behavior, where liquefaction often reoccurs at the same location. These

investigations give information about the possibility of earthquake occurrence and potential of liquefaction.

2.4.7. Grain Size Distribution

Liquefaction susceptibility is remarkably influenced by gradation. Liquefaction susceptibility of poorly graded soils is higher in comparison the well graded soils. As far as well graded soils are considered, it is observed that small particles are placed between large particles. Hence, in well graded soils, volume change is comparatively low. Field investigations conducted in some post-earthquake shows that liquefaction failures occur more often in uniformly poorly graded soils. (Steven Lawrence Kramer, 1996).

According to the 1st Chinese Criteria which is proposed by Wang (1979) there are three pre-requisites for fine cohesive soils to be potentially liquefiable type and character. First of all, they include less than 15% clay fines with weight of grains and shall size smaller than the diameter 0.005mm $\leq$ 0.15. Secondly, liquid limit (LL) shall be less than or equal to 35%. Finally current in-situ water content is equal to or higher than 90% of the liquid limit. Figure 2.8 shows the 1st Chinese Criteria chart which was proposed by Wang (1979), in terms of liquid limit (LL) versus natural water content, (W_n).

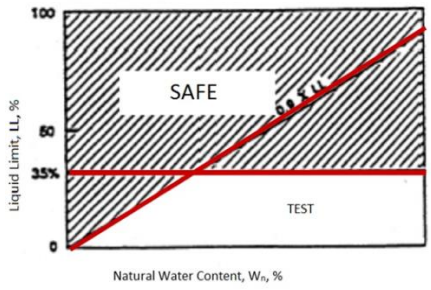

Figure 2.8. The 1st Chinese Criteria
(Source: Wang, 1979)

Wang (1981) has identified three new categories of liquefiable soils through 2nd Chinese criteria. First of the referred categories is for saturated sand, at particular levels

of earthquake intensity and at low values of effective overburden pressure, if Standard Penetration Test (SPT) blows counts is lower than a critical value. Second is; saturated slightly cohesive silty soils with a water content higher than 90% of its liquid limit and with a liquidity index smaller than 0.75. Third and the last category is for the unconfined compressive strength with less than 50 kPa, meaning a SPT blow count to be 4 or less and having a sensitivity in excess of 4. Figure 2.9 illustrates the new recommendadations of 1st and 2nd Chinese criteria.

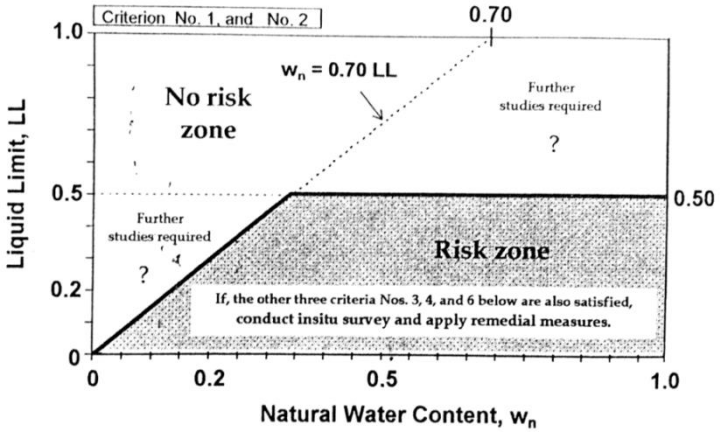

Figure 2.9. The 1st and the 2nd Chinese Criteria
(Source: Tezcan & Özdemir, 2004)

Figure 2.10 shows the Chinese Criteria, also known as the Modified Chinese Criteria developed by Andrews and Martin (2000). It suggests that if a soil has less than 10% clay fines (<0.002mm) and a liquid limit (LL) of the minus #40 sieve is less than 32%, it will be considered as potentially liquefiable. Also, soils having more than 10% clay fines and LL ≥ 32% are unlikely to be liquefaction susceptible.

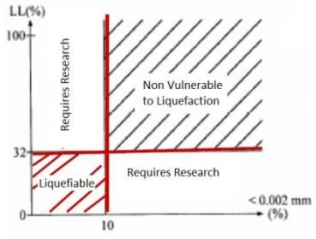

Figure 2.10. Modified Chinese Criteria
(Source: Tezcan & Özdemir, 2004)

2.4.8. Grain Shape

Liquefaction susceptibility can be influenced by particle shape as well. In comparison to soils with angular grains, soils with rounded particles are more susceptible to densification. Hence, rather than angular-grained soils, soils with rounded particle shapes are usually more susceptible to liquefaction. Soils with rounded particles more frequently observed in the fluvial and alluvial environments, where loosely deposited saturated soils are found more often. Also, in those areas, liquefaction susceptibility is often high.

2.4.9. Depositional Environment

Soil deposits are susceptible to liquefaction and are formed within a relatively narrow range of geological environments. (T. Youd, 1991). Soil deposit's potential is due to depositional environment, hydrological environment and age of the soil deposit (Youd & Hoose, 1977).

The environment of the deposited soil is constituted by the size, shape and arrangement of grains, hydraulic conductivity and lateral continuity of deposits (Arulmoli, Arulanandan, & Seed, 1985).

Geologic processes producing high liquefaction potential soil deposits are divided into two groups as uniform grain size soils and those in loose states. Hence, in saturated conditions, fluvial deposits and colluvial and aeolian deposits are subject to liquefaction along with alluvial fans in alluvial plains, brach terraces, playa and estuarine deposits.

2.4.10. Age of Deposits

Another factor to influence the liquefaction potential is the age of deposits which is related to its density, degree of soil cementation, ability to transmit earthquake energy and hydraulic conductivity. New soil deposits are subjected to higher levels of liquefaction risk than older deposits.

2.4.11. Initial Confining Pressure

In cases where the confining pressure increases, the liquefaction potential of a soil deposit reduces. An increase in initial confining pressure results with an increase in the stress required to initiate liquefaction under cyclic load conditions. Niigata earthquake (1964) demonstrates that soils having less than 2.7 meters of fill remained stable and the same soils surrounding the fill liquefied extensively (Seed & Idriss, 1971).

2.4.12. Drainage Conditions

If the soil is under drained conditions, where pore water dissipates quickly, liquefaction may not be observed with the following exceptions. Firstly in the cases where coarse, gravelly soils are surrounded and encapsulated by finer and less pervious materials. Secondly, when drainage is prevented by finer soils, which fill-in the void spaces between the coarser particles. Thirdly is when depth of the layer (or stratum) of the coarse soil is too large.

With regards to these three exceptional cases, the potential of liquefaction in coarse soils increases. Hence risk should be evaluated carefully (Seed et al., 2001).

2.5. **Assessment of Liquefaction Potential**

The first step in liquefaction engineering is to determine if soils of interest are potentially liquefiable or not. For this purpose, a number of approaches to evaluation of the potential for initiation of liquefaction have been developed over the years. Simplified procedures (e.g., Seed and Idriss 1971, Dobry et al. 1982, Law et al. 1990, Kayen and Mitchell 1997) are commonly used in engineering practice. There are two approaches for the simplified procedures: (1) the cyclic stress approach and (2) the cyclic strain approach.

2.5.1. The Cyclic Stress Approach

One of the most popular procedures is the simplified procedure which characterizes both earthquake loading and soil liquefaction resistance in terms of cyclic stress. This procedure is developed by Seed and Idriss in 1971 after the Niagata Earthquake. According to the procedure liquefaction is expected to occur at locations, where the demand exceeds the resistance capacity and the factor of safety (FS) is less than unity. (In the Eurocode 8-98 FS $\geq$ 1.25)

$$FS= \frac{\text{Capacity}}{\text{Demand}} = \frac{\text{CRR}}{\text{CSR}} \tag{2.4}$$

Where CRR= cyclic stress ratio, CSR= cyclic resistance ratio. An earthquake motion is converted to an equivalent series of uniform cycles of shear stress. The number of equivalent cycles, a function of the duration of the motion is correlated with the magnitude of the earthquake (Lee and Seed, 1967). The time history of shear stress at any point in a soil during an earthquake has an irregular form. Hence, the average equivalent shear stress is used for M_w magnitude of 7.5. Seed et al. (1983) proposed the following formula to calculate the CSR due to earthquake shaking.

$$CSR= \frac{\tau_{av}}{\sigma'_{vo}} \tag{2.5}$$

Where, τ_{av} is the average horizontal shear stress developed on the soil element, and σ'_{vo} is effective vertical overburden pressure.

The capacity of the soil to resist liquefaction (CRR) is determined by use of field tests, by correlations or by means of laboratory tests which are cyclic triaxial and cyclic simple shear tests. Liquefaction resitance is expressed in terms of the number of cycles required to produce failure of a soil at a particular level of cyclic shear stress. To evaluate the liquefaction resistance, three different in-situ testing methods can be used. These are standart penetration test (SPT), using cone penetration test (CPT) and shear wave velocity tests (V_s).

2.5.1.1 Determining CRR Based on Standart Penetration Test

One of the methods for evaluating the CRR is based on standart penetration tests. Values of N_m which can be obtained from the field SPT tests are needed to be corrected using the following formula;

$$(N_1)_{60} = N_m \, C_N \, C_E \, C_B \, C_R \, C_S \tag{2.6}$$

Where $(N_1)_{60}$ is the corrected SPT number, in which N is measured standart penetration resistance and C_N,C_E, C_B, C_R, C_S are correction factors. Also, the SPT tests and the formula for correcting the measured parameters will be described in detail in Chapter 3 under the section 3.4.1.

According to the SPT based Cyclic Resitance Ratio finding for valuation of liquefaction potential at different magnitude earthquakes, Seed et al. (1985) proposed practical charts which represent a series of curves for sand with different $(N_1)_{60}$ values and with different fines contents. When normalized SPT value of soil is known, the CRR can be obtained from these charts for the earthquake magnitude of M_w=7.5. Figure 2.11 shows the relationship between CRR and $(N_1)_{60}$ for different fines content which are proposed by Seed at al. in 1985.

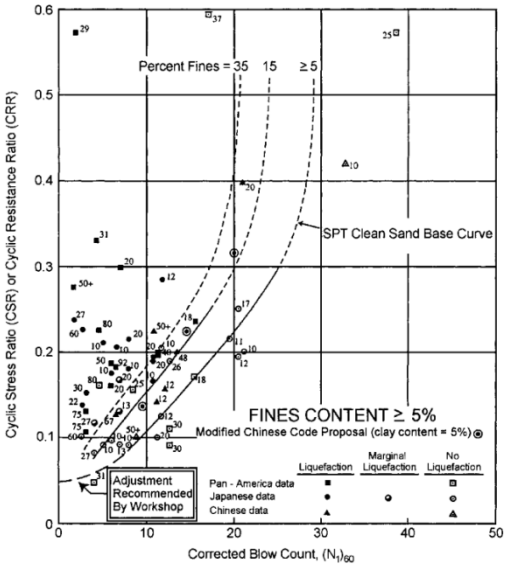

Figure 2.11. Relationship between CRR and $(N_1)_{60}$
(Source: Seed at al., 1985)

In Figure 2.11, a curve shown as "SPT Clean Sand Base Curve" was reshaped and approximated by the following formula for clean sand in 1996 NCEER Workshops on evalutation of liquefaction resistance of soils.

$$CSR_{7.5} = \frac{1}{34 - (N_1)_{60}} + \frac{(N_1)_{60}}{135} + \frac{50}{[10 - (N_1)_{60} + 45]^2} - \frac{1}{200} \qquad (2.7)$$

In 1996 NCEER Workshop it was also noted that this equation is valid for $(N_1)_{60} < 30$. For $(N_1)_{60} > 30$, clean granular soils are too dense to liquefy and are classed as non liquefiable.

2.5.1.2. Determining CRR Based on Cone Penetration Test

Another method for evaluating the CRR is based on cone penetration tests (CPT). It is one of the in-situ tests and has more advantanges than SPT. Procedure, testing method and advantages of CPT will be described in detail in Chapter 3 under the section 3.4.2. It is basically known that cone penetration resistance (q_c), effective overburden pressure (σ'_{vo}) data can be obtained from CPT. These values are also needed to be corrected and normalized to evaluate the liquefaction resistance. There are numbers of equations in the literature to convert the in-situ measured CPT values to an effective value due to a reference overburden pressure (Kayen et al. 1992, Liao and Whitman 1986, Jamiolkowski et al. 1985). Correction the q_c value requires the steps as follows;

$$q_{c1} = C_Q \; q_c \qquad (2.8)$$

where; C_Q is the correction factor for cone penetration resistance and q_c is cone penetration resistance measured in the field.

A method that uses cone penetration resistance for the assessment of liquefaction potential was first developed by Robertson and Campanella in 1985. Other similar CPT based charts were aslo developed by Seed and De Alba (1986), Shibata and Teparaska (1988), Mitchell and Tseng (1990), where the cone tip resistance is expressed in the form of q_{c1} and cyclic resistance ratio CRR.

After these studies, q_c values was adjusted to be normalized and made dimensionless by the following expressions;

$$q_{c1N} = C_Q \frac{q_c}{P_a} \tag{2.9}$$

$$C_Q = \left(\frac{P_a}{\sigma'_{vo}} \right)^m \tag{2.10}$$

$$m = 0.784 - 0.521 D_r \tag{2.11}$$

where;

q_{c1N} = normalized cone penetration resistance

q_c = cone penetration resistance measured in field

C_Q = correction factor for cone penetration resistance

P_a = atmospheric pressure (0.1 MPa)

σ'_{vo} = effective vertical overburden pressure

m = factor based on soil density

Robertson and Wride (1998) constructed a procedure, referred to the soil behavior type index (I_c) method in order to calculate the effect of fines content of soils on the cone penetration tip resisatance. The soil behavior index (I_c) method depends on grain size characteristic and also obtained from the following equation as suggested by Robertson and Wride (1998);

$$I_c = \sqrt{(3.47 - \log Q)^2 + (1.22 + \log F)^2} \tag{2.11}$$

$$Q = \frac{q_C - \sigma_{vo}}{P_a} \left(\frac{P_a}{\sigma'_{vo}} \right)^m \tag{2.12}$$

$$F = \frac{f_s}{q_C - \sigma_{vo}} 100 \tag{2.13}$$

Where;

Q= normalized and modified cone resistance

F= normalized friction ratio in percent

f_S= CPT sleeve friction resistance measured insitu

According to these deterministic studies and using data from different sites, Robertson and Wride proposed a useful chart for the direct determination of CRR for clean sands (FC≤ 5%) from CPT data. This figure was developed from CPT case history data compiled from several investigations, including those by Stark and Olson (1995) and Suzuki et al. (1995). The chart, valid for magnitude 7.5 earthquakes only, shows the calculated cyclic resistance ratio plotted as a function dimensionless vary against, corrected, and normalized CPT resistance $q_{c1N.}$ (Figure 2.12)

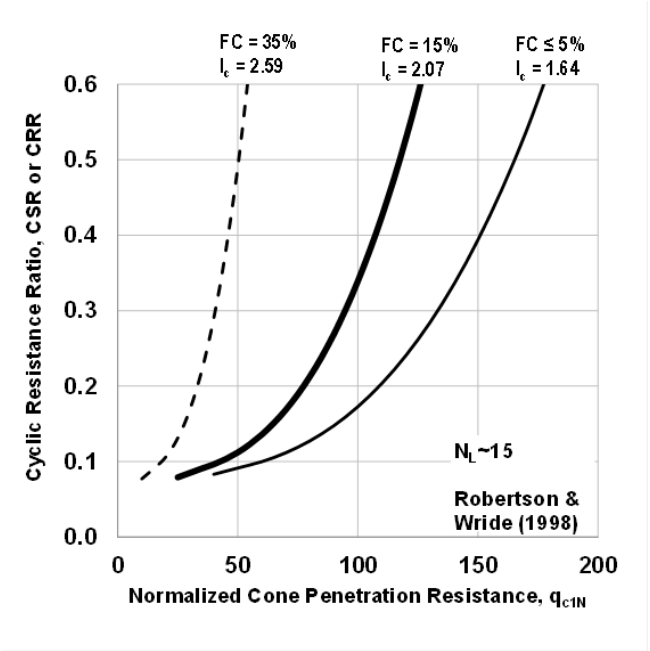

Figure 2.12. Curve recomenmended for calculation of CRR based on CPT (Source: Robertson and Wride,1998).

Note that the practical CRR curve given in Figure 2.12 can be used only for clean sands. For other soil tpyes an equivalent clean sand value should be obtained by means of a correction factor for grain characteristics K_c as follows;

$$(q_{c1N})_{cs} = K_c \; q_{c1N} \tag{2.14}$$

Where;$(q_{c1N})_{cs}$ = the normalized dimensionless tip reistance equivalent to clean sand and K_c= correction factor based on grain size characteristics.

K_c, the correction factor, for grain characteristics, is defined by the following equations (Robertson and Wride 1998):

$$K_c = 1 \quad \text{if} \quad I_c \leq 1.64 \tag{2.15a}$$

$$K_c = 1 \quad \text{if} \quad 1.64 < I_c < 2.36 \text{ and } F < 0.5 \tag{2.15b}$$

$$K_c = \alpha \quad \text{if} \quad 1.64 < I_c < 2.36 \tag{2.15c}$$

$$K_c = \text{Not used} \quad \text{if} \quad I_c \geq 2.36 \tag{2.15d}$$

$$\alpha = -0{,}403\, I_C^{\,4} + 5.581 I_C^{\,3} - 21.63 I_C^{\,2} + 33.75 I_C - 17.88 \tag{2.16}$$

Where; I_c = soil behavior type index.

In NCEER 1998 Workshop, the CRR- q_{c1N} chart proposed by Roberston and Wride (Figure 2.12) was reproducted for clean sand having equivalent normalized tip resistance $(q_{c1N})_{cs}$ and plotted as in Figure 2.14. Aslo, the clean-sand base curve in Figure 2.14 was approximated by the following equation (Robertson and Wride 1998):

$$CRR = 0.833 \frac{(q_{c1N})_{cs}}{1000} + 0.05 \quad \text{if} \quad (q_{c1N})_{cs} < 50 \tag{2.17a}$$

$$CRR = 93 \left(\frac{(q_{c1N})_{cs}}{1000} \right)^3 + 0.08 \quad \text{if} \quad 50 \leq (q_{c1N})_{cs} < 160 \tag{2.17b}$$

Where; $(q_{c1N})_{cs}$ = the normalized dimensionless tip reistance equivalent to clean sand.

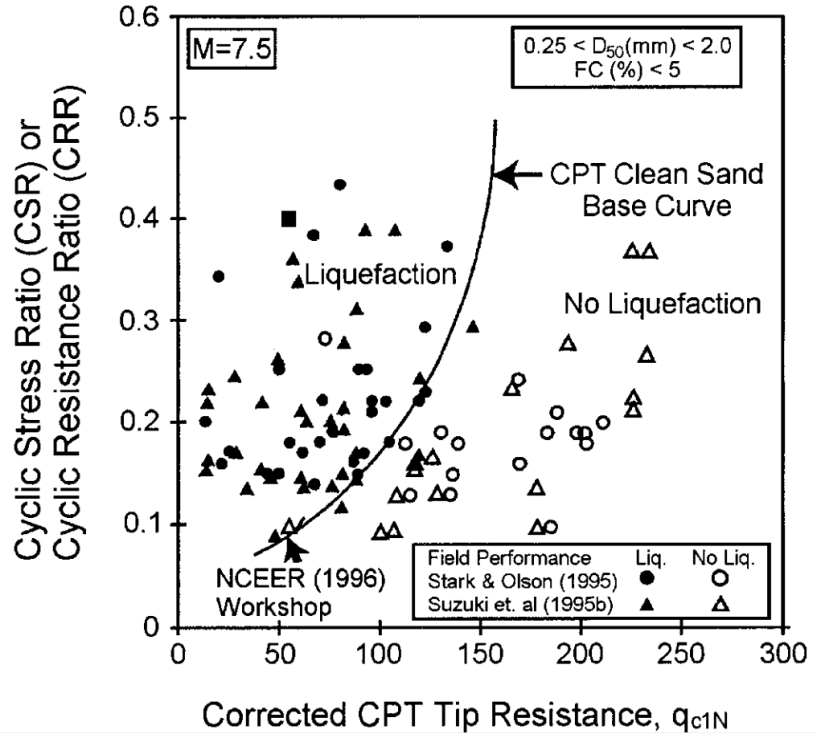

Figure 2.13. Curve Recommended for Calculation of CRR from CPT Data along with Empirical Liquefaction Data from Compiled Case Histories (Reproduced from Robertson and Wride 1998)

2.5.1.3. Determining CRR Based on Shear Wave Velocity

Another method for evaluating the CRR is based on simplified shear wave velocity. The simplified shear wave velocity (V_s) procedure requires measuring the shear wave velocity from insitu tests. In this study, Seismic Cone Piezocone Test (SCPTu) was performed to provide the V_s data which is decirbed in detail in Chapter 3, section 3.4.3. For a sand of constant void raito, the shear wave velocity will increase with depth because of the effects of increased effective confining pressure. Hence it is belived that results have been normalized with respect to effective overburden pressure (Robertson and Finn, 1992). This suggestion is in harmony with the tradition of normalizing penetration resistance parameters due to overburden pressure. Robertson and Finn (1992) have suggested the following equation for calculating the normalized shear wave velocity (V_{s1});

$$V_{s1}=V_s\left(\frac{P_a}{\sigma'_{vo}}\right)^{0.25} \quad (2.18)$$

Where;

Vs=is the measured in situ shear wave velocity,

P_a = atmospheric pressure (0.1 MPa),

σ'_{vo} = effective vertical overburden pressure.

Both V_s and CRR are similary influenced by soil density, overburden pressure, stress history and soil type. Several researches have developed relationships between Vs and CRR (Dobry et al. 1992, Tokimatsu and Uchida 1990, Robertson et al. 1992, Kayen et al. 1992, Andrus and Stokoe 1997 and Andrus et al 1999). 1999 NCEER Workshop participants also recommend this equation for correcting the V_s, (Youd and Idriss, 2001, Andrus et al., 2001). The relationship developed by Andrus et al. (1999) is the relationship recommended by the 1996 NCEER workshop (Youd and Idriss, 2001). Figure 2.14 shows the compilation of seven relationships between liquefaction resistance and overbuden stress-corrected shear wave velocity values suggested by researchers mentioned above and relationship developed by Andrus et al (1999).

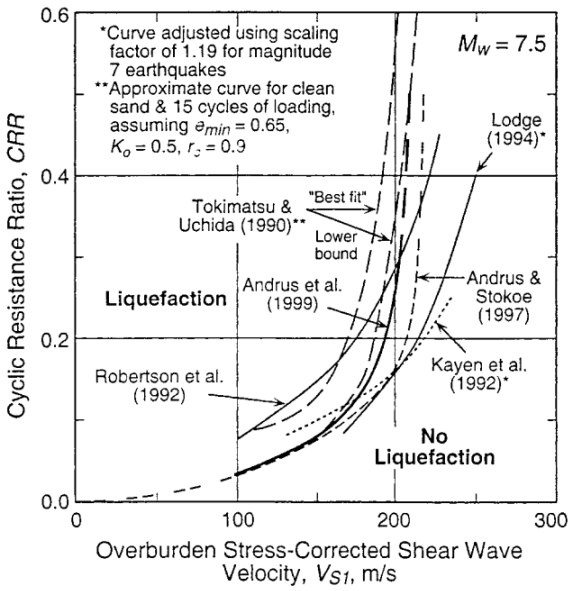

Figure 2.14. Compretion of Seven Reltionships between Liquefaction Resistance and Overbruden Stress-Corrected Shear Wave Velocity for Granular Soils (Source: NCEER 1996 and 1998 Workshop)

The relationship developed by Andrus et al (1999) also can be described using the following equation;

$$CRR = r\left(\frac{V_{s1}}{100}\right)^2 + s\left(\frac{1}{V_{s1c}-V_{s1}} - \frac{1}{V_{s1}}\right) \quad (2.19)$$

Where;

CRR= cyclic resistance ratio

V_{s1} = normalized shear wave velocity,

V_{s1c} = limiting upper value of V_{s1} for liquefaction occurrence,

r = curve fitting parameter equal to 0.03

s = curve fitting parameter equal to 0.9

The limiting upper value of Vs1 for liquefaction occurrence, V_{s1c} depend upon fines content and these values are;

V_{s1c} = 220 m/s for sand with fines content (FC) < 5%

V_{s1c} = 210 m/s for sand with fines content (FC) = 20%

V_{s1c} = 200 m/s for sand with fines content (FC) > 35%

Figure 2.15 shows the curves with various fines contents recommended for calculation of CRR from V_{s1} (after Adnrus, et al. 1999).

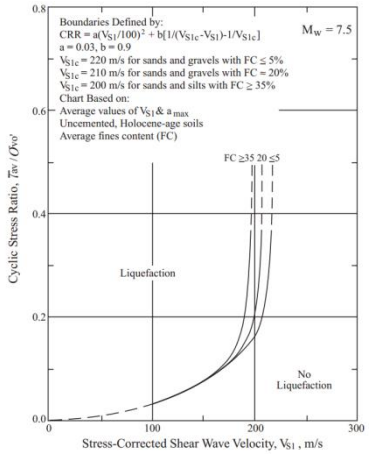

Figure 2.15. Curves with various fines contents recommended for calculation of CRR from V_{s1} (after Adnrus, et al. 1999) (Source; NCEER workshop summary report)

2.5.2. The Cyclic Strain Approach

The cyclic strain approach for evaluating the liquefaction potential was first introduced by Dobry et al. (1982). In this approach, shear strain, rather than shear stress, is the main parameter that controls both densification and liquefaction in sands. Dobry et al. (1982) found a strong relationship between cyclic shear strain and pore water pressure generation, as presented in Figure 2.16. The data shown in Figure 2.16 were obtained from cyclic strain-controlled triaxial tests performed on two types of clean sands. The pore water pressure response of both sands after ten loading cycles revealed the existence of a cyclic threshold shear strain of approximately 0.01%, below which no densification of the soil (if allowed to drain) or pore water pressure generation occurs. The trend of these data also showed that approximately 10 cycles of 1% cyclic shear strain would generate a pore water pressure ratio (r_U) of 1.0, which corresponds to zero effective stress and thus initial liquefaction of the specimen.

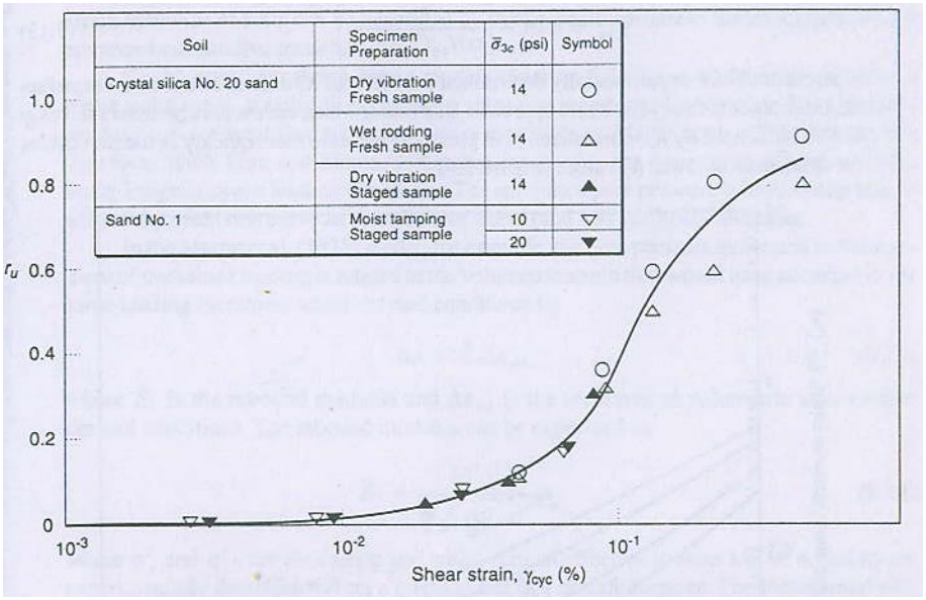

Figure 2.16. Measured pore pressure ratio after 10 cycles of loading in strain controlled cyclic triaxial tests. (after Droby and Ladd 1980) (Source; Geotechnical Earthquake Engineering Book, S.Kramer)

The evaluation of liquefaction potential in the cyclic strain approach is based on the prediction of pore water pressures from the earthquake-induced cyclic shear strain and the expected number of strain cycles. The cyclic shear strain, γ_{cyc}, is calculated by:

$$\gamma_{cyc} = 0.65 \frac{a_{max}}{g} \frac{\sigma_v \, r_d}{G_{(\gamma_{cyc})}} \qquad (2.20)$$

Where;

a_{max} = the peak horizontal acceleration at the ground surface,

g = the acceleration of gravity

σ_{vo} = the initial total vertical stress at the depth of interest

$G_{(\gamma cyc)}$ = the shear modulus of the soil at shear strain level,

r_d = the stress reduction factor at the depth of interest to account for the flexibility of the soil column. Equation 2.20 must be used iteratively, as the value of G is based on the computed value of γ_{cyc}.

CHAPTER 3

FIELD TESTS

3.1. **Introduction**

Studying the liquefaction potential screening requires a well-planned experimental program which includes field and laboratory studies. Therefore, in this study a field working plan was created and standardized to obtain data which is accurate and useful for liquefaction analysis.

Field tests are important components of the research for the analysis of liquefaction and they provide the opportunity to test the soil under itsnatural conditions. Although field tests have advantages e.g. testing in undisturbed conditions, they have some disadvantages for example testing conditions are not controlled, time dependent phenomenon are difficult to control due to large scale and measurements and instrumentation is rather a difficult task.Field tests are needed when it is difficult to obtain "undisturbed" samples, in case of cohesionless soils.

In this study, five different in-situ tests were performed. These are (1) Standard Penetration Test (SPT), (2) Piezocone Penetration Test (CPTu), (3) Seismic Cone Penetration Test (SCPT), (4) Pore Pressure Dissipation Test (PPDT) and (5) Direct Push Permeability Test (DPPT). An illustration of the field tests conducted in this study is shown in Figure 3.1. Some of them need a boring hole like SPT. SPT boring holes have been used both to take disturbed samples for laboratory test and to measure the ground water level. This chapter explains the testing area, experimental program of field tests and details of the test setups.

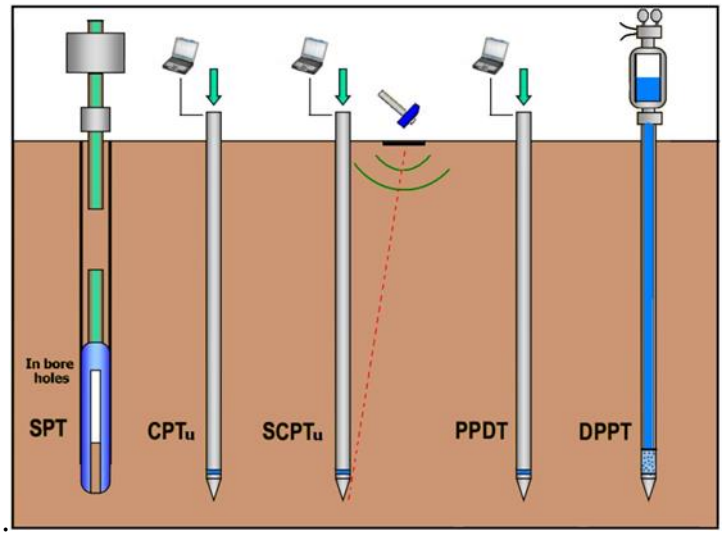

Figure 3.1. An illustration ofthe field tests conducted in this study

3.2. Field Testing Area

Aegean and West Anatolian Regionsare one of the most seismically active regions of Turkey. Izmir is seismically most active part of the Aegean area. It shows a very complex, active and rapidly changing tectonic pattern due to the relative motions of surrounding tectonic plates. Figure 3.2 shows active faults in Izmir which were presented in Izmir Metropolitan Municipality Earthquake Master Plan Project (1999). These are; Guzelhisar Fault, Menemen Fault, Foca-Bergama Fault, Izmir Fault, Bornova Fault, Tuzla Fault, Seferihisar Fault, Gulbahce Fault and Gumuldur Fault. Figure 3.3 illustrates the probability of liquefaction zones in Izmir Metropolitan Municipalityaccording to the RADIUS Izmir Metropolitan Municipality Earthquake Master Plan Project, (1999). In addition to that, Eskişar (2008) determined the soil properties of the northern coast of Izmir Gulf by collecting data from geotechnical surveys in amount of 461 sounding conducted between 1984 and 2006. Using the knowledge from previous studies, soil properties of the northern coast of Izmir Gulf were determined. According to the research, the area between Karsiyaka and Cigli (the northern coasts of the Izmir Gulf) is known for content of sand, silt, silty sand and sandy silt deposits. Proposed testing area is shown at Figure 3.4.

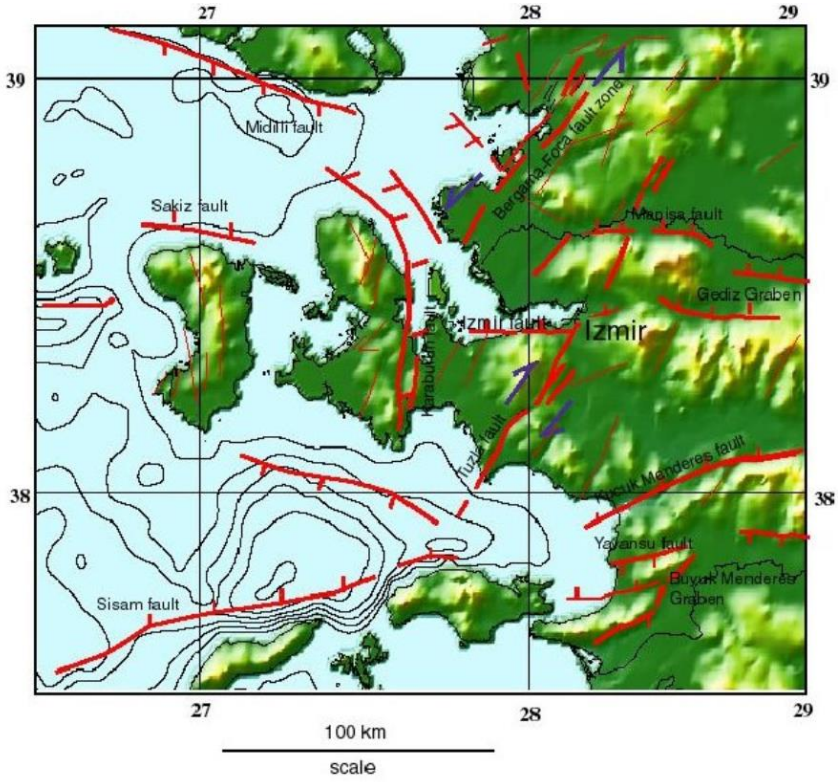

Figure 3.2. Active faults in Izmir seismic zone
(Source: Izmir Metropolitan MunicipalityEarthquake Master Plan Project, 1999)

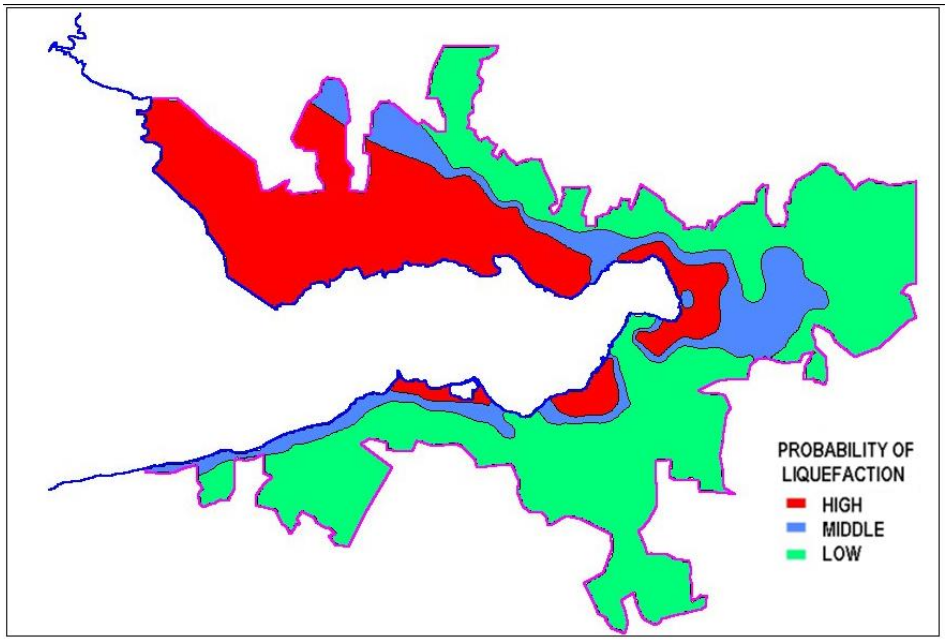

Figure 3.3. Liquefaction probability of Izmir Metropol
(Source: Izmir Metropolitan MunicipalityEarthquake Master Plan Project, 1999)

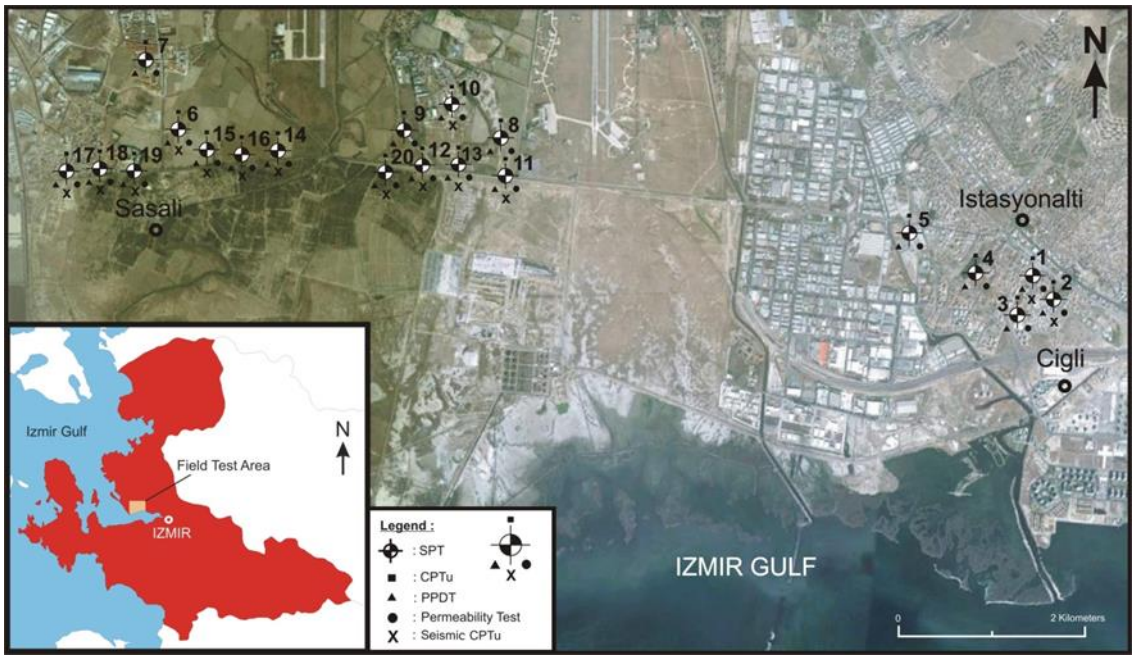

Figure 3.4. Map showing the location of the points of field tests and wells

In testing area 20 pints had been selected which was estimated to contain silty sand with different silt content. The coordinates of the testing locations were determined with GPS in field and shown on map in Figure 3.4. The GPS coordinates were given inTable 3.1 .

Table 3.1. GPS coordinates of test locations

Location	GPS Coordinates			Location	GPS Coordinates		
	--	mE	mN		--	mE	mN
SC1	35S	505663	4260272	SC11	35S	500120	4260979
SC2	35S	505641	4260267	SC12	35S	500096	4260992
SC3	35S	505559	4260191	SC13	35S	499481	4260937
SC4	35S	505182	4260297	SC14	35S	497560	4260813
SC5	35S	504314	4260660	SC15	35S	497139	4260852
SC6	35S	496637	4261074	SC16	35S	497237	4260815
SC7	35S	496454	4261763	SC17	35S	495643	4260500
SC8	35S	499987	4261056	SC18	35S	495721	4260512
SC9	35S	499043	4261014	SC19	35S	496024	4260568
SC10	35S	499509	4261481	SC20	35S	499156	4260993

3.3. **Locating of the Tests**

The set of field tests was conducted at significant distance from each other in order to prevent effects from previous soundings at each location. Figure 3.5 shows the schematic representation of test points with distances and the location of the field tests around the well. As shown in the Figure3.5 a and b, each sounding was applied around SPT borehole with 1.5m distance. This application keeps the tests away at least 1.5m far from each other.

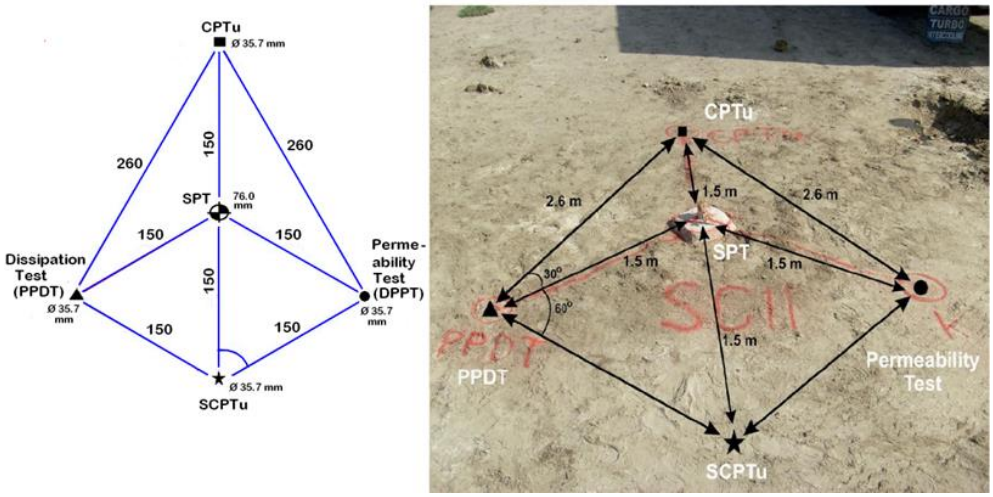

(a) (b)

Figure 3.5. (a) Schematic representation of test points, (b) Photo of test applications point around well in field

3.4. **Field Tests**

The five field tests which had been done in field were described in detail in this part, including test equipments, testing methods and progress of the work. These tests are;

1. Standard Penetration Test (SPT)
2. Piezocone Penetration Test (CPTu)
3. Seismic Cone Penetration Test (SCPT)
4. Pore Pressure Dissipation Test (PPDT)
5. Direct Push Permeability Test (DPPT)

3.4.1. Standard Penetration Test (SPT)

In this study, Standard Penetration Tests (SPT) were conducted in order to determine the soil mechanical proprieties and observe the soil profile of field. Another and most important scope of this test was to handle the soil samples which were needed for the laboratory tests.

SPT is one of the most commonly used in-situ tests for site investigation because of its low cost, simplicity and versatility.The SPT procedure initially appeared from a necessity to obtain cheap additional information during small-diameter sampler driving. One of the advantages of SPT is that it is carried out in routine exploration boreholes of varying diameters. So, the test provides a simple, universally applicable, testing method instead of sophisticated boring or testing rig.

3.4.1.1. Historical Background

The history of SPT was started in 1902 with exploratory borings using 1-inch diameter drive samplers made by Charles R. Gow. During the late 1920s and early 1930s; Mohr developed a slightly larger diameter split-spoon drive sampler and recorded the number of blow counts per foot of penetration. Adoption of the split spoon sampling procedure was formed in 1938 by ASCE's Committee on Sampling and Testing of the Soil Mechanics and Foundations Division, thanks to Terzaghi and Casagrande's research.

The first study about SPT procedure was carried out by Terzaghi in 1947. Then, Henwood began producing the Mohr 2-inch diameter split spoon sampler in the early 1950s and finally it became a nation-wide standard in 1958 when the materials and procedures were officially adopted by the American Society for Testing and Materials (ASTM). Nowadays, SPT can be performed according to thetesting standard named as "ASTM D1586; Standard Test Method for SPT and Split-Barrel Sampling of Soils", which was revised in 1984. Figure 3. 6 a to c illustrates some examples of the SPT samplers from the first developed to the most current one.

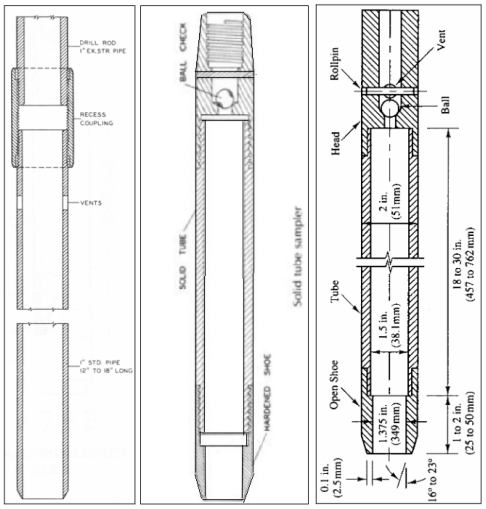

(a) (b) (c)

Figure 3. 6. (a) Gow Pile Sampler (1902), (b) SPT split spoon sampler as developed by Mohr in 1930s, (c) Details of a SPT sampler as given in ASTM D1586. (Source: Notes on the Standard Penetration Test, Advanced Engineering Geology & Geotechnics, Spring 2004)

3.4.1.2. Test Equipments

Standard Penetration Test requires a set-up consisting of various equipments for drilling, casing the hole, blowing and taking samples. All these equipments were described and classified according to their features, functions and types in Table 3.1.

Table 3.2. SPT and drilling equipments

	Equipment	Dimensions	Comment
Drilling System	Drag, Chopping, and Fishtail Bits,	57 mm < d < 165 mm	can be used in Open-hole rotary drilling or casing advancement drilling methods.
	Roller-Cone Bits,	57 mm < d < 165 mm	
	Hollow-Stem Continuous Flight Augers	57 mm < d < 165 mm	used in continuous flight hollow-stem auger method
	Solid, Continuous Flight, Bucket and Hand Augers,	57 mm < d < 165 mm	used in Continuous flight solid auger method
	Drill Rods	d= 28.5 mm (inside) d= 41.3 mm (outside) L = 2,3,4 and 6 m	can be used in all drilling methods
Hammer and Anvil System	Donut Hammer	w= 63.5 kg	Open System, Lost energy ~ %40
	Safety Hammer	w= 63.5 kg	Closed System, Lost energy ~ %40
	Automatic Hammer	w= 63.5 kg	Safest System, Lost energy ~ %10
Hammer Drop System	Rope-cathead	-	
	Rope-trip	-	
	Automatic	-	
Sampler	Split-Barrel Sampler	* Explained in figure	

Note: d= diameter, w= weight, L= lenght

In this study, for the SPT running, barrel auger was used as a driller, drill rods with length of 2m, 3m, 6m and donut hammer with rope-trip system. Schematic representation of Split-Barrel sampler was also shown in details in Figure 3.7a and Figure 3.7b shows Split-Barrel sampler filled with soil in field.

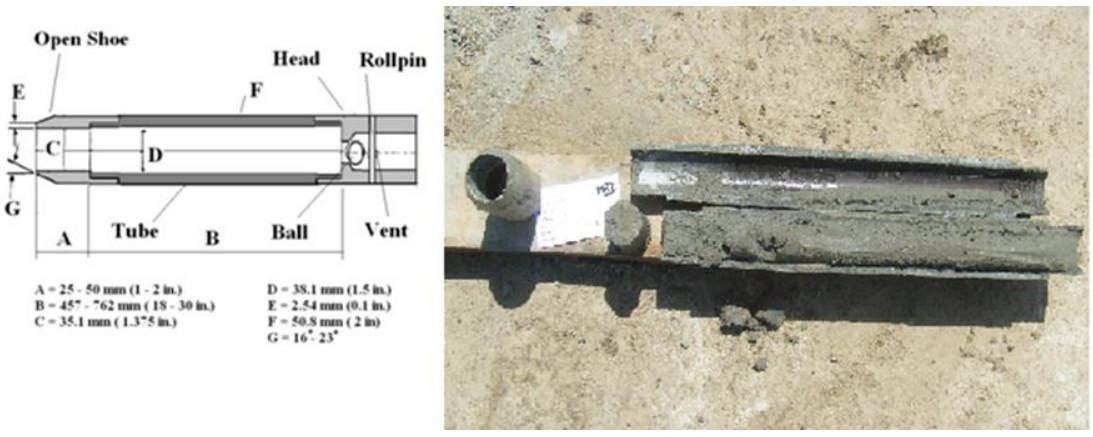

(a) (b)

Figure 3.7. (a)Schematic representations of Split-Barrel Sampler as given in ASTM D1586, (b) Split-Barrel Sampler with soil sample in field

3.4.1.3. Testing Procedure

There are several drilling methods for a SPT and the method should be chosen according to the subsurface conditions. These are;

1. Open-hole rotary drilling method
2. Continuous flight hollow-stem auger method.
3. Wash boring method.
4. Continuous flight solid auger method.

In this study, open-hole rotary drilling method was conducted with casing advancement. Drilling, sampling and testing procedures which were done can be described as follows (Figure 3.8 and Figure 3.9);

1. The borehole was drilled incrementally to permit intermittent or continuous sampling, drilling was paused at depth intervals of 1.5m, and soil sample was taken from last 0.5m depth of drilling using by barrel auger.
2. After the borehole had been advanced to the desired testing elevation and excessive cuttings had been removed,split-barrel sampler was attached to the

sampling rods and put into the borehole carefully to notallow the sampler to drop onto the soil.

3. After the hammer had been positioned above and the anvil had been attached to the top of the sampling rods, the drill rods was marked in three successive 0.15m increments so that the advance of the sampler under the impact of the hammer was easily observed for each 0.15m increment (Figure 3.8).
4. The sampler was driven with blows from the 63.5kg hammer through 0.76m height and counted the number of blows applied in each 0.15m increment (Figure 3.8 and Figure 3.9).
5. A total of 50 blows have been applied during any one of the three 0.15m increments, a total of 100 blows have been applied for 0.45m increments or there is no observed advance of the sampler during the application of 10 successive blows of the hammer, when one of the previous situations occurred, the blowing stopped and it was noted on boring log.
6. The number of blows (N) requiredadvancing the sampler each 0.15m of penetration was recorded manually. The first 0.15m was considered to be a seating drive. The sum of the number of blows required for the second and third 0.15m of penetration was termed as“standard penetration resistance”, the “N-value” or “N_m” (Figure 3.9).
7. After the SPT had been done, testing equipment and spilt barrel sampler were removed to the ground surface, the soil sample was taken from sampler. The soil sample was classified according to the Soil Classification Cheat Sheet, and then one or more representative portions of the sample were placed into sealable moisture-proof zip lock bag without ramming or distorting any apparent stratification. Each disturbed sample bag was stored with a label that the name of location, depth and name of the sample, soil classification according to the first field observation writing on, to bring them to the laboratory (Figure 3.7).
8. The drilling setup was positioned with barrel auger into the borehole again, and the drilling has been run on for another 1.5m depth. The procedure had been repeated for each 1.5m interval depth until the last SPT test was done at 15m depth.

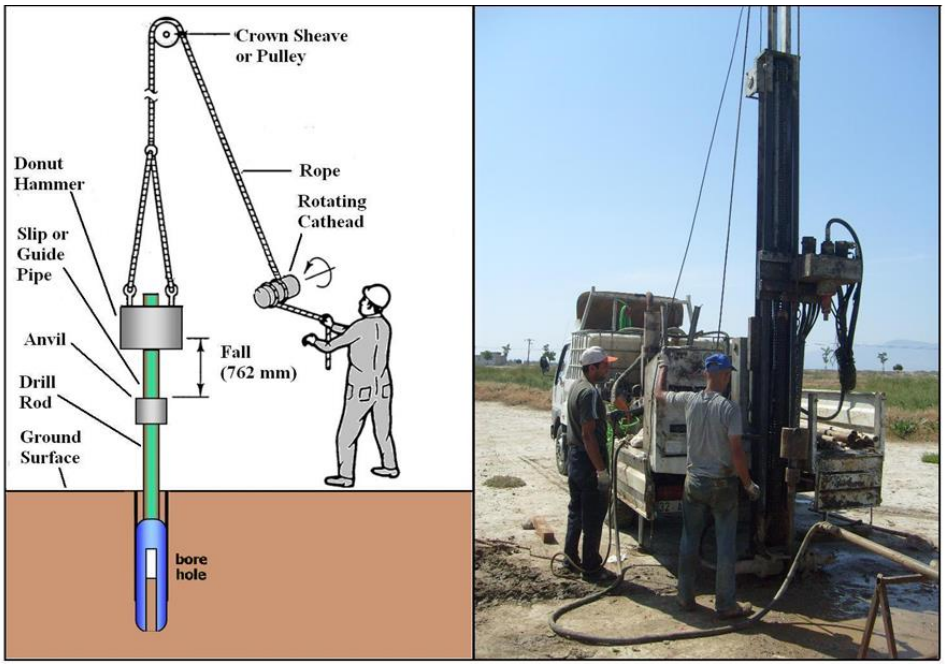

(a) (b)

Figure 3.8. (a) Schematic representations of SPT setup, (b) application of SPT in the field

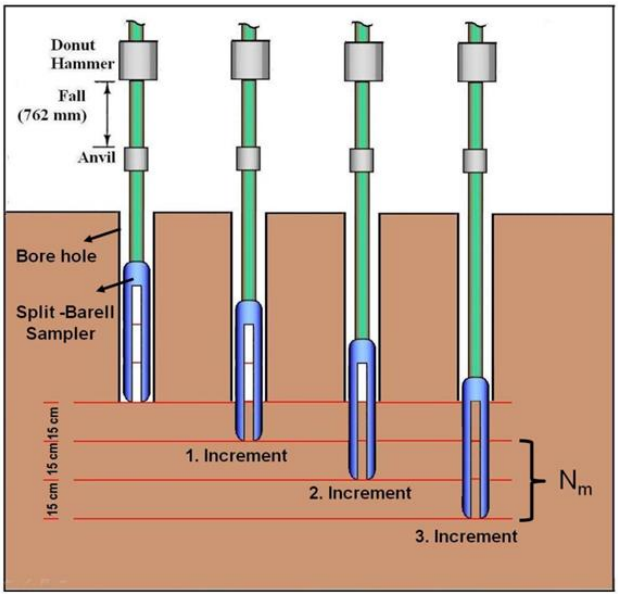

Figure 3.9. Schematic illustrations of SPT penetrations and measuring increments

For each borehole, a data sheet was formed as “Boring Log” to record all information related to borehole. The boring log includes information about project name

and location, borehole name and coordinates, date of test, type of drilling method, size and type of bit, type of sampler, number of sample and number of SPT tests, completion depth of borehole, ground water level, inspector name, sample description, test depth, blow count of SPT and the number of sample photo. For all 20 test locations, boring logs of boreholes are given in Appendix A.

3.4.1.4 Correction of Standard Penetration Resistance

In a Standard Penetration Test, a number of parameters influence the measured standard penetration resistance (N value). N value can be affected by varying of hammer type, sampler type, length of the sampling rods or drilling rods, diameter of borehole. Not all the energy from the falling hammer is used in driving the sampler into the ground. A lot of energy is lost through inefficiencies of the hammer, bending of the rods and in pushing the sampler into the ground. Therefore, some corrections are needed to estimate the normalized standard penetration resistance of the soil and the measured N value is standardized by multiplying it by the ratio of the measured energy transferred to the rod to 60% of the theoretical potential energy. Using by all parameters the N value has been normalized according to the following equation (Robertson and Wride, 1998);

$$(N_1)_{60} = N\, C_N\, C_E\, C_B\, C_R\, C_S \tag{3.1}$$

Where;

$$C_N = \frac{2.2}{1.2+(\frac{\sigma_{vo}'}{P_a})} \tag{3.2}$$

C_N is specified by Seed and Idriss (1982). Pa=1atm=100 kN/m2, σ_{vo}'= effective overburden pressure.C_N, C_E C_B C_R C_S are the correction factors which are listed in Table 3.3 by Robertson and Wride (1998).

Table 3.3. Correction factors of SPT N values

Term	Factor	Equipment Variable	Correction
C_N	Overburden Pressure	-	$=2.2 / (1.2+(\sigma_{v0}/P_a)) \leq 1.7$
C_E	Energy Ratio	Donut Hammer	0.5 -1.0
		Safety Hammer	0.7-1.2
		Automatic Hammer	0.8-1.3
C_B	Borehole Diameter	65-115 mm	1.0
		150 mm	1.05
		200 mm	1.15
C_R	Rod Lenght	<3 m	0.75
		3 - 4 m	0.8
		4 - 6 m	0.85
		6 - 10 m	0.95
		10 - 30 m	1
C_S	Sampling Method	Standard Sampler	1
		Sampler without liners	1.1 -1.3

For this study, to calculate the normalized standard penetration ratio, $(N_1)_{60}$, correction factors was estimated as follows; C_E=0.6,(correction for donut hammer energy ratio of 60%), C_B= 1 (correction factor for 65-115 mm borehole diameter) C_R= 0.8(correction factor for 3-4 m rod length), C_S= 1(correction for standard samplers). All normalized standard penetration resistance was calculated and recorded, using the equation and factors given above.

3.4.1.5 Ground Water Level

In this study, at the end of the each SPT running, PVC well screens with 5cm diameter which were used to ensure the flow of groundwater into the wells were placed into the boreholes in order to prevent the deformation of wells. During the field work progress, these wells were used as groundwater observation wells and ground water level measurements were performed in regular time intervals by means of electronic water level indicator. Figure 3.10 shows an application of measuring the depth of water level with water level indicator at one of the test locations. A ground water level observation data sheet was formed as “well construction log” for each well including information such as project name, location, casing type, diameter and length, screening type, diameter and length. Moreover, it consists of each measurement of water depth

with date and time. For all 20 test locations, average ground water levels were given in Table 3.4.

Figure 3.10. Measuring the depth of water level with water level indicator at one of the observation well

It was observed that the ground water levels were very variable, depending on the season. The shallowest ground water depth was at around 1m while the deepest one was around 3.5m. It means the field working area has a very shallow ground water depth which plays a significant role in liquefaction occurring cases.

Table 3.4. Average ground water levels of borholes

Borehole Number	Ground Water Level (m)	Borehole Number	Ground Water Level (m)	Borehole Number	Ground Water Level (m)	Ground Water Level (m)	Ground Water Level (m)
SC1	1,84	SC6	2,26	SC11	1,85	SC16	2,81
SC2	2,78	SC7	1,84	SC12	1,06	SC17	1,93
SC3	3,4	SC8	1,67	SC13	1,41	SC18	1,35
SC4	2,3	SC9	1,56	SC14	2,36	SC19	1,81
SC5	1,70	SC10	1,76	SC15	1,56	SC20	1,56

3.4.1 Piezocone Penetration Test (CPTu)

In this study, total of 20 Piezocone Penetration Tests (CPTu) were conducted in order to estimate the geotechnical parameters to provide results for the liquefaction analysis. Definition of the Cone Penetration Test (CPT) can be expressed as follows; a penetration test which is aimed to measure the soil resistance and performed with a setup includes series of rods and a cone connected to end of rods to push into the ground. Also, cone penetration provides measurements of resistance of a surface sleeve and pore pressure by a sensor. The CPTu is most practical field test and has several main advantages over the traditional method of borings and other testing. These advantages can be listed as follows;

1. It provides continuous data during the penetration.
2. The data are repeatable and reliable.
3. The applicability of test saves time and cost.

The procedures for performing CPTs are standardized by the United States Bureau of Reclamation as USBR 7020, 7021 and in the American Society for Testing and Materials as ASTM D-5778, D-6067. CPTu tests were done according to the ASTM D-5778 and D-6067 standards according to the test procedure explained in section 3.4.2.3.

3.4.2.1. **Historical Background**

The Cone Penetration Test (CPT) system can be divided into three main groups according to technical features of penetrometers in their historical background. These are mechanical cone penetrometers, electric cone penetrometers and piezocone penetrometers.

CPT was introduced in northern Europe in 1930s by P. Barentsen. It was a mechanical penetrometer that incrementally measured the cone tip resistance and named as Dutch cone. In the 1960, mechanical cones, known as Begemann friction cones, measured both the tip resistance and the side resistance along a sleeve above the cone tip, were developed. Mechanical cone penetrometers are still used because of their low cost and simplicity.

The first electric cone penetrometer whichwas called as the ‘‘Rotterdam cone’’, was developed in 1948 by Bakker in Holland. In an electric cone penetrometer system the signals were transmitted to the ground surface through a cable inside the rods. In 1960s, the CPT was introduced in North America with an electric cone penetrometer that used electrical transducers to measure the tip and side resistance. In recent years, a large number of electric cone penetrometers have been developed all around the world.

The use of electronics allowed the incorporation of additional sensors in the cone system, including those for pore water stress, temperature, inclination, acoustic emissions, and down-hole seismic. Penetrometers capable of measuring dynamic or static pore water pressures are called piezometric cones or piezocones.In 1974, Janbu and Senneset firstlyused a conventional electrical piezometer to measure pore water pressures during the penetration. Schmertmann also pushed into a piezometer a probe and presented the importance of pore water pressure measurement for the interpretation of CPT data. For last two decades, a number of piezocone test system have been developed, including probes with two or three filter positions or cordless data transferring. Figure 3. 11 illustrates some examples of the cone penetrometers from first developed mechanical penetrometer to the one of the most popular earlier piezocones. Also Figure 3.12 shows the most recent penetrometers developed over time.

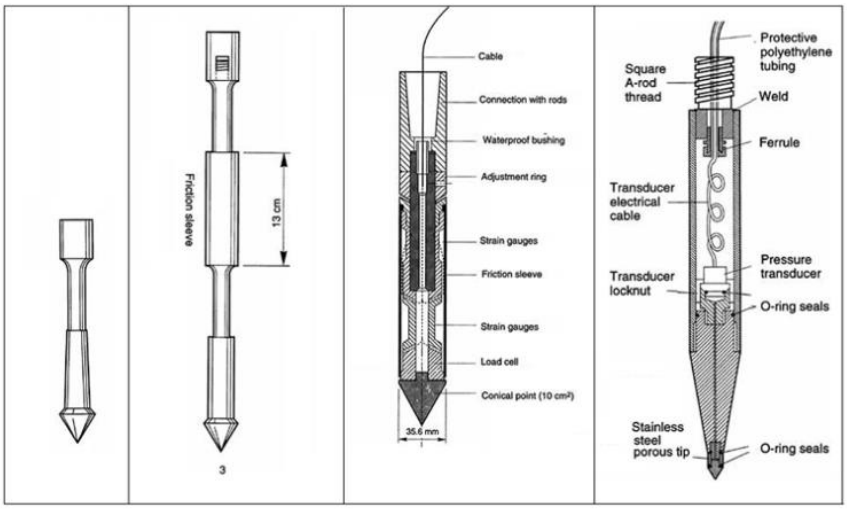

(a) (b) (c) (d)

Figure 3. 11. (a) Duch cone (1932),(b) Begemann type mechanical cone (1972), (c) Fugro electrical cone (1971), (d) Wissa piezometer probe (1975) (Source: CPT in GeotechnicalPractice Lunne,1997)

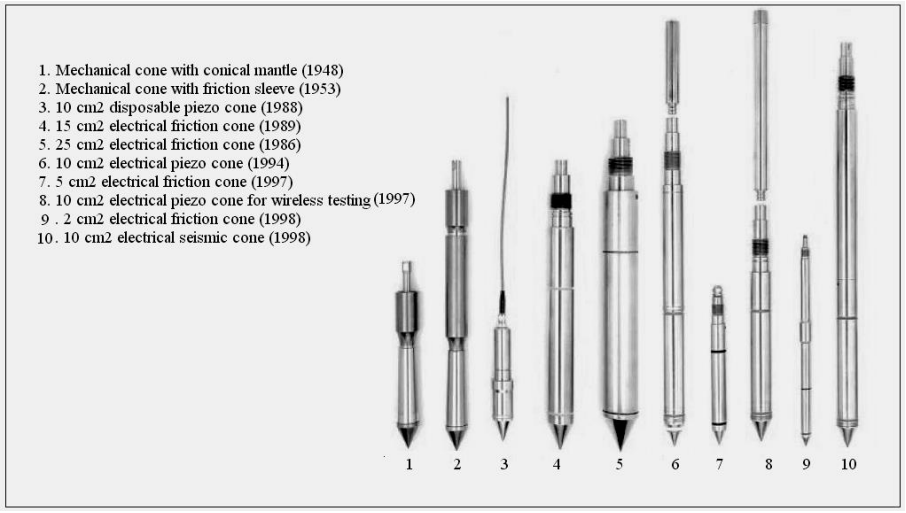

Figure 3.12. Penetrometers developed over time, with their features and patented years (Source: A P van den berg Co. official website; *www.apvandenberg.com*)

3.4.2.2. **Test Equipments**

The CPT equipments can be divided into three parts; cone penetrometer, pushing equipment and data acquisition system.There are several piezocones with different size and features as shown in Figure 3.12. Piezocone consists of a 60° conewith 10 cm^2 base area (35.7 diameters) and a 150 cm^2 friction sleeve located above the cone. This modelis the most widely used and accepted reference test equipment. In the piezocones, pore pressure is measured typically at three different locations as shown in Figure 3.13. These pore pressures sensors are known as: on the cone (u_1), behind the cone (u_2) and behind the friction sleeve (u_3).

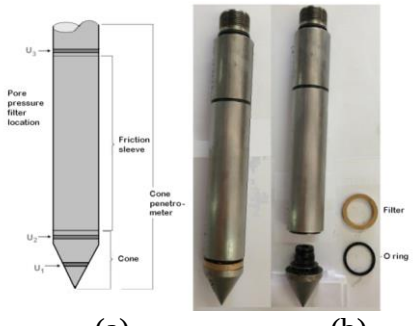

(a) (b)

Figure 3.13. (a) Schematic presentation of the piezocone, (b) piezocone with its filter and O-ring elements

In this study, a wireless piezocone was used with a cone tip of 35.7 mm in diameter, a 10 cm^2 base area, an angle of 60 degrees and friction sleeve of 150 cm^2. The wireless piezocone probe was shown in detail in Figure 3.14. Components of probe were numbered in figure as follows; 1)Cone, 10 cm^2, 2) O-ring, 3) Filter Ring, 4) X-ring, 5) Support Ring, 6) O-ring, 7) O-ring, 8) O-ring, 9) Friction Sleeve, 10) Cone Body, 11) O-ring (Geotech Nova CPT Acoustic Manual)

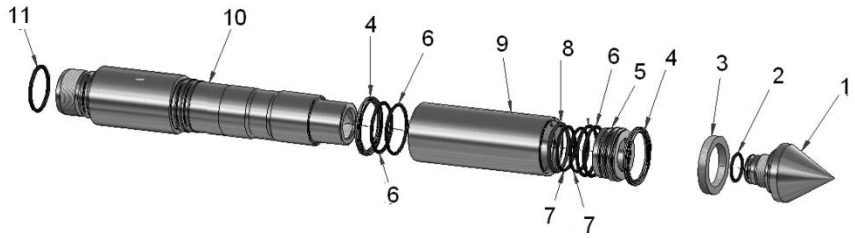

Figure 3.14. CPTu Probe with components

The pushing equipment consists of a trust mechanism, a reaction system and push rods. For CPT tests, there are special designed trucks including hydraulic jacking system, rigs with enough trust capacity. The rigs used for penetrating the probe and rods into the soil. The trust capacity of these trucks generally varies between 10 and 20 tones. For this study a truck belongs to Zemin Teknolojleri Merkezi Company with 30 tones capacity was used which was shown in Figure 3.15.

Figure 3.15. CPTu test truck

Data acquisition systemis a part of the CPTu setup which is including lots of electrical components and software. The components of the system were listed and described as follows and also illustrated in Figure 3.16.

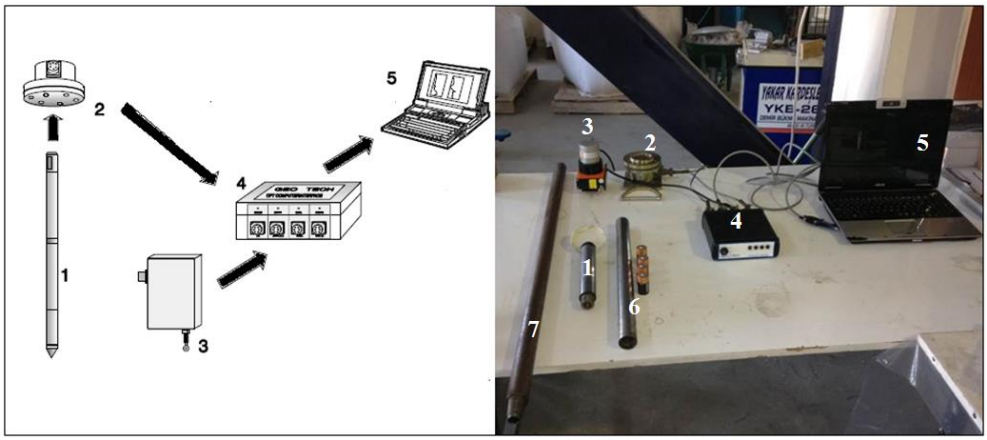

(a) (b)

Figure 3.16. (a) Schematic illustration of Geotech Nova CPT Acoustic Manual, (b) connections of all data acquisition system equipments

Components of CPTu data acquisition system were numbered in figure as follows; 1) CPT probe, 2) Microphone, 3) Depth encoder, 4) Computer interface box, 5) Computer, 6) Nova and 7) Rod.

The system does not require a cable to transmit measured data, from probe to soil surface. This is done acoustically; the digitized coded data string is converted into a high frequency acoustic signal by a piezoelectric element in the probe. The signal is then transmitted up through the steel of the rods to a microphone on the rig or penetrometer. No cable is used for transmitting the data from probe to the recorder at the surface. The absence of a cable makes the system very easy and time efficient to use. From the microphone, the signals are transmitted to a computer interface box, which also receives depth information, from a depth encoder. The data is then sent to a computer. The data are presented simultaneously on the PC screen as curves and digits.

For this study, data acquisition system, piezocone and other equipments for CPTu test were manufactured by Geotech Co, Sweden.

3.4.2.3. **Testing procedure**

The pore water pressure meter is normally a pressure transducer of the membrane type. The sensor shows insignificant deformation during loading. It communicates with a porous filter on the surface of the cone penetrometer via a liquid chamber. The filter element and other parts of the pore pressure system are saturated with a liquid before field use. This saturation should be maintained until the cone penetrometer reaches the groundwater surface or saturated soil. The filter should be saturated with de-aired glycrine, silicone oil or similar which makes it easier to maintain saturation throughout the test. It is good practice to cover the filter element with a rubber membrane, which will burst when the penetrometer comes into contact with the soil. The cone penetrometer is designed in such a way that it is easy to replace the filter and that the liquid chamber is easy to saturate. In general, filter elements are saturated in the laboratory and kept saturated in airtight containers until assembly in the field. One commonly used procedure to assemble and saturate the piezocone in the field, when using glycerin or silicone oil, is to use a plastic funnel (Figure 3. 17).

To saturate the piezocone with a plastic funnel, some procedure was done in field. First, the cone penetrometer was turned upside down and the cone was removed. The funnel was mounted and slowly filled with glycerin or silicone oil. Using a plastic syringe and hypodermic needle, the cavities in the penetrometer were saturated. The filter was carefully transferred from its container to the funnel and all parts were assembled while submerged in the liquid. Figure 3. 17 shows the mounting the filter elements to the probe in a funnel full of glycrine.

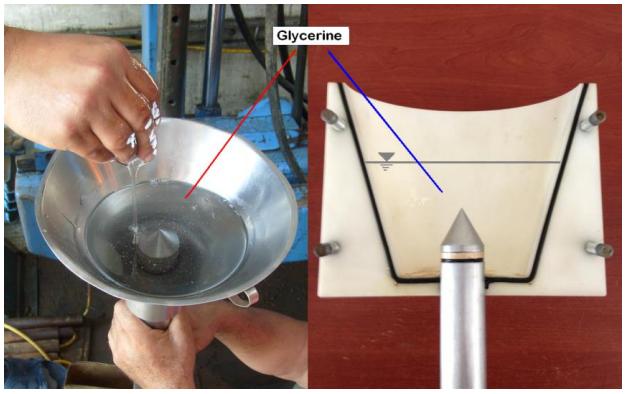

(a) (b)

Figure 3. 17. Mounting the filter element with a glycerin funnel (a) in the field, (b) in the laboratory

Truck should be leveled with the help of truck hydraulic leveling feet on the test point in the field. The truck can be anchorage to the ground to improve the stability of truck using by anchorage feet, if it is necessary (Figure 3.18. a). CPTu test is a non-stop penetration test, the penetration velocity should be constant during the test.Therefore, rigs, ram and hydraulic pushing system should be controlled before starting a CPTu sounding.All leveling procedures and controls were completed about truck and pushing system.

Before the probe was mounted on the nova, batteries of nova were controlled. The rods, which were made of steel, were mounted to probe. Each rod has 1m length, the penetrating part of the test setup including probe, nova and rods were prepared to perform, and the microphone was placed at top of the setup. This process should be exact to achieve good sound transmission. Apparatus and all cables of data acquisition system, including microphone, computer interface box, depth encoder, data cables, power cables and computer were connected.

Before each CPTu test, it is essential to perform a zero load test of the cone tip and sleeve friction, while the probe is suspended vertically in the air. After zerotestwas recorded, CPTu test was ready to sound. Figure 3.18 shows a schematic illustration of CPTu setup and truck, penetration system inside the CPTu truck and cone penetration into the ground during a sounding. In this figure apparatus of system were numbered as follows; 1) rods, 2) rams, 3) rigs and 4)computer.

(a) (b) (c)

Figure 3.18. (a) Schematic illustration of CPTu setup and truck, (b) Penetration system inside the CPTu truck, (c) cone penetration into the ground

3.4.2.4. **Measured Parameters**

CPTu sounding was started after all the preparation mentioned before had been completed. While theprobewas beingpenetrated into the soil, the transmitter received the digital multiplexed measured data of cone resistance (q_c), sleeve friction (f_s) and pore water pressure (u_2) from the probe. The results were viewed on the screen on the computer. Penetration velocity was constant during the sounding and 2 cm/sec as standard reference for the test (ASTM D 3441).

During the test, cone resistance (q_c), sleeve friction (f_s) and pore water pressure (u_2) values was seen instantly as a graphical review on the computer screen. The CPTu wireless sounding system provides to read data for each 2cm depth. To read the data, software named "Geo-Log" was used. Also, "Geo-Pro" software provides some interpretations, calculations and assumptions about mechanical proprieties of tested soil. Figure 3.19 shows a graphical illustration of a CPTu sounding including cone resistance, sleeve friction, pore water pressure graphics with soil classification according to the Robertson 1990 soil classification chart as an export of Geo-Pro program. Unified Soil Classification System symbols were added manually according to the laboratory soil classification test. The symbols of USGS will be explained in section Chapter 4. Soil group numbers and soil type definitions of Robertson 1990 soil classification system were shown in Figure 3.19 All CPTu test exports were given in Appendix B.

The soil types of samples according to the USGS which obtained from laboratory soil classification test and soil types of test profile according to the Robertson 1990 classification system obtained from CPTu soundings were compared for all tests. It was observed that, both systems classified the silty sands and clean sands similarly. However, a number of soil samples were classified by CPTu software according to the Robertson 1990 classifiaction system as Clay, Silty clay (3) and/or Silt mixtures, Clayey silt (4) while laboratory soil clasifiaction tests gave different results as Clayey sand (SC) and/or Silty Sand (SM) for same samples.

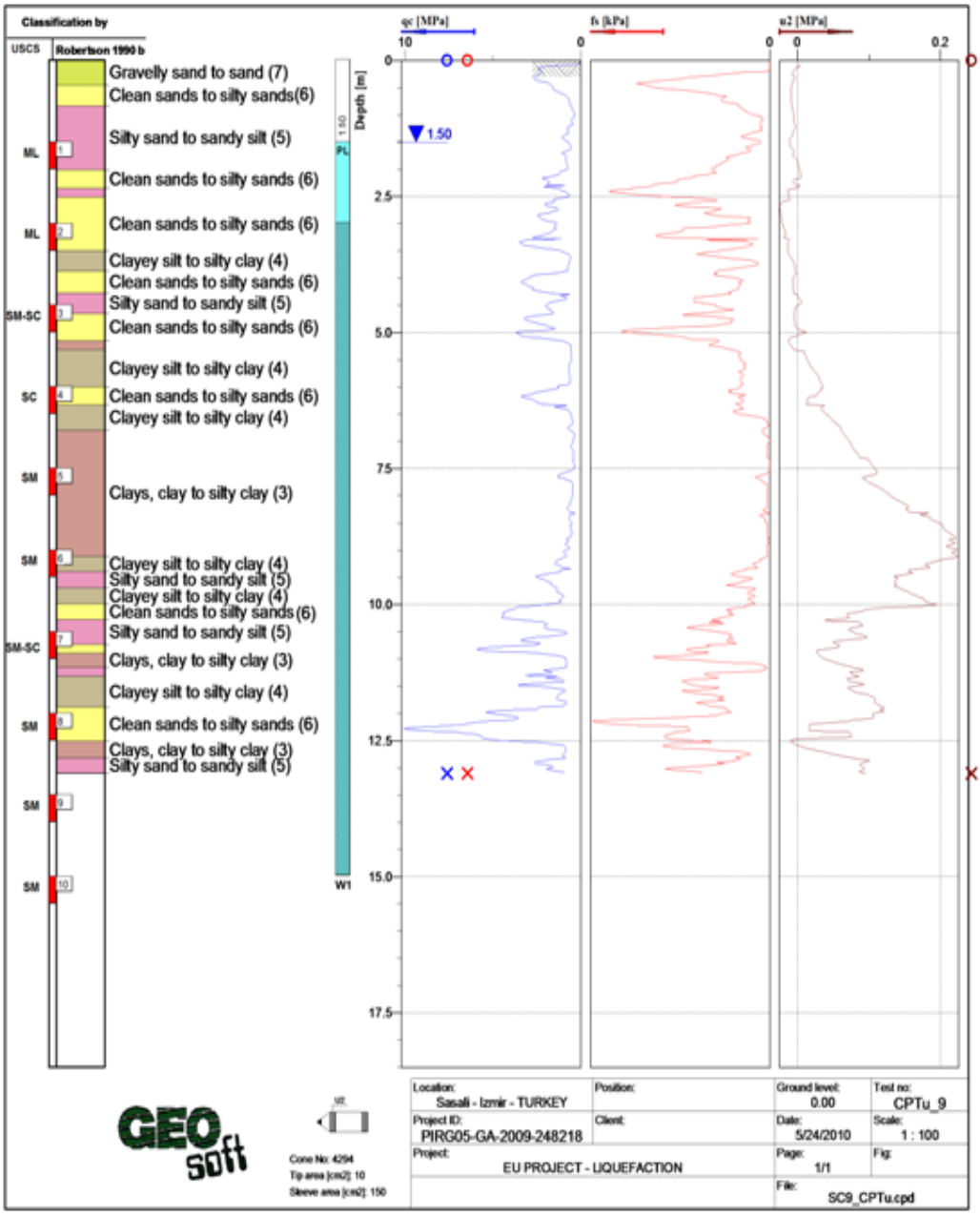

Figure 3.19. Graphics of a CPTu sounding as export of Geo-Pro software

Table 3.5. Soil classification chart of Robertson 1990

Soil Group No	Soil Type (Robertson 1990)	Soil Group No	Soil Type (Robertson 1990)
1	Sensitive, fine grained	6	Sand; clean sands to silty sands
2	Organic soils-peats	7	Gravelly sand to sand
3	Clays, Clay to silty clay	8	Very stiff sand to clayey sand
4	Silt mixtures clayey silt to silty clay	9	Very stiff fine grained
5	Sand mixtures; silty sand to sandy silt		

CPTu test procedure requires some normalization of measured cone tip resistance. This normalization provides to figure out a dimensionless normalized cone penetration resistance, q_{c1N}. Normalized cone penetration resistance was suggested by Youd et. al. (2001) as equations stated below;

$$q_{c1N} = C_q \left(\frac{q_c}{P_a} \right) \tag{3.3}$$

$$C_q = \left(\frac{P_a}{\sigma_{vo}'} \right)^n \tag{3.4}$$

Where;

P_a = 1 atm atmospheric pressure in the same units used for q_c

σ_{vo}'=effective vertical stress in the same units as P_a

n= stress exponent.

3.4.3. Seismic Cone Penetration Test (SCPT)

In recent years, a downhole method with a seismic piezocone has more advantages for seismic researches. The combination of the seismic downhole method and the CPT logging provide an extremely rapid, reliable and economic means of determining stratigraphic, strength and modulus information in one sounding. Recent version of seismic cone was developed at University of British Columbia by Campanella and Robertson in 1986 (Figure 3.20).

SCPT is performed to measure seismic waves. There are two different type of waves P waves and S waves through the soil. P waves arrive at the detector first and they are called as primary waves. Primary waves are longitudinal or compressional waves which mean the vibrations are along the same direction as the direction of travel. P waves depend upon the bulk modulus of elasticity for the material as well as its density. S-waves arrive at the detector of a seismometer second and they are called as secondary waves. Secondary waves are transverse waves which mean the vibrations are at right angles to the direction of travel. S waves depend upon a resistance to transverse or "shear" force. Also, the seismic waves are called as “compression (P) waves” and “shear (S) waves”. S waves travel typically 60% of the speed of P waves. During a

SCPT sounding a P wave is generated with a hitting vertically to P plate to compute compression waves velocity and a S wave is generated with a horizontal hitting to S plate to compute shear wave velocity (Figure 3.21).

In this study, seismic cone penetration test (SCPT), is generated by adding geophones and accelerometers to standard CPT setup.

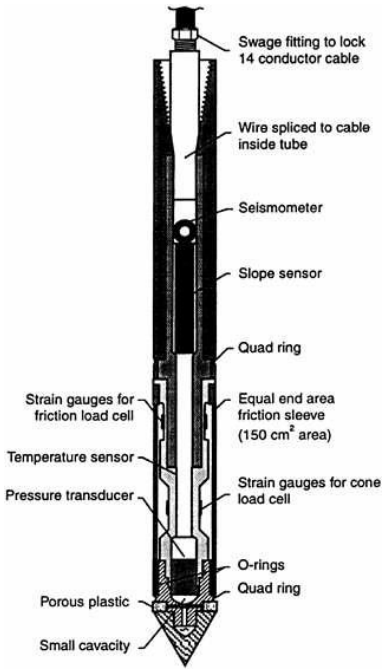

Figure 3.20. Seismic Cone developed by Campanella and Robertson in 1986

3.4.3.1. Test Equipment

It is easy to change a CPTu system into a seismic CPTu system with a seismic adapter mounted on a CPT cone and seismic acquisition box conducted to system. Therefore, CPT needs some additional equipment to sound seismic measurements. the equipments for Seismic-CPT purchased from Geotech Company are shown in Figure 3.21.

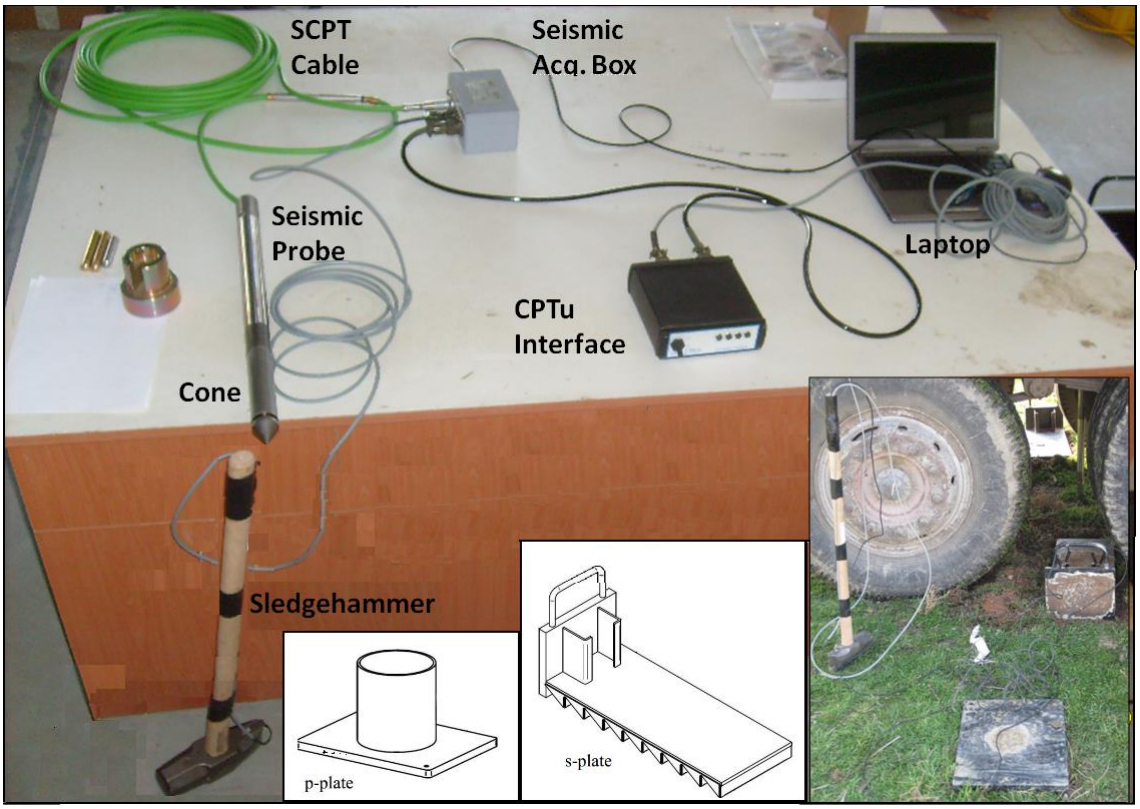

Figure 3.21. Equipment of SCPT setup and S-P wave plates with representation in field

Computer interface box, data cables and other components of CPT test setup were already described in CPTu equipments part. For seismic measurements, new additional apparatus were listed and described as follows;

Seismic Probe; a small rugged velocity seismometer has been incorporated into the cone penetrometer to obtain the measurement of dynamic shear modulus. The miniature seismometer is a Geospace with 1.7cm diameter with a nominal natural frequency of 28Hz. The seismometer is placed in the horizontal direction and orientated transverse to the signal source to detect the horizontal component of the shear wave arrivals. Figure 3.20 shows the seismic probe in detail.

Sledgehammer is a heavy wooden beam with steel ends, with 7 kg weight which triggering to seismic software to run has been connected to the system and used to generate a seismic wave on the ground surface, (Figure 3.21)

Bottom Plates for S and P wave; are steel plates placed on the ground during test to generate either P-wave or S waves (Figure 3.21).

SCPT Data Acquisition Box; a hardware connected to CPT interface box to transmit the seismic data.

SCPT Cable; SCPT test has been performed by a different mechanism from coreless CPT system which has included a cable for transition of data.

3.4.3.2. Testing procedure

First, all equipment including rods and data acquisition system of SCPT, SCPT probe, sledgehammer, plates for seismic source and pushing equipment with CPTu testing truck was brought to the field and connected as shown in (Figure 3.21). The truck was placed on the test location and pushing system was leveled to provide the rods and probe standing vertical. P and S plates were placed on the ground by applying a static load on them.

The seismic cone penetrometer was pushed into the gorund and penetration is stopped at 1 m intervals. During the pause in penetration, a compression wave was generated at the ground surface. Hitting with a sledgehammer to the P plate vertically generated this seismic wave. Also for generating a shear wave, ends of the S plates were hammered horizontally. Creating the S wave sound signals were repeated two times with two different S plates, placed with same horizontal distance to boring hole, called “left” and “right”. When the hammer made a contact with the bottom plate, it completed an electrical circuit, allowing the discharge of a capacitor. This discharge caused the timer module to generate an output pulse of the voltage source for 2-4 second duration. The rise time of the pulse was typically 100ns. Once the pulse finished, the circuit was automatically stopped. A polarized shear wave was generated in borehole and the time was measured for the shear wave to travel a known distance to the geophone in the borehole. A schematic illustration and test application on field are shown in the Figure 3. 22.

The time required for the shear wave to reach the seismometer in the cone was recorded by software. The velocity of the sound generated on the ground surface can be calculated using the following formula;

$$V = \frac{L}{t} \tag{3.5}$$

Where, V = the velocity of the sound in soil (m/sec), L= the distances between ground surface and the seismometer in the cone in meter, t= the sounds arrival time in second.

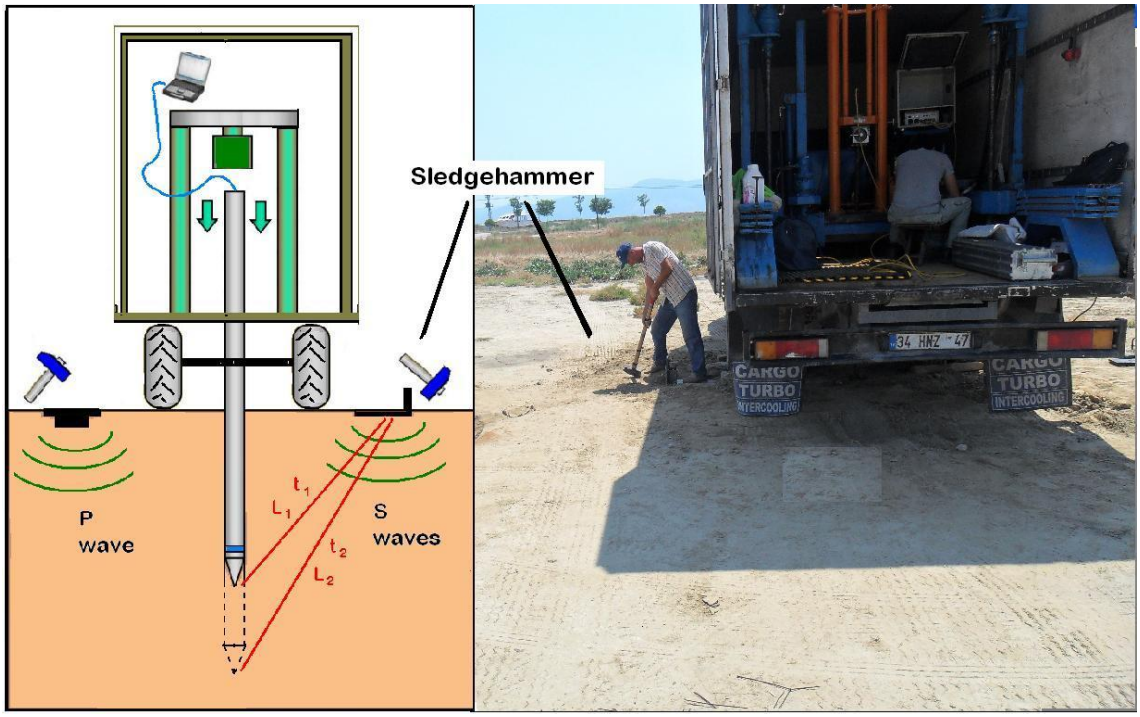

(a) (b)

Figure 3. 22. (a) Schematic representation of SCPT, (b) application of CPTu on field with investigation truck

In this study, seismic measurements were repeated for each interval 1m through the all depth for 14 different test locations and the measuring velocity of sounds were recorded as raw data.

3.4.3.3. Analysis of Signals

The raw data was processed by seismic CPT analysis software named SCPT-Analysis to reach the shear wave velocity values. This software is purchased from Geotech Company. There are two methods in this program: (1) Cross correlation method and (2) Reverse polarity (Cross-over) method to reach the shear wave velocity values from the data taken from field.

In the reverse polarity (cross-over) method, two files which correspond to reversely polarized waves (left and right) acquired at the same depth are selected as first depth and again two files selected for a greater depth as second depth. For each depth a crosshair point selected which illustrates the same acceleration changes versus time. The program simply calculates the duration between these two points. The time interval between two depths is founded by subtracting the cross-over time at the lower depth from that at the greater depth. The distance from interval is calculated from the difference between the sloping distances from the source to receiver locations. As shown in Figure 3. 22 the interval shear velocity V_s is calculated by the distance interval (L_2-L_1) divided by the time interval (t_2-t_1). Also the signals recorded with an accelerometer and filtered with spectral analysis were illustrated for reverse polarity method in Figure 3. 23.

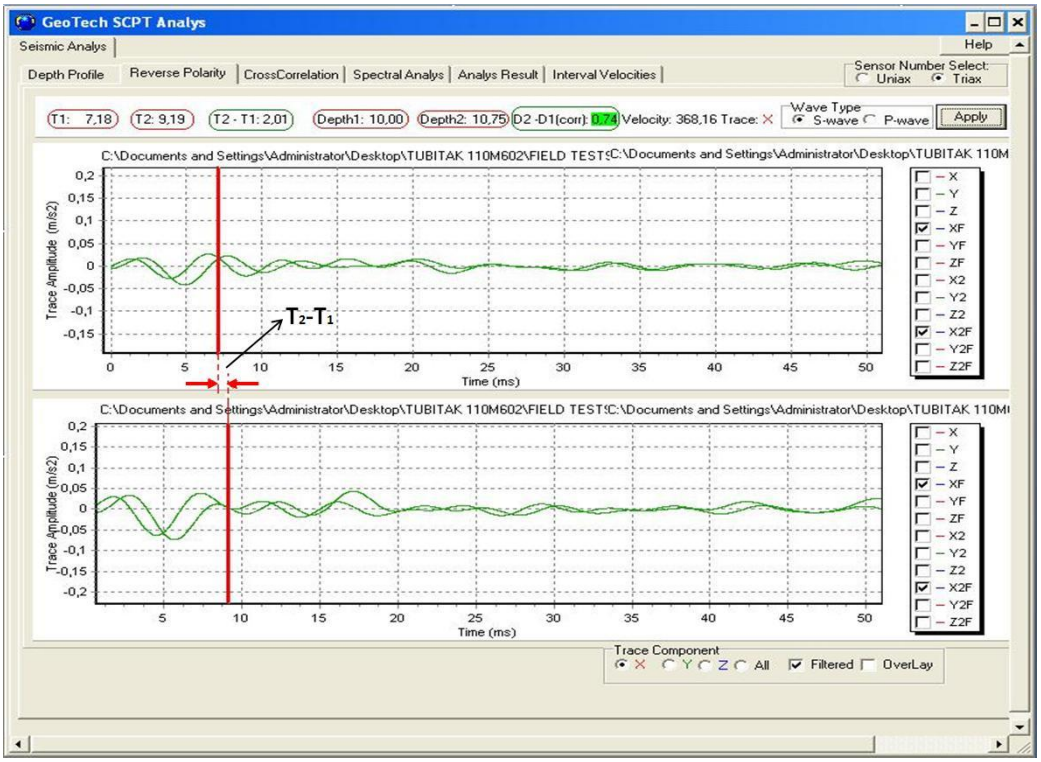

Figure 3. 23. Reverse polarity method for time interval (Geotech SCPT-Analysis Program)

The other method for analyzing the seismic data is cross correlation method. The cross correlation of signals at consecutive depths is determined by shifting the lower signal to upper signal. At each shift, the sum of the products of the signals amplitudes at each interval gives the cross-correlation for that shift. After shifting through all of the time intervals the cross correlation can be plotted versus time shift. The time shift giving the greatest sum is taken as the time shift interval used to calculate the interval velocity (Campanella et al, 1992). Figure 3.24 shows a screen of the cross correlation during the analysis.

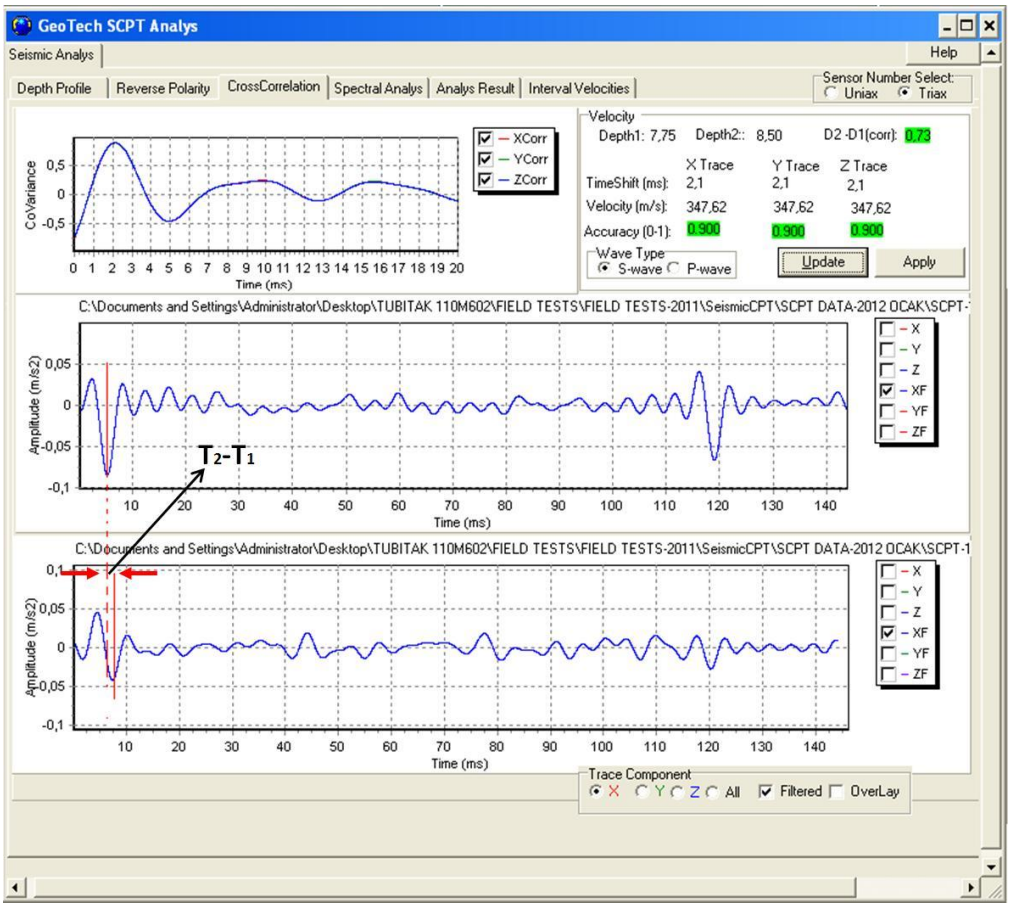

Figure 3.24. Cross correlation method for time interval of Geotech SCPT-Analysis Program

For this study, cross correlation method was used for the analysis and determined the shear wave velocity for each interval 1m through the all depth for 14 different test locations.

3.4.4. Pore Pressure Dissipation Test (PPDT)

It was referred to that one of the advantages of the piezocone test is that it can be used to measure to pore pressure with sensors located on the CPT probe. The pore pressure is measured typically at three different locations as shown in Figure 3.13. These locations of pore pressures sensors are known as: on the cone (u_1), behind the cone (u_2) and behind the friction sleeve (u_3) (Figure 3.13). In saturated clays and silts, large excess pore water pressures are generated during penetration of the piezocone. When the penetration stops the excess pore water pressure starts to dissipate. Pore pressure dissipation test (PPDT) is performed to investigate the change in the excess pore pressure (Δu) with time, which is defined as;

$$\Delta u = u_i - u_0 \tag{3.6}$$

Where; u_i is the measured pore pressure at the depth of interest and u_0 is the equilibrium in situ pore pressure at the depth of interest. Interpretation of dissipation records is generally based on a normalized excess pore-pressure ratio (U) which was defined as;

$$U = \frac{\Delta u_t}{\Delta u_i} = \frac{(u_t - u_0)}{(u_i - u_0)} \tag{3.7}$$

Where; Δu_t = excess pore pressure at any time t after penetration is stopped, Δu_i = initial excess pore pressure at t = 0 (on stopping penetration) and u_t = total pore pressure at any time t. For standard dissipation records, where the excess pore pressure shows a monotonic decrease with time, U varies between 1 (at t=0) and 0, when 100% dissipation of the excess pore pressure has occurred.

Also if the ground water level is known, hydrostatic water pressure of the depth can be required and the duration for decreasing excess pore water pressure to hydrostatic water pressure values can be defined as t_{100}. The dissipation of pore pressure can occur rapidly in sands, but it can take several days in clays.

In this test, the main scope is to determine the time value for 50% dissipation of excess pore water pressure (U= 50%), known as "t_{50}". This value is essential to estimate

the coefficient of consolidation (c_h) and permeability of soil in the field. The graphical technique suggested by Torstensson (1977), yields a value for t_{50}, which corresponds to the time for 50% consolidation. The results from PPDT, as normalized excess pore-pressure ratio (U) and time for 50% dissipation, (t_{50}) can be interpreted to provide estimates of the in situ horizontal coefficient of consolidation (c_h), horizontal coefficient of permeability and also compressibility. These relationships were explained in Chapter 2.

In this study, PPDT tests were performed for each 1m interval depth for each test location. After PPDT had been performed, the normalized excess pore-pressure ratio versus time in log scale was plotted and the times for 50% consolidation t_{50} values were figured out. An example of graphical method to find t_{50} value from dissipation data was given in Figure 3.25.

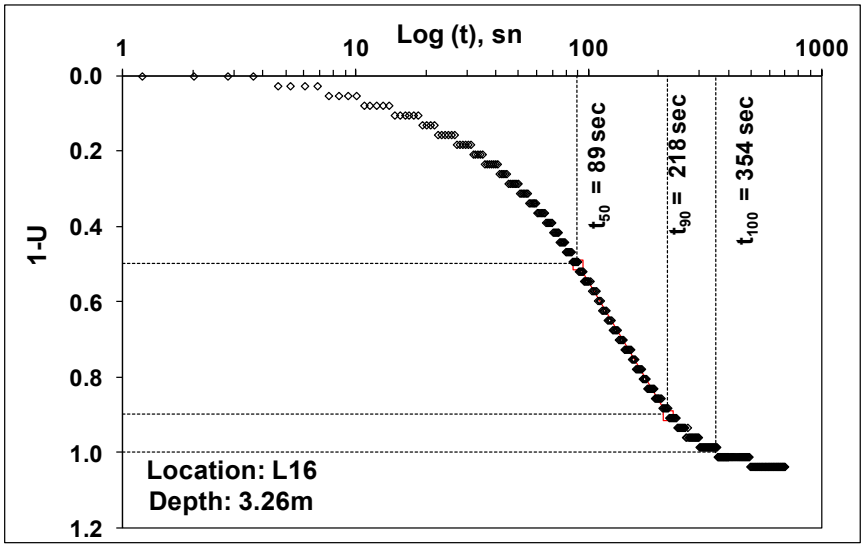

Figure 3.25. An example of finding t50 value from dissipation data for SC16 borhole and depth of 3.26m

In sands PPDT dissipation is very quick so it is not possible to find t_{50} value correctly. Therefore the PPDT values were not used to find t_{50} and it was discussed in Chapter 5 in detail.

3.4.5. Direct Puh Permeability Test (DPPT)

Direct push permeability test (DPPT) is an in-situ geotechnical experiment which scopes to obtain independent evaluations of in-situ hydraulic conductivities along the cone sounding path. For DPPT can be performed with an in-situ permeameter setup which was fabricated by Lee et al in 2008.In situ permeameter setup includes a screen probe which is fabricated to mount to the CPTu rods and a mechanism of a specially fabricated cylinder which has valves to control water and compressed gas. The screen probe is fabricated with tip angle of 60o and 35.7mm diameter cone. Also, screened probe were fabricated with a slot size of 0.3 mm, corresponding to a No. 10 screen and 45 mm length.

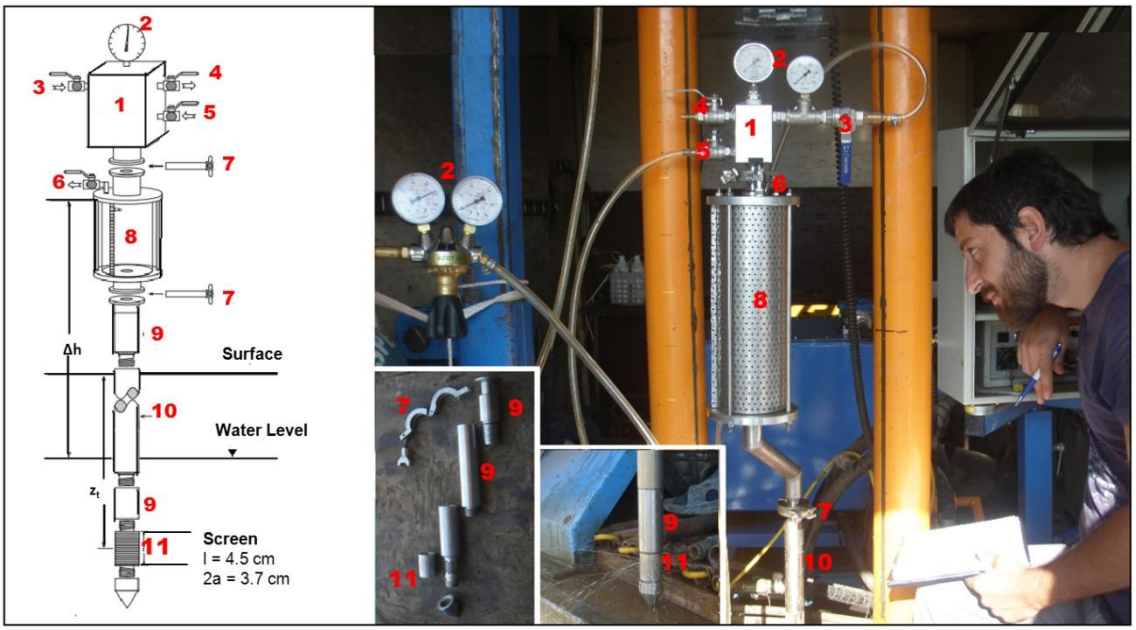

(a) (b)

Figure 3.26. (a) An schematic illustration of permeameter setup created by Lee, (b) application of permeameter setup in field

Figure 3.26 shows a schematic illustration of permeameter set-up and application of the setup in field. Components of permeameter setup were numbered in this figure as follows; 1) Gas cylinder, 2) Pressure gauge, 3) N2 gas in valve, 4) N2 gas out valve, 5) water in valve, 6) Air out valve, 7) Airtight coupling, 8) Water cylinder, 9) Coupling, 10) CPT rods, 11) Screen.

Direct push permeability test provides to measure the flow speed of the water manually as a volume discharged over a measured time under constant pressure. This mechanism rapidly pressurizes the water column in the tank that stand on ground surface using by compressed nitrogen gas to perform the measurement (Lee at al, 2008).

Following the testing procedure, first screened probe was penetrated to the depth of test conducted. Test was started by rapidly pressurizing the water column. Flow rate, Q, was measured manually as a volume discharged over a measured time. It is known that if the soil is permeable as like sand, the test can be done with free flowing condition, but if the permeability of soil is too low, it is needed to increase the pressure adding by compressed nitrogen gas into the water column. The tests were repeated for each interval 1m through the all depth to 15m to measure the flow rate of the water. According to the boring logs data, some of the depths were performed with free flowing conditions while a number of the depths were conducted with increasing the pressure adding by compressed nitrogen gas into the cylinder. In situ permeameter tests were completed for all 20 locations and flow rates were recorded.

Hydraulic conductivity k_h was calculated through the spherical form of Darcy's law; from the applied excess head, Δh and measured volumetric flow, Q through the spherical form of Darcy's law (Lee et al., 2008):

$$k_h = \frac{Q}{4\pi \Delta h a_s} \tag{3.8}$$

Where, Δh = applied excess head, Q = measured volumetric flow, and a_s = effective radius of the spherical injection zone. Effective radius can be defined as;

$$a_S = \sqrt{\frac{1}{2} al} \tag{3.9}$$

Where; a = radius of screen, l = length of the screen.

CHAPTER 4

LABORATORY STUDIES

4.1. **Introduction**

Laboratory tests are necessary to appropriately select the types and quantities of soils for geotechnical research. A careful review of all data obtained during the field investigation is essential to develop an appropriately scoped laboratory testing program.

This chapter provides the laboratory test methods including testing equipment, general procedures related to each test, and parameters measured by the tests. Laboratory tests were conducted in order to determine the index properties of the soil. Also, results of these tests were presented in this chapter. These are; soil particle size tests including sieve analysis and hydrometer test, Atterberg limits tests, specific gravity test, and maximum and minimum void ratio tests.

4.2. **Sample Collection**

The laboratory testing program includes basic soil characterization tests for disturbed soil samples. The borehole was drilled incrementally to permit intermittent or continuous sampling, drilling was paused at depth intervals of 1.5m, and soil sample was taken from last 0.5m depth of drilling using by barrel auger. This sample was named with a number as “Sample 1”. After SPT split-barrel sampler was inserted into borehole and SPT test was performed, the disturbed soil samples were retrieved from the sampling tube and SPT spoon almost at 1.5m intervals. About 45cm long soil samples are procured from the SPT spoon. The first 15cm interval of the split spoon sample typically is disregarded because of the soil disturbance. The usable portion of the sample is taken from the bottom 2/3 of the split spoon (about 15-45cm) and named with its test number as “SPT1”.

All sample taken from barrel auger and SPT spoon were placed into sealable moisture-proof zip lock bag without ramming or distorting any apparent stratification.

Each disturbed sample bag was stored with a label that the name of location, depth and name of the sample, soil classification according to the first field observation writing on, to bring them to the laboratory. Figure 4.1 ilustrates an example of the disturbed sample in sealable moisture-proof zip lock bag with its lebel.

Figure 4.1. An example of the disturbed sample in zip lock bag.

4.3. **Laboratory Tests**

Laboratory tests; 1) Soil particle size tests; sieve analysis, hydrometer tests,2) Atterberg limits tests; liquid limit and plastic limit tests, 3) Specific gravity test, 4) Maximum and minimum void ratio tests.

4.3.1. Soil Particle Size Tests

Soil grain size distribution is a geotechnical process that allows us to classify soils by determining the different percentages of aggregate diameters in the sample. To know the grain size distribution or soil classification is necessary for any classification method of soil. The process utilizes two tests; Mechanical Sieve Analysis is used for larger diameter aggregates (4.75 mm to 0.075 mm) while the Hydrometer is used for aggregates passing the last sieve (diameters less than 0.075 mm). These methods are

standardized as ASTM D 422 - Standard Test Method for Particle-Size Analysis of Soils.

4.3.1.1. Mechanical Sieve Analysis Test

In sieve analysis test, a series of sieves with different size openings which are stacked on top of each other are used to determine the grain size distribution and plot the distribution curve of soil samples whose the finest particle size is 0.075 mm.

Figure 4.2. Sieve analysis setup with sieve shaker and sieves that ranged the #4 to #230.

The sieve screens are wire fabric with rectangular openings. The sieve with largest openings is placed at the top of the sieve stack, each sieve is placed on the finer one and the sieve with the smallest openings is placed on bottom of the stack with a pan under it. Figure 4.2 shows the setup include the sieve stack and sieve shaker. Also, Table 4.1 shows the detail about the sieves such as sieve size or number and dimensions of openings according to the ASTM E11 standard.

Table 4.1. Sieve size or number with dimensions of openings

Sieve Size or Number	Openings (mm)	Sieve Size or Number	Openings (mm)	Sieve Size or Number	Openings (µm)
4"	100	0.375"	9.5	#20	850
3.5"	90	0.3125"	8	#25	710
3"	75	0.25"	6.3	#30	600
2.5"	63	#3.5	5.6	#35	500
2"	50	#4	4.75	#40	425
1.75"	45	#5	4	#45	355
1.5"	38.1	#6	3.35	#50	300
1.25"	31.5	#7	2.8	#60	250
1"	25	#8	2.36	#70	212
0.875"	22.4	#10	2	#80	180
0.75"	19	#12	1.7	#100	150
0.625"	16	#14	1.4	#120	125
0.5"	12.5	#16	1.18	#140	106
0.4375"	11.2	#18	1	#150	100
				#170	90
				#200	75
				#230	63
				#270	53
				#325	45
				#400	38

For this study, sieves of number #4, #8, #16, #18, #20, #30, #40, #50, #60, #100, #150, #200, #230 were used and sieve analysis tests were performed.

The calculations used in sieve analysis are based upon the principle that the percentage of the soil weight either pass through or retained on the each sieve can be calculated. The formula for calculating the Percent Retained (R) for any sieve is:

$$R=\frac{\text{WeightRetained}}{\text{Soil Weight}}\ \text{x}\ 100 \tag{4.1}$$

Cumulative Percent Retained (C) is another value which is needed for sieve analysis. For a given sieve size, C is derived by adding the percent retained for the given sieve size to the percent retained for all sieves with larger openings. For example, the formula for calculating the C for the sieve #18 is;

$$C_{\#18}= R_{\#4} + R_{\#8} + R_{\#16} \tag{4.2}$$

Where; R is Retained Percent for each sieve

The last value is the Percent Finer shows the total percentage of the soil grain distribution that is smaller than the size of the sieve opening for the given sieve an it is calculated by subtracting the cumulative percent retained from 100% as follows;

$$F_N = 100 - C_N \quad (4.3)$$

According to the knowledge given above, The Percent Retained, The Cumulative Percent Retained and Percent Finer was calculated and recorded on data form. Table 4.2 shows the values for sieve analysis on the data form for one of the soil samples.

Table 4.2. Sieve analysis data form of one of the soil samples.

Location No:	SC16	**Sample No:**	SPT 10	**Depth (m):** 15.00 -15.45			
Sieve No	Sieve Size	Weight Tare + Sample	Weight Tare	Weight Retained	Percent Retained (R)	Cumulative Retained (C)	Finer (F)
	mm	gr			%	%	%
#1 1/2 "	38.1	0	0	0.00	0.0	0.0	100.0
#3/4 "	19	0	0	0.00	0.0	0.0	100.0
#3/8 "	9.5	0	0	0.00	0.0	0.0	100.0
#4	4.75	470.8	470.8	0.00	0.0	0.0	100.0
#8	2.36	445.9	445.9	0.00	0.0	0.0	100.0
#16	1.18	420.3	420.3	0.00	0.0	0.0	100.0
#18	1	433.4	433.3	0.10	0.1	0.1	99.9
#20	0.85	399.5	399.2	0.30	0.2	0.2	99.8
#30	0.6	406.7	399.6	7.10	3.8	4.0	96.0
#40	0.425	406.7	399.9	6.80	3.6	7.6	92.4
#50	0.3	382.2	375.7	6.50	3.5	11.1	88.9
#60	0.25	392.4	390.2	2.20	1.2	12.2	87.8
#100	0.15	398.4	371.1	27.30	14.5	26.7	73.3
#150	0.1	284.3	227.3	57.00	30.3	57.0	43.0
#200	0.075	307.8	270.6	37.20	19.8	76.8	23.2
#230	0.063	343.9	323.1	20.80	11.1	87.9	12.1
Pan	-	277.9	255.1	22.80	12.1	100.0	0.0
Total Weight	-	-	-	188.10	100.0	-	-

Finally, according to the data form Grain Size Distribution Diagram was plotted. This graph shows both sieve size, number and the corresponding grain size on the horizontal axis and Percent Finer on the vertical axis. Figure 4.3 shows the grain size distribution graph according to the data given in Table 4.2 which belongs to soil sample named as SPT10 from test location SC16.

Sieve analysis test was done 248 times for each soil sample and the graphs of grain size distributions of soils included the hydrometer test results were given in Appendix C.

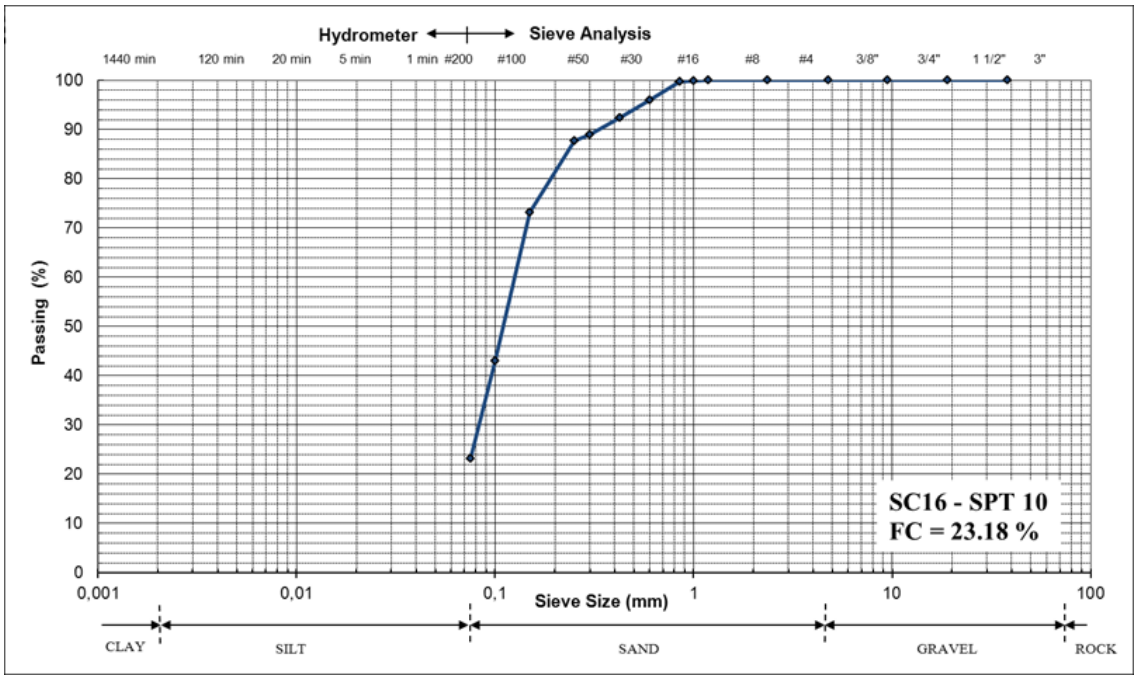

Figure 4.3. Grain size distribution graph of one of the soil sample which is "SPT10" from borehole "SC16" according to the sieve analysis.

4.3.2.1. **Hydrometer Analysis Test**

Hydrometer analysis is used to provide an indication of grain size distribution for soil grains between 0.075mm to 0.001mm. The hydrometer test is based upon the assumption that the soil grains will settle as individual according to the Stoke's Law. The velocity of a particle as it settles through a water column can be expressed as;

$$v = \frac{\Delta H}{\Delta T} \tag{4.4}$$

Where, v= velocity of particle, ΔH= change in particle altitude in a column of water, ΔT= time elapsed.

There are four possible sources of error that must be corrected for hydrometer analysis. One of them is that, the hydrometer is calibrated to be read at temperature of 20 ^{0}C, but it is not possible to do the test at this constant temperature. Second one is the deflocculating agent changes the specific gravity of the solution. Last one of the error sources is that the hydrometer is manufactured to be read at the bottom of the meniscus

and all readings must be made at the top of the meniscus during the test. There is a hydrometer composite correction factor (HCCF) to correct the errors that accounts for the differences in reading the meniscus at the top and for the variations in temperature and specific gravity. It will be explained in details in hydrometer test analysis section.

Before the hydrometer tests were done, specific gravity tests had been performed which will be explained in another section. Because specific gravity value of soil sample was needed to determine some constant that was essential for analysis of hydrometer test result.

The cylinder was set on the table and the time of the starting for reading was recorded, it was t=0. Hydrometer readings and the temperature of the slurry was recorded at the following intervals of elapsed time (ΔT); 1, 2, 5, 15, 30, 60, 120, 250, 1440 minute (Figure 4.4). For each hydrometer reading, temperature, and elapsed time were recorded on the data form (Table 4.4).

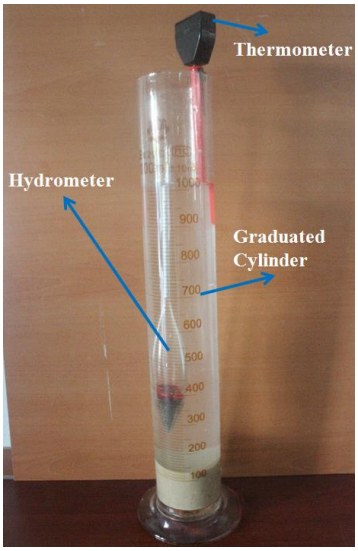

Figure 4. 4. Hydrometer reading setup with graduated cylinder, thermometer and hydrometer

Scope of the hydrometer test results analysis is to plot a grain size distribution for fines on the same graph as that used for the sieve analysis.

Analysis of hydrometer test results requires calculating some correction factors. First one is Hydrometer Composite Correction Factor (HCCF) which related with the error of reading. To determine HCCF values, a graphical method is used, this method was not explained in detail in this section. According to the knowledge about highest

and lower temperature and the hydrometer readings, HCCF was assumed as equal to 4. Second term which is related with specific gravity of the soil and temperature and known as K was needed to determine. Table 4.3 was used to determine the K value. The distance from the suspension surface to the depth which the density of the suspension had been measured, called L, also was needed. L values were determined according to the hydrometer readings and presented in Table 4.4.

Table 4.3. Values of K for hydrometer test analysis

Values of K	Specific Gravity of Soil								
Tempreature ^{0}C	2.45	2.50	2.55	2.60	2.65	2.70	2.75	2.80	2.85
16	0.01510	0.01505	0.01481	0.01457	0.01435	0.01414	0.01394	0.01374	0.01356
17	0.01511	0.01486	0.01462	0.01439	0.01407	0.01396	0.01376	0.01356	0.01338
18	0.01492	0.01467	0.01443	0.01421	0.01399	0.01378	0.01359	0.01339	0.01321
19	0.01474	0.01449	0.01425	0.01403	0.01382	0.01361	0.01342	0.01323	0.01305
20	0.01456	0.01431	0.01408	0.01386	0.01365	0.01344	0.01325	0.01307	0.01289
21	0.01438	0.01414	0.01391	0.01369	0.01348	0.01328	0.01309	0.01291	0.01273
22	0.01421	0.01397	0.01374	0.01353	0.01332	0.01312	0.01294	0.01276	0.01258
23	0.01404	0.01381	0.01358	0.01337	0.01317	0.01297	0.01279	0.01261	0.01243
24	0.01388	0.01365	0.01342	0.01321	0.01301	0.01282	0.01264	0.01246	0.01229
25	0.01372	0.01349	0.01327	0.01306	0.01286	0.01267	0.01249	0.01232	0.01215
26	0.01357	0.01334	0.01312	0.01291	0.01272	0.01253	0.01235	0.01218	0.01201
27	0.01342	0.01319	0.01297	0.01277	0.01258	0.01239	0.01221	0.01204	0.01188
28	0.01327	0.01304	0.01283	0.01264	0.01244	0.01255	0.01208	0.01191	0.01175
29	0.01312	0.0129	0.01269	0.01249	0.01230	0.01212	0.01195	0.01178	0.01162
30	0.01298	0.01276	0.01256	0.01236	0.01217	0.01199	0.01182	0.01165	0.01149

Table 4. 4. Values of L for hydrometer test analysis

Hydrometer Reading	L (cm)	Hydrometer Reading	L (cm)	Hydrometer Reading	L (cm)	Hydrometer Reading	L (cm)
0	16.3	16	13.7	32	11.1	48	8.4
1	16.1	17	13.5	33	10.9	49	8.3
2	16.0	18	13.3	34	10.7	50	8.1
3	15.8	19	13.2	35	10.6	51	7.9
4	15.6	20	13.0	36	10.4	52	7.8
5	15.5	21	12.9	37	10.2	53	7.6
6	15.3	22	12.7	38	10.1	54	7.4
7	15.2	23	12.5	39	9.9	55	7.3
8	15.0	24	12.4	40	9.7	56	7.1
9	14.8	25	12.2	41	9.6	57	7.0
10	14.7	26	12.0	42	9.4	58	6.8
11	14.5	27	11.9	43	9.2	59	6.6
12	14.3	28	11.7	44	9.1	60	6.5
13	14.2	29	11.5	45	8.9		
14	14.0	30	11.4	46	8.8		
15	13.8	31	11.2	47	8.6		

For the hydrometer test the grain size is given as follows;

$$D=K \times \sqrt{(L \times \Delta T)} \tag{4.5}$$

Where, D = particle diameter (mm), K= constant depending on suspension temperature and specific gravity of the soil, L= distance (cm) from the suspension surface to the depth at which the density of the suspension is being measured by hydrometer for that reading, ΔT= time intervals (minutes).

Also, Corrected Hydrometer Readings (R) must be determined by subtracting the HCCF from the hydrometer readings.

Table 4. 5. Values of a for hydrometer test analysis

Specific Gravity	Value of a
2.95	0.94
2.9	0.95
2.85	0.96
2.8	0.97
2.75	0.98
2.7	0.99
2.65	1.00
2.6	1.01
2.55	1.02
2.5	1.03
2.45	1.04

For calculating the Percent Finer for each particle diameter the following equation is used;

$$F = \frac{R \times a}{W} \times 100 \tag{4.6}$$

Where; F= Percent finer, R= corrected hydrometer reading, W= weight of soil sample, a = correction factor used for hydrometer analysis to account for the difference in the specific gravity of the soil. Correction factor “a” was presented in Table 4.5.

The values for hydrometer analysis includes elapsed time, temperature, hydrometer reading, corrected hydrometer reading, value of K, value of L, particle diameter and percent finer are respectively determined and recorded in data form as given Table 4.6.

Finally, according to the data form of hydrometer analysis, grain size distribution graph for fine grains was added to grain size distribution diagram of mechanical sieve analysis. This graph shows both particle diameter on the horizontal axis and the percent finer on the vertical axis. Figure 4.5 shows the grain size distribution graph according to the data taken from both mechanical sieve analysis and hydrometer analysis which belongs to soil sample named as SPT10 from test location SC16.

Hydrometer tests were conducted for 112 soil samples using by method which was explained below and standardized by ASTM as "ASTM- D422 Standard Test Method for Particle-Size Analysis of Soils".

Table 4. 6. Hydrometer test result data form for one of the soil samples

Sample No:	SC 16	**Sample No:**	SPT 10	**Depth (m):**	15.00-15.45	**Weight of Sample (gr)**	50
G_S	2.68	**HCFF**	4	**a**	0.98		

ΔT	**Tempeture**	**Hydrometer Reading**	**Corrected HR**	**K**	**L**	**Particle Diameter**	**Percent Finer**
Min	C	-	-	-	cm	mm	%
1	21	25	21	0.01344	12.9	0.04827	41.2
2	21	18.5	14.5	0.01344	13.9	0.03543	28.4
5	21	14	10	0.01344	14.7	0.02304	19.6
15	21	10.5	6.5	0.01344	15.3	0.01355	12.7
30	21	8.5	4.5	0.01344	15.6	0.00968	8.8
60	21	7.5	3.5	0.01344	15.7	0.00688	6.9
120	21	6	2	0.01344	16.0	0.00491	3.9
250	21	5.5	1.5	0.01344	16.1	0.00341	2.9
1440	21	4.5	0.5	0.01344	16.2	0.00143	1.0

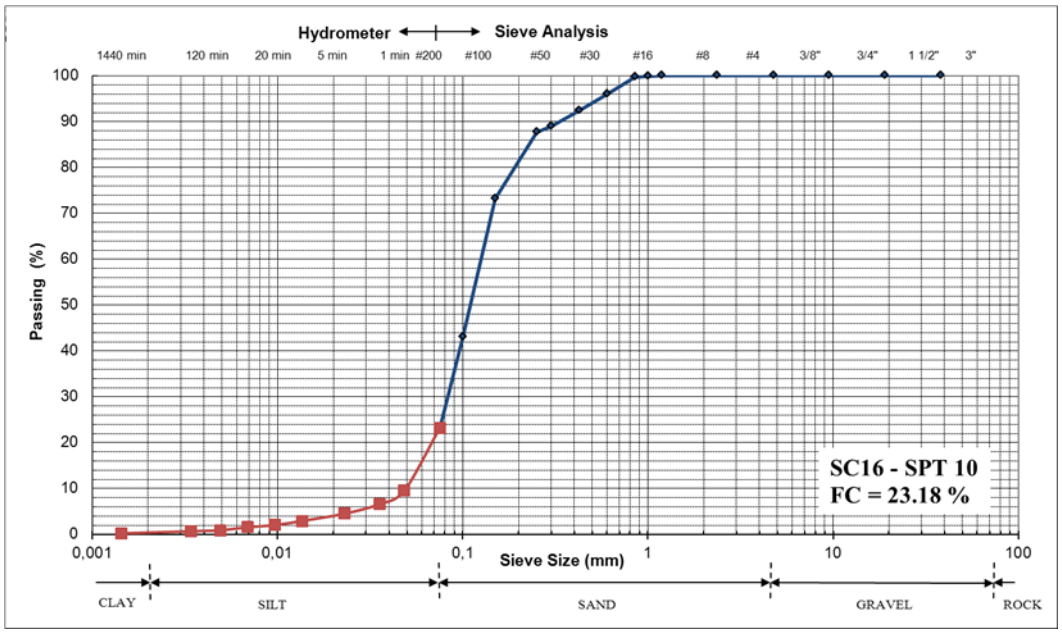

Figure 4.5. Grain size distribution of soil according to both sieve analysis and hydrometer analysis

Soil classification methods requires to determine some coefficient as uniformity coefficient (C_u) and coefficient of gradation (C_c) which were computed as follows;

$$C_u = \frac{D_{60}}{D_{10}} \tag{4.7}$$

$$C_c = \frac{(D_{30})^2}{D_{60} \text{ x } D_{10}} \tag{4.8}$$

Where, D_{10} is the diameter through which 10% of the total soil mass has passed also named as effective size, D_{30} is diameter through which 30% of the total soil mass has passed and D_{60} is diameter through which 60% of the total soil mass has passed.

$D_{10,}$ D_{30} and D_{60} values were found by entering the grain size chart at the 10% finer line, following the line horizontally to its intersection with the grain size distribution curve, then reading the grain size directly from the horizontal axis of the chart. Then, uniformity coefficient (C_u) and coefficient of gradation (C_c) values were determined for each sample and recorded to use for soil classification that described section 4.3.

4.3.2. Atterberg Limits Tests

In the early part of the twentieth century a Swedish agriculturist named Atterberg devised a method for classifying and describing the properties of cohesive soils, based on their moisture content. Several types of limits include the liquid limit, and the plastic limits were presented by Atterberg in this method. The liquid limit and the plastic limit tests are always performed together to yield another indicator about the soil referred to as the plasticity index (PI). Plasticity index is calculated by subtracting the plastic limit from liquid limit. It is important to note that both tests are conducted only on material passing the #40 sieve. Liquid limit test and plastic limit test procedures are standardized by ASTM as "ASTM- D4318 Standard Test Methods for Liquid Limit, Plastic Limit, and Plasticity Index of Soils".

4.3.2.1. Liquid Limit Test

The sample was placed into a pan and mixed with enough water to create slurry, then poured the slurry through the #40 sieve and allowed the slurry to pass the sieve. The consistency of soil sample was checked and added water as needed in 1 ml to 5ml increments to adjust the moisture content. The test was started with the lowest moisture content and used successively higher moisture contents for each trial. A portion of soil was placed on the brass cup of the liquid limit device and leveled using by spatula. A clean sharp groove which extended through the center line of the cup was formed using the grooving tool. The cup was lifted and dropped at the rate of about two drops per second using the hand crack. This motion (lifting and dropping) is named as blow. It was continued creating (continue to create) the blows until the soil came together enough to close the groove for a length of 1 mm (Figure 4.7). The number of blows was recorded. A portion of soil sample was removed from the brass cup and weighted to determine the moisture content. A soil sample was prepared again adding additional water which allows to soil to close the groove on the next trial with fewer blows. All of these steps were repeated for a minimum total of three trials. A graph was plotted using by the moisture content and blows count for each trial. The numbers of blows were plotted on the horizontal axis with logarithmic scale and moisture contents were plotted on the vertical axis with arithmetic scale (Figure 4.6). A line which is referred to as the

flow curve was drawn through the points plotted in step 10 (Figure 4.6). Figure 4.6 shows an example of the flow curve for sample “SC16-SPT10”.

A line extended vertically upward from the 25 blows point on the horizontal axis to intersect with the flow curve and then another line was extended from this intersection point horizontally to the vertical axis. At the point of intersection with the vertical axis is defined as the liquid limit

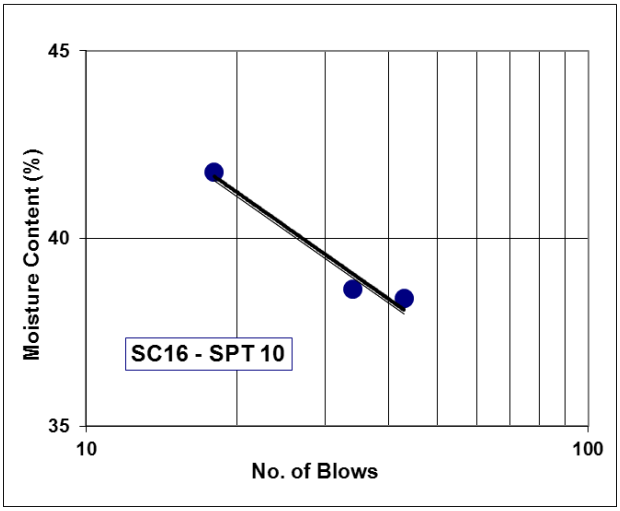

Figure 4.6. An example of flow curve to define the liquid limit

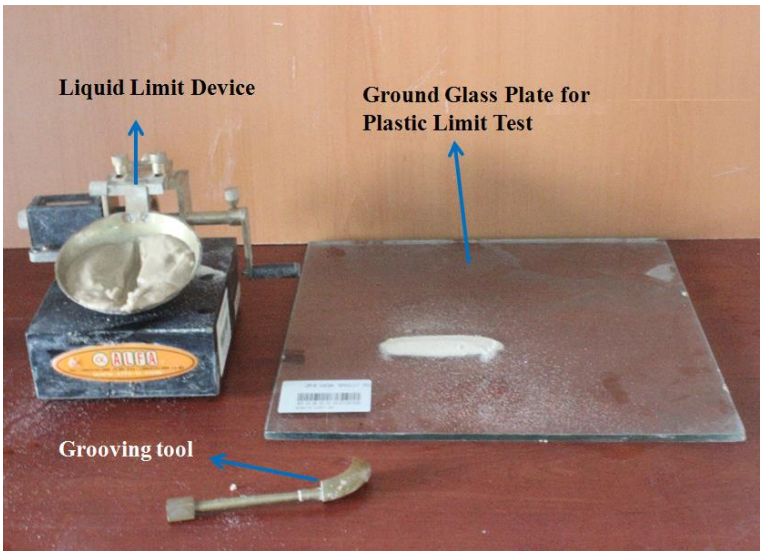

Figure 4.7. Setup including liquid limit device and tool, ground glass plate for plastic limit test

4.3.2.2. **Plastic Limit Test**

About 20 grams of soil sample was removed from liquid limit test preparation cup and its moisture content was increased gradually mixing thoroughly between additions of water until the soil was easy to shape into a ball. After the soil sample was formed into a small ball, it was placed on the ground glass plate and rolled using hand with a moving parallel to the plate. Rolling was being continued until the tread had a diameter of 3mm. It is known that if the tread breaks before it becomes 3 mm diameter it is at moisture content below the plastic limit, if the thread rolls out to a diameter smaller than 3 mm without any cracking it is at a moisture content higher than the plastic limit. According to this knowledge step 2 and 3 was repeated until the soil was at a moisture content such that it began cracking while it was rolled into a 3 mm diameter thread. Moisture content determination was performed for the sample at the plastic limit and the moisture content value was recorded as plastic limit.

For all soil samples, the liquid limit and the plastic limit tests were performed and recorded. Also for each sample Plasticity Index was calculated as follows and recorded;

$$PI = LL - PL \tag{4.9}$$

Where, PI is Plasticity index, LL is liquid limit and PL is plastic limit of soil.

4.3.3. Specific Gravity Test

The ASTM D854 standard test method was used to determine the specific gravity. This method proposes to use pycnometer and desicator to perform the test

The pycnometer was filled with distilled water and weighted; the weigh was recorded as weight of pycnometer with water (W_{WP}). Weight of the empty pycnometer was recorded as pycnometer tare (W_P). About 10 grams of soil portion was taken from the sample passed through sieve #4 which had been dried before and the weight was recorded as dry soil sample weight (W_S). 10 grams soil sample was poured into 100ml pycnometer using by pycnometer filling tube. Then, the pycnometer was filled with distilled water up to 1/3 height. For each sample three pycnometers were prepared as

mentioned in first two step and the pycnometers were placed into the dessicator to take the entrapped air out. Vacuum pomp was connected to desiccator and pycnometers filling with slurry were vacuumed. During the vacuum, bubbling was seen inside the slurry. The pycnometers had been exposed to vacuum until bubbling was stopped, at least 2 hours. After pycnometers were taken from dessicator, they were filled with distilled water and weighted again and the weight was recorded as pycnometer weight filled with soil and water (W_{SWP}). Temperature of distilled water and all weight data were recorded in data form as shown in Table 4.7

Figure 4.8. Specific gravity test setup including vacuum pump, pycnometers

Then specific gravity was computed as follows;

$$G_S = \frac{k \times W_S}{W_S + (W_{SWP} - W_{WP})} \tag{4.10}$$

Where; G_S = specific gravity of soil, W_{WP} = weight of pycnometer with water, W_S = weight of dry soil sample, W_{SWP} = pycnometer weight filled with soil and water, k = temperature coefficient for water that taken from ASTM standard.

Table 4.7. Specific gravity test data form for soil sample SC16-SPT10

Water Temperature 25,4		k 0,9971					
Sample No.	Test No.	Volume of Pycnometer	Weight of Dry Sample (W_S)	Weight of Pycnometer + Water+Sample (W_{SPW})	Weight of Pycnometer + Water (W_{PW})	Specific Gravity G_s	Avarage Specific Gravity G_s
#	#	ml	gr	gr	gr	gr/cm^3	%
SC16-SPT10	1	100	10,00	129,695	123,400	2,691	2,68
	2	100	10,00	138,680	132,500	2,610	
	3	100	10,00	129,755	123,400	2,736	

Specific gravity tests were performed three times for each soil sample, calculating by average of these three tests result, G_S values for each sample were recorded and given in laboratory test summary table.

4.3.4. Maximum and Minimum Void Ratio Test

The ASTM D 4253 standard test method was used to determine the maximum void ratio. The ASTM D 4254 standard test method was used to determine the minimum void ratio.

Before starting to perform the test, the interior diameter (d) and the height (h) of the mold were measured, the volume of the mold (V_m) was calculated and the mold was weighted, (M_m). The oven dried specimen was mixed in a spout to provide an even distribution of particle sizes. The soil was filled into the mold with loose sand spiraling motion to minimize segregation. A pouring funnel was used to pour the soil from spout into mold as loosely as possible, holding the poring funnel vertical. Height of the spout was adjusted to maintain a free fall of the soil of about 13 mm. The pouring funnel was moved in a spiral path on mold to form each layer of nearly uniform thickness. The mold filled approximately to 25 mm above the top of the mold and excess soil level was trimmed off using leveling tool. Mold full with soil was weighted and recorded.

All data taken from the test such as volume of the soil, weight of the dry loose soil were recorded as shown in Table 4.8. Firstly, minimum dry index density of soil was calculated using formula given below;

$$\rho_{dmin} = \frac{M_S}{V_s} \tag{4.11}$$

Where; ρ_{dmin} = minimum index density, M_S = mass of the tested dry soil, V_S = volume of the tested dry soil.

Maximum void ratio of soil was calculated as follows;

$$e_{max} = \frac{\rho_W x G_S}{\rho_{dmin}} \tag{4.12}$$

Where; e_{max} = maximum void ratio of soil, ρ_W = density of water (1 g/cm^3), G_S = specific gravity, ρ_{dmin} = minimum index density.

ASTM standard requires that minimum void ratio test can be done just after maximum void ratio test using same mold filled with soil. According to this knowledge for each sample maximum and minimum void ratio tests were conducted respectively.

Also, ASTM test standard requires that, for special mold, the total mass of the surcharge base plate and surcharge weight should be equivalent to a surcharge stress of 13.8 kPa. For creating the standard stress, the surcharge base area of mold was calculated as 81.71 cm^2. A surcharge weight of 8.79 kg was created which gives a weight of 11.26 kg with surcharge base plate to be equal equivalent to a surcharge stress of 0.138 kg/cm^2 on the mold surface.

The surcharge weight was placed on the mold and twisted slightly to make it in contact with the surface of the soil. The mold was attached to the vibrating table. Mold assembly and specimen were vibrated for 8 min. The weight and surcharge base plate were removed and mold was detached from vibration table. The volume of the soil was measured after vibration and also the weight of the soil was checked again. All data were recorded in data form. (Table 4.8)

Figure 4.9. Mold and weight placed on vibrating table

Firstly, maximum dry index density of soil was calculated to determine the minimum void ratio using formula given below;

$$\rho_{dmax} = \frac{M_S}{V_{s(av)}} \tag{4.11}$$

Where; ρ_{dmax} = maximum dry index density, M_S = mass of the tested dry soil, $V_{S(av)}$ = volume of the tested dry soil after vibration.

Minimum void ratio of soil was calculated as follows;

$$e_{min} = \frac{\rho_W x G_S}{\rho_{dmax}} - 1 \tag{4.12}$$

Where; e_{min} = minimum void ratio of soil, ρ_W = density of water (1 g/cm^3), G_S = specific gravity, ρ_{dmax} = maximum index density.

Maximum and minimum void ratio tests were conducted for all samples and e_{max} and e_{min} values were recorded as shown in Table 4.8. For all samples, maximum and minimum void ratio values were given in laboratory test summary table (Table 4.10)

Table 4.8. An example of data form for maximum and minimum void ratio for soil sample SC16-SPT10

Location Name	Sample Name	Specific Gravity Gs	Mold Tare	Mold Volume	Soil Volume	Weight of Loose Soil + Mold (Dry)	Weight of Dry Loose Soil	$\rho_{dry-min}$	e_{max}	Soil Volume After Compaction	$\rho_{dry-max}$	e_{min}
#	#		gr	cm^3	cm^3	gr	gr	gr/cm^3	-	cm^3	gr/cm^3	-
SC16	SPT10	2,68	4204,0	1372,8	416,7	4614,6	410,6	0,99	1,72	294,17	1,40	0,92

4.4. **Soil Classification According to the USGS**

According to the laboratoary studies which includes a serial of tests; sieve analysis and hydrometer tests, Atterberg limits tests, specific gravity tests, maximum and minimum void ratio tests, each sample of soil type was determined. To classify the soil type, Unified Soil Classification System (USCS) was used and the soil types of samples were recorded with their symbols. The soil type symbols of USCS were given in Table 4.9 with their definitions.

Table 4.9. Soil classification type symbols and describitions in the USCS

Soil Type Symbol	Soil Type Definition
GW	well-graded gravel, fine to coarse gravel
GP	poorly graded gravel
GM	silty gravel
GC	clayey gravel
SW	well-graded sand, fine to coarse sand
SP	poorly graded sand
SM	silty sand
SC	clayey sand
ML	silt
CL	clay of low plasticity, lean clay
OL	organic silt, organic clay
MH	silt of high plasticity, elastic silt
CH	clay of high plasticity, fat clay
OH	organic clay, organic silt
Pt	peat

For all samples, all data obtained from laboratuary studies were given in laboratoary test summary table in Table 4.10. Table 4.10 shows in detail sample name, sample depth, soil classification, D_{50}, C_u, C_c values, liquit limit and plastic limit, grain size percentage, specific gravity, maximum and minimum void ratio for each sample.

Table 4.10. Laboratory test results summary sheet

LABORATORY TEST SUMMARY SHEET

Boring Number	Sample Number	Depth	Classification (Method: USGS)	D_{50}	C_u	C_c	Atterberg Limits			Grain Size			Hydrometer		Gs Specific Gravity	e_{max} (Dry)	e_{min} (Dry)
							Liquid Limit	Plastic Limit	PI	Gravel	Sand	FC	Silt	Clay			
-	-	m					(%)	(%)	(%)	(%)	(%)	(%)	(%)	(%)	-	-	-
SC1	SPT1	1,50 - 1,95	SW	1,00	14,17	1,23	27,7	NP	NP	17,2	**79,0**	3,8	-	-	2,64	-	-
	SPT2	3,00 - 3,45	SP-SM	0,35	6,40	0,90	29,8	25,5	4,3	0,9	**88,4**	10,7	-	-	2,50	1,17	0,86
	SPT3	4,50 - 4,95	SM	0,17	-	-	39,6	27,5	12,1	0,0	**78,8**	21,2	-	-	2,52	1,42	1,04
	SPT4	6,00 - 6,45	SP-SM	0,76	10,67	0,77	NP	NP	NP	23,0	**71,9**	5,1	-	-	2,50	0,70	0,54
	SPT5	7,50 - 7,95	SP	5,00	50,00	0,86	21,7	NP	NP	47,0	**49,7**	3,3	-	-	-	-	-
	SPT6	9,00 - 9,45	SP	0,35	2,87	0,97	NP	NP	NP	0,2	**96,6**	3,2	-	-	2,54	0,93	0,72
	SPT7	10,50 - 10,95	SP	1,80	18,67	0,62	22,2	NP	NP	25,3	**70,1**	4,5	-	-	-	0,78	0,48
	SPT8	12,00 - 12,45	SM	0,22	-	-	39,6	29,3	10,3	0,3	**84,0**	15,7	-	-	2,58	1,78	1,13
	SPT9	13,50 - 13,95	SM	0,11	-	-	47,1	26,6	20,5	0,0	**70,5**	29,5	-	-	2,52	1,85	1,08
	SPT10	15,00 - 15,45	SM	0,24	-	-	53,4	38,5	14,9	0,0	**82,5**	17,5	-	-	2,65	2,67	1,65
SC2	SPT1	1,50 - 1,95	SW	0,79	12,00	1,61	12,7	NP	NP	10,1	**85,6**	4,4	-	-	2,53	0,75	0,88
	SPT2	3,00 - 3,45	SM	0,55	8,88	0,89	20,0	NP	NP	10,8	**82,0**	7,3	-	-	2,57	-	-
	UD1	4.50	SM	-	-	-	37,7	26,4	11,3	0,0	**75,2**	24,8	21,1	3,7	2,48	-	-
	SPT3	6,00 - 6,45	SP	0,90	9,00	0,69	20,4	NP	NP	27,0	**69,8**	3,3	-	-	2,62	-	-
	SPT4	9,00 - 9,45	SM	0,44	4,40	0,91	16,4	NP	NP	8,7	**85,9**	5,4	-	-	2,75	-	0,79
	SPT5	10,50 - 10,95	SP	0,27	2,38	0,99	NP	NP	NP	0,0	**96,9**	3,1	-	-	-	1,09	0,85
	SPT6	11,00 - 11,45	SP	0,34	3,36	1,10	NP	NP	NP	0,0	**95,7**	4,3	-	-	2,63	1,07	0,75
	SPT7	15,00 - 15,45	SP	0,54	3,75	1,67	NP	NP	NP	3,0	**92,8**	4,2	-	-	2,75	0,92	0,78
SC3	SPT1	3,00 - 3,45	SW-SM-SC	0,79	12,00	1,69	24,4	19,8	4,6	10,9	**79,7**	9,4	-	-	2,56	1,90	0,73
	SPT2	4,50 - 4,95	SP-SM	0,49	9,33	0,76	26,5	25,0	1,5	12,8	**77,5**	9,6	-	-	2,46	-	-
	SPT3	6,00 - 6,45	No Sample	-	-	-	-	-	-	-	-	-	-	-	-	-	-
	SPT4	7,50 - 7,95	SC	0,30	-	-	28,5	21,1	7,4	7,9	**72,0**	20,1	18,9	1,2	2,57	1,23	0,93
	SPT5	9,50 - 9,95	SP-SC	0,23	4,71	0,85	33,0	20,0	12,9	0,0	**88,1**	11,9	-	-	2,44	2,00	0,89
	UD1	10.50	SC	-	-	-	43,3	24,5	18,8	0,0	**60,4**	39,6	34,1	5,5	2,45	-	
	SPT6	13,00 - 13,45	SC	0,23	-	-	47,8	26,6	21,3	0,0	**73,8**	26,2	22,2	3,9	2,54	4,02	1,38
	SPT7	16,50 - 16,95	SC	0,12	-	-	48,3	27,1	21,2	0,0	**76,5**	23,5	20,7	2,8	2,51	3,82	1,20
	UD2	18.00	SM	-	-	-	42,5	35,5	7,0	0,0	**60,4**	39,6	34,5	5,2	2,45	-	-
SC4	SPT1	1,50 - 1,95	SP-SC	0,40	6,50	0,87	40,9	23,3	17,7	4,0	**87,4**	8,5	-	-	2,51	1,27	0,92
	SPT2	3,00 - 3,45	SC	0,26	-	-	30,9	22,2	8,7	0,8	**80,1**	19,1	18,0	1,1	2,53		1,10
	UD1	4.50	SM	-	-	-	30,9	28,9	2,0	9,4	**62,4**	28,2	23,4	4,8	2,39	1,70	-
	SPT3	6,00 - 6,45	SC	0,16	-	-	29,7	20,5	9,2	0,0	**81,0**	19,0	-	-	2,70	1,35	0,91
	SPT4	7,50 - 7,95	SP-SM	0,17	2,38	0,95	NP	NP	NP	0,0	**93,5**	6,5	-	-	2,60	1,02	0,69
	SPT5	9,00 - 9,45	SP-SM	0,24	2,95	1,29	NP	NP	NP	0,0	**93,9**	6,1	-	-	2,60	0,80	0,67
	SPT6	11,00 - 11,45	SP-SM	0,17	2,38	1,03	NP	NP	NP	0,0	**93,5**	6,5	-	-	2,55	0,79	0,68
	SPT7	12,50 - 12,95	SM	0,18	-	-	54,7	29,5	25,2	0,0	**80,0**	20,0	-	-	2,61	2,13	1,26
	UD2	13.50	SM	-	-	-	45,9	30,3	15,6	0,0	**61,5**	38,5	33,9	4,6	2,61		-
	SPT8	15,00 - 15,45	SC	0,23	-	-	29,9	17,6	12,2	0,0	**85,4**	14,6	13,3	1,3	2,66	1,47	0,93
SC5	SPT1	1,50 - 1,95	SC	0,21	-	-	66,9	26,9	39,9	0,0	**78,6**	21,4	13,3	8,1	2,46	1,03	0,76
	SPT2	3,00 - 3,45	No Sample	-	-	-	-	-	-	-	-	-	-	-	-	-	-
	SPT3	4,50 - 4,95	SC	0,17	-	-	49,3	20,5	28,8	0,0	**75,1**	24,9	22,1	2,7	2,61	2,68	1,55
	UD1	6.00	SM	-	-	-	39,9	31,0	8,9	0,0	**58,0**	42,0	36,1	5,9	2,59	-	-
	SPT4	8,00 - 8,45	SC	0,14	-	-	28,3	20,4	7,8	0,0	**73,8**	26,2	23,6	2,6	2,57	2,16	1,29
	SPT5	9,00 - 9,45	SC	0,15	-	-	47,6	25,0	22,6	0,0	**73,3**	26,7	22,9	3,7	2,63	2,09	1,12
	SPT6	10,50 - 10,95	SM	0,10	-	-	23,0	NP	NP	0,0	**79,2**	20,8	20,6	0,2	2,73	-	-
	SPT7	12,50 - 12,95	SP	0,14	1,88	0,83	NP	NP	NP	1,3	**93,9**	4,8	-	-	2,73	-	-
	SPT8	13,50 - 13,95	SM	0,16	-	-	49,8	30,7	19,0	0,0	**81,0**	19,0	17,2	1,8	2,64	2,85	1,53
	SPT9	15,00 - 15,95	SC	0,12	-	-	53,4	24,5	29,0	0,0	**67,6**	32,4	31,4	1,0	2,61	2,35	1,42
SC6	SPT1	1,50 - 1,95	SM	0,09	-	-	26,7	23,0	3,7	0,0	**61,7**	38,3	37,3	1,0	2,75	1,71	1,09
	SPT2	3,00 - 3,45	SC	0,18	-	-	27,8	18,8	9,1	0,0	**82,7**	17,3	15,1	2,3	2,65	1,10	0,72
	SPT3	4,50 - 4,95	SM-SC	0,18	-	-	23,0	16,5	6,4	0,0	**84,3**	15,7	13,7	2,0	2,62	0,90	0,72
	Sample 1	6,00	SP-SC	0,27	3,90	1,33	35,2	23,7	11,5	0,3	**90,4**	9,4	-	-	2,57	2,09	1,29
	SPT4	7,50 - 7,95	SP	0,28	1,94	0,98	NP	NP	NP	0,2	**96,0**	3,9	-	-	2,81	1,05	0,86
	SPT5	9,00 - 9,45	SP	0,18	2,47	0,97	NP	NP	NP	0,0	**97,1**	2,9	-	-	-	1,02	0,72
	SPT6	10,50 - 10,95	SP	0,20	1,52	1,02	NP	NP	NP	0,0	**97,4**	2,6	-	-	2,69	-	0,78
	SPT7	12,00 - 12,45	SC	0,12	-	-	35,7	23,1	12,6	0,0	**61,1**	38,9	35,0	3,9	2,57	1,79	1,13
	UD1	14.00	SM	-	-	-	40,1	29,7	10,4	0,0	**56,9**	43,1	39,2	3,9	2,63	-	-
	SPT8	15,00 - 15,45	SM	0,15	-	-	46,5	30,5	15,9	0,0	**70,3**	29,7	-	-	2,52	2,21	1,12
SC7	SPT1	1,50 - 1,95	No Sample	-	-	-	-	-	-	-	-	-	-	-	-	-	-
	SPT2	3,00 - 3,45	SC	0,10	-	-	27,7	19,5	8,2	0,0	**61,9**	38,1	35,4	2,7	2,60	1,67	1,00
	SPT3	4,50 - 4,95	SC	0,12	-	-	37,3	24,0	13,3	0,4	**69,0**	30,6	27,2	3,4	2,68	2,01	1,22
	SPT4	6,50 - 6,95	SP-SM	0,28	5,67	1,13	NP	NP	NP	23,5	**66,2**	10,2	-	-	2,65	1,22	0,77
	SPT5	8,00 - 8,45	SP-SM	0,14	1,92	0,85	NP	NP	NP	9,4	**83,6**	7,1	-	-	2,63	1,02	0,77
	SPT6	9,00 - 9,45	SP-SM	0,20	0,33	0,08	NP	NP	NP	11,9	**79,2**	8,9	-	-	2,63	0,97	0,56
	SPT7	10,50 - 10,95	No Sample	-	-	-	-	-	-	-	-	-	-	-	-	-	-
	SPT8	12,00 - 12,45	SP	0,40	4,82	0,69	NP	NP	NP	0,0	**96,6**	3,4	-	-	2,64	1,11	0,71
	SPT9	13,50 - 13,95	No Sample	-	-	-	-	-	-	-	-	-	-	-	-	-	-
	SPT10	15,00 - 15,45	SP-SC	0,51	6,87	3,05	29,2	19,4	9,8	0,0	**91,0**	9,0	-	-	2,64	1,35	0,73

(Cont. on next page)

Table 4.10. (cont.)

LABORATORY TEST SUMMARY SHEET (cont.)

Boring Number	Sample Number	Depth	Classification (Method: USGS)	D_{50}	C_u	C_c	Atterberg Limits			Grain Size			Hydrometer		Gs Specific Gravity		
							Liquid Limit	Plastic Limit	PI	Gravel	Sand	FC	Silt	Clay		e_{max} (Dry)	e_{min} (Dry)
-	-	m					(%)	(%)	(%)	(%)	(%)	(%)	(%)	(%)	-	-	-
SC8	SPT1	3,00 - 3,45	SC	0,10	-	-	43,5	22,4	21,1	0,0	**59,7**	40,3	36,3	4,0	2,57	1,80	1,04
	SPT2	4,50 - 4,95	SC	0,08	-	-	29,0	21,8	7,2	0,0	**52,0**	48,0	47,1	1,0	2,65	2,07	1,18
	SPT3	6,00 - 6,45	SC	0,14	-	-	38,0	21,8	16,3	0,0	**75,3**	24,7	22,0	2,7	2,59	2,31	1,29
	UD1	7.50	SM	-	-	-	31,7	29,7	2,0	0,0	**60,5**	39,5	37,1	2,4	2,62	-	-
	SPT4	9,00 - 9,45	SM	0,82	-	-	27,8	NP	NP	0,0	**54,5**	45,5	42,3	3,2	2,56	2,14	1,32
	SPT5	10,50 - 10,95	SC	0,90	-	-	31,7	20,8	11,0	0,0	**59,5**	40,5	38,0	2,4	2,66	2,07	1,35
	SPT6	12,00 - 12,45	SM	0,16	-	-	NP	NP	NP	0,0	**87,7**	12,3	-	-	2,68	1,41	0,99
	SPT7	13,50 - 13,95	SP-SM	0,19	2,35	1,32	NP	NP	NP	0,0	**94,4**	5,6	-	-	2,77	1,13	0,86
	SPT8	15,00 - 15,45	SP-SM	0,14	2,05	0,80	NP	NP	NP	0,0	**93,2**	6,8	-	-	2,65	1,53	0,89
SC9	SPT1	1,5 - 1,95	ML	-	-	-	37,7	31,3	6,5	0,0	32,9	**67,1**	62,4	4,7	2,72	3,27	1,70
	UD1	3.00	ML	-	-	-	31,2	27,2	4,0	0,0	44,1	**55,9**	53,1	2,8	2,60	-	
	SPT2	4,5 - 4,95	SM-SC	0,08	-	-	26,1	19,2	6,9	0,0	**53,6**	49,4	46,7	2,7	2,61	1,41	0,94
	SPT3	6,0 - 6,45	SC	0,10	-	-	28,1	20,4	7,7	0,0	**67,7**	32,3	30,0	2,3	2,55	1,88	1,12
	SPT4	7,5 -7,95	SM	0,14	-	-	39,5	27,7	11,8	0,0	**73,2**	26,8	21,4	5,4	2,65	1,85	1,27
	SPT5	9,0 - 9,45	SM	0,10	-	-	22,0	NP	NP	0,0	**79,2**	20,8	18,1	2,7	2,62	2,17	1,30
	SPT6	10,5 - 10,95	SM-SC	0,09	-	-	27,7	21,8	5,9	0,0	**64,4**	35,6	32,4	3,2	2,59	2,03	1,25
	SPT7	12,0 - 12,45	SM	0,85	-	-	38,6	29,0	9,5	0,0	**54,7**	45,3	41,3	4,1	-	2,94	1,57
	UD2	13.50	SM	-	-	-	NP	NP	NP	0,0	**78,6**	21,4	-	-	2,64	-	
	SPT8	15,0 - 15,45	SM	0,80	-	-	31,5	27,4	4,2	0,0	**53,6**	46,4	43,6	2,8	2,60	1,64	0,96
SC10	SPT1	1,5 - 1,95	SC	0,15	-	-	36,9	17,4	19,6	0,5	**72,9**	26,6	24,5	2,1	2,59	1,83	1,02
	SPT2	3,0 - 3,45	SM	0,10	-	-	45,7	28,5	17,3	0,0	**60,6**	39,4	33,9	5,5	2,55	2,19	1,11
	UD1	4.50	SM	-	-	-	57,5	37,4	20,1	0,0	**76,7**	23,3	19,8	3,5	2,55	-	
	SPT3	6,0 - 6,45	SM	0,11	-	-	39,0	29,0	10,0	0,0	**62,9**	37,1	32,6	4,4	2,69	2,21	1,32
	SPT4	7,5 - 7,95	SM	0,76	-	-	38,7	25,8	12,9	0,0	**51,0**	49,0	47,0	2,0	2,47	2,48	1,29
	SPT5	9,0 - 9,45	SM	0,13	-	-	NP	NP	NP	0,0	**79,7**	20,3	-	-	2,54	1,42	0,87
	SPT6	10,5 - 10,95	SM	0,15	2,08	0,81	NP	NP	NP	0,0	**90,4**	9,6	-	-	-	1,23	0,90
	Sample 1	12,0	SM	0,14	-	-	46,5	29,1	17,4	0,0	**70,1**	29,9	23,7	6,1	2,53	2,01	1,12
	SPT7	13,0 - 13,45	SM	0,15	-	-	45,6	27,0	18,6	0,0	**86,6**	13,4	-	-	-	3,31	1,75
	SPT8	15,0 - 15,45	SM	0,19	-	-	42,5	33,8	8,7	0,0	**85,8**	14,2	-	-	2,46	2,56	1,43
SC11	Sample 1	1.00 - 1.50	SM	0,17	5,83	0,43	41,4	26,9	14,5	0,0	**80,9**	19,1	17,75	1,38	2,74	1,77	1,05
	SPT1	1,50 - 1,95	SC	0,15	2,77	0,85	30,3	20,7	9,6	0,0	**84,44**	15,56	15,21	0,34	2,68	2,07	1,31
	Sample 2	2,50 - 3,00	SM	0,18	4,84	0,54	44,1	30,2	13,9	0,0	**84,37**	15,6	14,66	0,97	2,72	1,60	0,99
	SPT2	3,00 - 3,45	SM	0,11	2,17	0,93	28,3	NP	NP	0,0	**71,9**	22,1	0,97	0,97	2,64	1,85	1,28
	Sample3	4,00 - 4,50	SP - SM	0,21	3,56	0,68	NP	NP	NP	0,0	**94,0**	6,0	21,68	0,32	2,63	1,99	1,23
	SPT3	4,50 - 4,95	SM	0,10	2,18	1,09	NP	NP	NP	0,0	**76,8**	23,3	23,17	0,09	2,70	1,69	1,16
	Sample 4	5,50 - 6,00	SM	0,11	2,00	1,13	24,7	NP	NP	0,0	**79,6**	20,4	20,11	0,31	2,81	2,08	1,18
	SPT4	6,00 - 6,45	SP - SM	0,13	1,63	1,06	NP	NP	NP	0,0	**91,9**	8,1	-	-	2,69	1,64	0,82
	SPT5	7,50 - 7,95	SM-SC	0,13	3,33	0,68	29,0	24,4	4,6	0,0	**79,8**	20,2	18,89	1,32	2,65	1,80	1,28
	SPT6	9,00 - 9,45	SP - SM	0,18	2,50	0,76	29,8	23,7	6,1	0,0	**91,4**	8,6	8,09	0,47	2,68	1,46	1,04
	Sample 5	10,00 - 10,50	SP - SM-SC	0,21	2,3	1,43	21,8	16,6	5,2	0,0	**93,7**	6,3	6,07	0,26	2,82	1,57	0,60
	SPT7	10.50 - 10.95	SP-SM	0,21	2,3	1,41	NP	NP	NP	0,0	**93,6**	6,4	-	-	2,73	1,33	0,52
	Sample 6	11,50 - 12,00	SP	0,19	2	1,45	22,1	15,4	6,7	0,0	**96,1**	3,9	-	-	2,74	1,44	0,71
	SPT8	12.00 -12,45	SP-SM	0,19	2,50	1,41	NP	NP	NP	0,0	**91,7**	8,3	-	-	2,77	3,18	1,09
	Sample 7	13,00 - 13,50	SP-SC	0,17	2,32	0,72	14,8	14,6	SC	0,0	**93,3**	6,7	-	-	2,74	1,34	0,47
	SPT9	13,50 -13,95	SP- SM	0,17	2,71	1,08	NP	NP	NP	0,0	**88,1**	11,9	11,82	0,07	2,79	1,24	0,87
	Sample 8	14,50 - 15,00	SM	0,11	2,06	0,99	NP	NP	NP	0,0	**82,2**	17,9	16,71	1,14	2,76	1,95	1,08
	SPT10	15,00 - 15,45	SP-SM	0,19	2,80	0,70	NP	NP	NP	0,0	**90,2**	9,8	-	-	2,69	1,27	0,69
SC12	Sample 1	1.00 - 1.50	SM	0,12	1,73	1,03	NP	NP	NP	0,0	**87,7**	12,3	11,75	0,55	2,81	2,06	1,22
	SPT1	1,50 - 1,95	SP-SM	0,14	2,27	0,95	NP	NP	NP	0,0	**88,8**	11,2	10,97	0,19	2,72	1,78	1,23
	Sample 2	2,50 - 3,00	CH	0,08	-	-	54,3	30,2	24,1	0,0	48,7	**51,3**	46,40	4,89	2,37	2,10	1,10
	SPT2	3,00 - 3,45	SP	0,22	2,5	1	NP	NP	NP	0,0	**96,9**	3,1	-	-	2,73	1,07	0,55
	Sample3	4,00 - 4,50	SP-SM	0,22	2,73	1,09	NP	NP	NP	0,0	**94,2**	5,8	-	-	2,74	1,32	0,69
	SPT3	4,50 - 4,95	SP	0,22	2,31	0,93	NP	NP	NP	0,0	**96,4**	3,6	-	-	2,69	1,11	0,62
	SPT4	6,00 - 6,45	No Sample	-	-	-	-	-	-	-	-	-	-	-	-	-	-
	SPT5	7,50 - 7,95	SP- SM	0,20	2,33	1,04	NP	NP	NP	0,0	**92,3**	7,7	-	-	2,74	1,11	0,63
	Sample 4	8,50 - 9,00	SP	0,20	2	1,47	NP	NP	NP	0,8	**95,3**	3,9	-	-	2,74	1,25	0,93
	SPT6	9,00 - 9,45	No Sample	-	-	-	-	-	-	-	-	-	-	-	-	-	-
	SPT7	10.50 - 10.95	SP- SM	0,12	1,87	1,05	NP	NP	NP	0,0	**89,7**	10,3	10,11	0,23	2,77	1,43	1,11
	SPT8	12.00 -12,45	No Sample	-	-	-	-	-	-	-	-	-			-	-	-
	SPT9	13,50 -13,95	SM	0,19	-	-	NP	NP	NP	0,0	**82,2**	17,8	16,09	1,74	2,78	1,84	1,35
	SPT10	15,00 - 15,45	SP- SM	0,13	1,88	0,92	NP	NP	NP	0,0	**92,0**	8,0	-	-	2,74	1,13	0,77
SC13	Sample 1	1.00 - 1.50	SP- SC	0,17	2,5	0,76	41,4	27,6	13,8	0,0	**91,6**	8,4	-	-	2,67	2,13	1,15
	SPT1	1,50 - 1,95	SM	0,10	-	-	25,6	25,0	0,6	0,0	**68,3**	31,7	29,13	2,60	2,68	1,90	0,61
	Sample 2	2,50 - 3,00	SP- SC	0,23	4,82	0,59	40,0	31,8	8,2	0,0	**92,1**	7,9	-	-	2,68	2,05	1,17
	SPT2	3,00 - 3,45	SC	0,11	2,31	0,83	40,1	30,9	9,2	0,0	**81,9**	18,1	-	-	2,53	2,29	1,19
	Sample3	4,00 - 4,50	SP	0,30	4,44	0,9	43,4	39,4	4,0	0,0	**95,2**	4,8	-	-	2,60	2,16	1,16
	SPT3	4,50 - 4,95	SC	0,12	2,33	0,79	34,9	27,4	7,5	0,0	**78,9**	21,1	-	-	2,75	2,83	1,02
	Sample 4	5,50 - 6,00	SP	0,33	4,42	0,9	60,0	38,8	21,2	0,0	**95,2**	4,8	-	-	2,58	1,99	0,83
	SPT4	6,00 - 6,45	SP-SC	0,17	2,50	0,76	36,7	30,4	6,3	0,0	**92,4**	7,6	-	-	2,63	2,21	0,91
	Sample 5	7,00 - 7,50	SP-SC-SM	0,19	3,07	0,77	31,9	27,2	4,7	0,0	**90,8**	9,2	-	-	2,64	1,71	0,93
	SPT5	7,50 - 7,95	SM	0,14	2,43	0,84	26,4	NP	NP	0,0	**87,7**	12,3	-	-	2,63	8,88	7,45
	Sample 6	8,50 - 9,00	SM	0,12	1,86	1,1	27,8	24,2	3,6	0,0	**87,4**	12,6	-	-	2,77	2,11	1,10
	SPT6	9,00 - 9,45	SP- SC	0,20	4,00	0,54	38,4	28,4	10,0	0,0	**90,4**	9,6	-	-	2,75	2,31	1,48
	Sample 7	10,00 - 10,50	SP- SM	0,15	2,00	0,84	NP	NP	NP	0,0	**92,7**	7,3	-	-	2,65	1,79	0,82
	SPT7	10.50 - 10.95	SP- SM	0,18	2,67	0,81	NP	NP	NP	0,0	**88,8**	11,2	-	-	2,70	1,66	0,73
	Sample 8	11,50 - 12,00	SP- SM	0,17	2,11	0,84	NP	NP	NP	0,0	**94,1**	5,9	-	-	2,64	1,50	0,79
	SPT8	12.00 -12,45	No Sample	-	-	-	-	-	-	-	-	-	-	-	-	-	-
	SPT9	13,50 -13,95	SP - SM	0,30	3,20	1,25	NP	NP	NP	0,0	**94,0**	6,0	-	-	2,56	1,18	0,60
	SPT10	15,00 - 15,45	SP - SM	0,22	3,67	0,86	NP	NP	NP	0,0	**94,1**	6,0	-	-	2,72	1,83	1,16

(Cont. on next page)

Table 4.10. (cont.)

LABORATORY TEST SUMMARY SHEET (cont.)

Boring Number	Sample Number	Depth	Classification (Method: USGS)	D_{50}	C_u	C_c	Atterberg Limits			Grain Size			Hydrometer		Gs Specific Gravity		
							Liquid Limit	Plastic Limit	PI	Gravel	Sand	FC	Silt	Clay		e_{max} (Dry)	e_{min} (Dry)
-	-	m					(%)	(%)	(%)	(%)	(%)	(%)	(%)	(%)	-	-	-
SC14	Sample 1	1.00 - 1.50	SM-SC	0,17	2,86	0,86	31,3	26,6	4,7	0,0	**86,4**	13,6	12,06	1,51	2,57	1,59	0,95
	SPT1	1,50 - 1,95	SM	0,12	1,86	1,33	NP	NP	NP	0,0	**86,3**	13,7	13,54	0,18	2,66	1,65	1,2
	Sample 2	2,50 - 3,00	SP- SM	0,15	2,00	0,95	NP	NP	NP	0,0	**92,8**	7,2	-	-	2,31	1,28	0,43
	SPT2	3,00 - 3,45	SP- SM	0,16	2,00	0,84	NP	NP	NP	0,0	**93,7**	6,3	-	-	2,68	1,70	0,79
	Sample3	4,00 - 4,50	SP -SM	0,17	2,38	0,80	20,8	20,7	0,1	0,0	**91,9**	8,2	-	-	2,68	1,51	0,84
	SPT3	4,50 - 4,95	SP- SM	0,16	2,00	0,75	NP	NP	NP	0,0	**94,9**	5,1	-	-	2,71	1,70	0,89
	Sample 4	5,50 - 6,00	SP-SM	0,19	2,35	0,85	NP	NP	NP	0,0	**92,6**	7,4	-	-	2,72	1,39	1,12
	SPT4	6,00 - 6,45	SP-SM	0,19	2,00	0,85	NP	NP	NP	7,1	**88,0**	4,9	-	-	2,68	1,53	0,71
	Sample 5	7,00 - 7,50	SP	0,24	3,00	1,08	16,7	15,3	1,4	0,0	**97,4**	2,6	-	-	2,71	1,40	0,56
	SPT5	7,50 - 7,95	No Sample	-	-	-	-	-	-	-	-	-	-	-	-	-	-
	Sample 6	8,50 - 9,00	SP	0,21	2,50	1,30	20,6	NP	NP	0,0	**97,0**	3,0	-	-	2,73	1,74	0,65
	SPT6	9,00 - 9,45	SP	0,32	2,77	1,03	NP	NP	NP	0,0	**98,2**	1,8	-	-	2,67	1,09	0,69
	Sample 7	10,00 - 10,50	SP	0,30	3,00	1,10	24,1	18,7	5,4	0,0	**98,3**	1,7	-	-	2,71	1,15	0,61
	SPT7	10.50 - 10.95	SP	0,33	2,92	1,82	NP	NP	NP	0,0	**98,2**	1,8	-	-	2,64	1,04	0,59
	SPT8	12.00 -12,45	SP	0,19	2	0,85	NP	NP	NP	0,0	**95,4**	4,6	-	-	2,72	1,30	0,77
	SPT9	13,50 -13,95	SP	0,21	2,70	1,07	NP	NP	NP	0,0	**95,3**	4,7	-	-	2,64	1,19	0,61
	SPT10	15,00 - 15,45	No Sample	-	-	-	-	-	-	-	-	-	-	-	-	-	-
SC15	Sample 1	1.00 - 1.50	SP- SM	0,18	1,6667	0,9	22,6	21,0	1,6	0,0	**93,3**	6,7	-	-	2,68	2,00	0,76
	SPT1	1,50 - 1,95	SM	0,13	1,33	1,13	NP	NP	NP	0,0	**87,9**	12,2	11,28	0,87	2,73	1,71	0,88
	Sample 2	2,50 - 3,00	SP- SM	0,13	1,3333	0,98	NP	NP	NP	0,0	**93,8**	6,2	-	-	2,64	1,72	1,28
	SPT2	3,00 - 3,45	SP	0,20	1,35	1,26	NP	NP	NP	0,0	**96,0**	4,0	-	-	2,63	1,50	0,71
	Sample3	4,00 - 4,50	SP - SM	0,19	1,5385	0,99	18,3	NP	NP	0,0	**94,5**	5,5	-	-	2,63	1,42	1,03
	SPT3	4,50 - 4,95	SP	0,20	1,31	1,16	NP	NP	NP	0,0	**96,4**	3,6	-	-	2,62	1,12	0,68
	Sample 4	5,50 - 6,00	SC	0,14	2,2222	3,375	49,8	33,3	16,5	0,0	**77,5**	22,5	18,54	4,01	2,64	2,57	1,10
	SPT4	6,00 - 6,45	SP- SM	0,20	1,50	0,93	NP	NP	NP	0,0	**94,1**	5,9	-	-	2,64	1,46	0,83
	Sample 5	7,00 - 7,50	SP	0,20	1,44	1,06	NP	NP	NP	0,0	**97,7**	2,3	-	-	2,69	1,42	0,61
	SPT5	7,50 - 7,95	SP	0,30	1,55	1,08	NP	NP	NP	0,0	**96,9**	3,1	-	-	2,66	1,04	0,63
	SPT6	9,00 - 9,45	SP	0,30	1,6	0,96	NP	NP	NP	0,0	**95,5**	4,5	-	-	2,65	1,04	0,61
	SPT7	10.50 - 10.95	No Sample	-	-	-	-	-	-	-	-	-	-	-	-	-	-
	SPT8	12.00 -12,45	SM	0,18	2,0952	0,72	NP	NP	NP	0,0	**85,0**	15,0	-	-	2,61	1,76	1,08
	SPT9	13,50 -13,95	SP-SM	0,23	1,5789	1,09	NP	NP	NP	0,0	**94,8**	5,2	-	-	2,67	1,31	0,75
	SPT10	15,00 - 15,45	SP- SM	0,18	1,83	0,82	NP	NP	NP	0,0	**91,1**	8,9	-	-	2,72	1,19	0,61
SC16	SPT1	1,50 - 1,95	SP	-	-	-	-	-	-	-	-	-	-	-	-	-	-
	Sample 1	2,50 - 3,00	SM	0,13	2,00	1,02	NP	NP	NP	0,0	**85,4**	14,6	13,96	0,67	2,66	1,74	1,00
	SPT2	3,00 - 3,45	SP	0,11	1,69	1,01	NP	NP	NP	16,1	**79,8**	4,2	3,72	0,45	2,76	2,30	1,27
	Sample 2	4,00 - 4,50	SM	0,14	2,29	0,89	NP	NP	NP	0,0	**69,1**	30,9	-	-	2,68	1,96	0,97
	SPT3	4,50 - 4,95	SP	0,20	2,8	0,6	NP	NP	NP	0,0	**95,3**	4,7	-	-	2,26	1,12	0,67
	Sample 3	5,50 - 6,00	SP	0,45	1,6	1	NP	NP	NP	0,0	**99,5**	0,5	-	-	2,66	1,45	0,80
	SPT4	6,00 - 6,45	SP	0,21	2,45	1,09	NP	NP	NP	0,0	**95,5**	4,5	-	-	2,70	-	-
	Sample 4	7,00 - 7,50	SP-SM	0,24	3,56	1	NP	NP	NP	0,0	**93,5**	6,5	-	-	2,34	1,48	0,94
	SPT5	7,50 - 7,95	SP	0,31	3,27	1,01	NP	NP	NP	0,0	**95,2**	4,8	-	-	2,76	1,18	0,77
	Sample 5	8,50 - 9,00	SP- SM	0,18	2,67	0,96	NP	NP	NP	0,0	**89,8**	10,2	-	-	2,76	2,04	0,57
	SPT6	9,00 - 9,45	SP - SM	0,30	4,63	1,09	NP	NP	NP	0,0	**91,0**	9,0	-	-	2,71	1,31	0,76
	SPT7	10.50 - 10.95	SP- SM	0,31	4,88	1,04	NP	NP	NP	0,0	**91,7**	8,3	-	-	2,86	1,41	0,85
	SPT8	12.00 -12,45	SP-SC	0,32	4,88	0,93	47,7	36,0	11,7	0,0	**91,9**	8,1	-	-	2,83	2,35	1,06
	SPT9	13,50 -13,95	SC	-	-	-	41,4	22,1	19,3	0,0	**70,5**	29,5	28,82	0,67	2,73	1,81	1,03
	SPT10	15,00 - 15,45	SM	1,05	2,50	1,11	40,3	31,8	8,5	0,0	**76,8**	23,2	22,82	0,36	2,68	1,72	0,92
SC17	Sample 1	1.00 - 1.50	SP- SC	0,2	2,75	0,82	37,6	27,9	9,7	0,0	**91,9**	8,1	-	-	2,69	1,72	0,63
	SPT1	1,50 - 1,95	SM-SC	-	-	-	27,4	22,7	4,7	0,3	**77,3**	22,4	21,05	1,32	2,72	1,89	1,32
	Sample 2	2,50 - 3,00	SM	0,13	2,14	0,95	NP	NP	NP	0,0	**85,1**	14,9	14,32	0,54	2,70	2,24	1,13
	SPT2	3,00 - 3,45	SP- SM	0,25	5,56	0,5	36,9	35,3	1,6	0,0	**94,9**	5,1	-		2,76	2,07	0,86
	Sample3	4,00 - 4,50	SP-SM	0,17	2,67	0,81	NP	NP	NP	0,0	**90,3**	9,8	-		2,82	1,74	0,95
	SPT3	4,50 - 4,95	SM-SC	0,14	2,57	0,79	29,4	23,1	6,3	0,0	**86,2**	13,8	12,91	0,86	2,80	2,03	1,27
	Sample 4	5,50 - 6,00	SM	0,13	2,14	0,95	29,7	28,7	1,0	0,0	**84,0**	16,0	15,58	0,42	2,77	2,10	1,10
	SPT4	6,00 - 6,45	SM	0,15	2,57	0,88	NP	NP	NP	0,0	**87,1**	12,9	12,06	0,84	2,82	1,62	1,02
	Sample 5	7,00 - 7,50	SP - SM	0,18	2,11	0,84	24,70	24,00	0,7	0,0	**95,0**	5,0	-	-	2,83	0,93	0,53
	SPT5	7,50 - 7,95	SP - SM	0,18	2,50	0,90	NP	NP	NP	0,0	**92,3**	7,8	-	-	2,77	1,54	0,92
	Sample 6	8,50 - 9,00	SP - SM	0,20	2,59	0,90	NP	NP	NP	0,0	**93,7**	6,3	-	-	2,76	1,49	0,91
	SPT6	9,00 - 9,45	SP- SM	0,20	2,59	1,2	NP	NP	NP	0,0	**91,8**	8,2	-	-	2,82	1,17	0,83
	SPT7	10.50 - 10.95	SP- SM	0,30	5,38	0,35	NP	NP	NP	0,0	**93,0**	7,0	-	-	2,80	1,37	0,78
	SPT8	12.00 -12,45	SP -SC	0,30	5,73	0,38	39,4	29,9	9,5	0,0	**89,0**	11,0	10,23	0,77	2,76	2,44	1,15
	SPT9	13,50 -13,95	SM	0,17	2,71	0,83	35,4	33,8	1,6	0,0	**86,6**	13,4	12,80	0,62	2,80	2,44	1,33
	SPT10	15,00 - 15,45	SM	0,19	1,85	1,93	29,1	28,8	0,3	0,0	**78,2**	21,8	20,17	1,65	2,82	2,38	1,05
SC18	Sample 1	1.00 - 1.50	SC	0,14	2,29	0,89	28,5	21,3	7,2	0,0	**85,7**	14,3	13,60	0,72	2,78	2,22	0,99
	SPT1	1,50 - 1,95	SP - SC	0,20	3,00	0,63	62,1	51,7	10,4	0,0	**91,0**	9,0	-	-	2,79	2,50	1,23
	Sample 2	2,50 - 3,00	SC	0,14	3,08	0,69	58,6	27,3	31,3	0,0	**83,1**	16,9	16,25	0,61	2,73	2,28	1,55
	SPT2	3,00 - 3,45	SP - SC- SM	0,17	2,5	0,76	33,0	27,4	5,6	0,0	**92,6**	7,4	-	-	2,73	2,66	1,18
	Sample3	4,00 - 4,50	SM	0,12	2,33	1,19	NP	NP	NP	0,0	**82,3**	17,7	17,11	0,59	2,81	2,48	1,19
	SPT3	4,50 - 4,95	SM	0,14	2,43	0,84	28,0	24,2	3,8	0,0	**87,0**	13,1	12,32	0,73	2,67	1,38	0,68
	Sample 4	5,50 - 6,00	SM	0,12	2,00	0,96	NP	NP	NP	0,0	**82,0**	18,0	17,02	1,01	2,82	2,66	1,00
	SPT4	6,00 - 6,45	SP- SM	0,14	2,14	0,95	NP	NP	NP	0,0	**89,2**	10,9	-	-	2,75	2,24	0,96
	Sample 5	7,00 - 7,50	SP- SM	0,14	2,14	0,95	NP	NP	NP	0,0	**88,3**	11,7	10,88	0,80	2,84	2,39	0,95
	SPT5	7,50 - 7,95	SP- SM	0,20	2,3	0,98	NP	NP	NP	0,0	**93,7**	6,3	-	-	2,82	1,40	0,97
	Sample 6	8,50 - 9,00	SP	0,20	2,10	1,07	NP	NP	NP	0,0	**95,3**	4,7	-	-	2,81	1,57	0,73
	SPT6	9,00 - 9,45	No Sample	-	-	-	-	-	-	-	-	-	-	-	-	-	-
	SPT7	10.50 - 10.95	SP - SC-SM	0,16	2,77	0,94	30,1	24,8	5,3	0,0	**89,7**	10,3	-	-	2,74	2,99	1,53
	SPT8	12.00 -12,45	SM	0,15	2,92	0,89	NP	NP	NP	0,0	**84,7**	15,3	14,81	0,50	2,79	1,86	0,66
	SPT9	13,50 -13,95	SM	0,15	2,57	0,79	NP	NP	NP	0,0	**84,8**	15,2	14,37	0,87	2,84	2,40	0,95
	SPT10	15,00 - 15,45	SP-SC-SM	0,19	2,67	0,81	34,9	29,7	5,2	0,0	**89,6**	10,4	-	-	2,74	2,39	1,05

(Cont. on next page)

Table 4.10. (cont.)

LABORATORY TEST SUMMARY SHEET (cont.)																	
Boring Number	Sample Number	Depth	Classification (Method: USCS)	D_{50}	C_u	C_c	Atterberg Limits			Grain Size			Hydrometer		Gs Specific Gravity		
							Liquid Limit	Plastic Limit	PI	Gravel	Sand	FC	Silt	Clay		e_{max} (Dry)	e_{min} (Dry)
-	-	m					(%)	(%)	(%)	(%)	(%)	(%)	(%)	(%)	-	-	-
SC19	Sample 1	1.00 - 1.50	SM	0,15	2,86	0,71	NP	NP	NP	0,0	**87,2**	12,8	12,38	0,38	2,80	2,07	1,03
	SPT1	1,50 - 1,95	SP- SM	0,16	2,40	0,90	NP	NP	NP	0,0	**89,7**	10,3	10,25	0,03	2,74	1,91	1,14
	Sample 2	2,50 - 3,00	SM	0,12	2,15	1,1	NP	NP	NP	0,0	**82,9**	17,1	17,01	0,06	2,79	2,20	1,36
	SPT2	3,00 - 3,45	SP	0,30	3,20	1,01	NP	NP	NP	0,0	**96,1**	3,9	-	-	2,73	1,36	0,60
	Sample3	4,00 - 4,50	SP- SM	0,21	3,00	1,17	NP	NP	NP	0,0	**93,0**	7,0	-	-	2,77	1,15	0,54
	SPT3	4,50 - 4,95	SP-SM	0,30	3,30	1,21	NP	NP	NP	0,0	**93,4**	6,6	-	-	2,71	1,12	0,54
	SPT4	6,00 - 6,45	SP	0,30	2,67	1,03	NP	NP	NP	0,0	**96,1**	3,9	-	-	2,78	1,10	0,61
	SPT5	7,50 - 7,95	SM	0,11	2,00	1,00	NP	NP	NP	0,0	**77,4**	22,6	22,40	0,22	2,83	2,06	1,32
	Sample 4	8,50 - 9,00	SM-SC	-	-	-	28,30	24,30	4,0	0,0	**59,6**	40,4	39,30	1,06	2,82	2,33	1,05
	SPT6	9,00 - 9,45	SM	-	-	-	NP	NP	NP	0,0	**67,7**	32,3	32,27	0,00	2,78	1,95	1,35
	SPT7	10.50 - 10.95	SC	-	-	-	31,2	23,9	7,3	0,0	**75,0**	25,0	24,60	0,41	2,79	2,58	1,30
	SPT8	12.00 -12,45	SM-SC	-	-	-	30,6	24,5	6,1	0,0	**69,6**	30,4	28,53	1,89	2,74	2,41	0,71
	SPT9	13,50 -13,95	SP-SM	0,17	2,67	0,81	NP	NP	NP	0,0	**88,5**	11,5	10,64	0,83	2,81	2,33	1,34
	SPT10	15,00 - 15,45	SP-SC	0,15	2,86	0,79	34,4	26,7	7,7	0,0	**87,1**	12,9	12,02	0,86	2,65	1,95	1,22
SC20	Sample 1	1.00 - 1.50	SM-SC	0,15	2,86	0,86	35,8	31,4	4,4	0,0	**87,9**	12,1	11,65	0,45	2,63	2,32	1,01
	SPT1	1,50 - 1,95	SP-SM	0,12	1,73	0,93	NP	NP	NP	0,3	**87,8**	11,9	11,59	0,30	2,73	2,18	1,42
	Sample 2	2,50 - 3,00	SM	0,10	1,83	0,97	NP	NP	NP	0,0	**77,3**	22,8	22,41	0,34	2,70	2,26	1,39
	SPT2	3,00 - 3,45	SP-SC	0,22	4,38	0,51	39,8	27,5	12,3	0,0	**91,9**	8,2	7,85	0,30	2,79	2,74	0,97
	Sample3	4,00 - 4,50	SC	0,18	2,86	0,79	44,8	24,9	19,9	0,0	**87,6**	12,4	12,13	0,24	2,69	1,81	1,26
	SPT3	4,50 - 4,95	SP	0,21	2,08	1,20	NP	NP	NP	0,0	**96,8**	3,3	-	-	2,73	1,30	0,86
	SPT4	6,00 - 6,45	SP-SC-SM	0,22	3	1,08	22,7	17,2	5,5	0,0	**94,9**	5,1	-	-	2,68	2,39	0,75
	Sample 4	7,00 - 7,50	SM	0,25	2,86	0,71	NP	NP	NP	0,0	**87,6**	12,4	12,00	0,41	2,73	1,88	0,74
	SPT5	7,50 - 7,95	SP-SM	0,20	2,94	1,06	21,9	18,4	3,5	0,0	**92,9**	7,1	-	-	2,67	2,46	0,61
	Sample 5	8,50 - 9,00	SP-SM	0,20	2,93	0,87	28,60	26,20	2,4	0,0	**89,7**	10,3	10,03	0,23	2,72	2,52	1,09
	SPT6	9,00 - 9,45	SM	0,12	2,31	1,03	NP	NP	NP	0,0	**82,9**	17,1	16,89	0,21	2,68	1,72	1,29
	SPT7	10.50 - 10.95	SM-SC	0,18	2,50	0,76	30,0	23,7	6,3	0,0	**75,4**	24,6	24,01	0,61	2,71	1,93	1,31
	SPT8	12.00 -12,45	SP-SM	0,18	2,50	0,76	NP	NP	NP	0,0	**92,1**	7,9	-	-	2,66	1,58	1,18
	SPT9	13,20 -13,65	SP-SM	0,17	2,38	0,80	NP	NP	NP	0,0	**91,9**	8,1	-	-	2,68	1,76	0,92

CHAPTER 5

ANALYSES OF LIQUEFACTION ASSESSMENT OF SOILS

5.1. **Introduction**

There are numbers of researches focused on liquefaction potential screening in the literature (e.g. Seed and Idriss 1971, Lee and Seed 1967, Seed and De Alba 1986, Shibata and Teparaska 1988, Mitchell and Tseng 1990, Stark and Olson 1995, Suzuki et al. 1995, Robertson and Wride 1998). All these relationships and researches are briefly described in Chapter 2. However, in these researches, the effects of fines content on liquefaction resistance and penetration resistance are not defined clearly. Also, in the literature, there are numerous studies about the effects of fines on cyclic resistance of soils (e.g. Zlatovic and Ishihara 1997, Polito and Martin, 2001; Thevanayagam and Martin 2002; Cubrinowski et al., 2010) and its effects on liquefaction screening using the cone penetration tests (e.g. Carraro et al. 2003, Huang et al. 2005, Kokusho et al. 2005). Huang et al. (2005). The related researches points out that it is not clear whether the existence of fines is beneficial to liquefaction resistance or not. Therefore, there is a need to understand the effects of non/low plastic fines on the liquefaction resistance, the cone penetration resistance, and the influence of fines content on the relationship between cone resistance and liquefaction resistance.

In this chapter, the field and laboratory tests explained in Chapters 3 and 4 are used in order to find the effects of fines content and relative density on consolidation characteristics and drainage effects of fines or consolidation characteristics of soils on cone penetration resistance at different relative densities. Also, the effects of relative density on liquefaction resistance of soils at different fines content (less than 30% by weight) are determined. Fines content over 30% by weight and/or high plasticity of fines can cause additional complications which can need different valuation methods, and this is beyond the scope of this study.

5.2. **Effect of Fines Content and Relative Density on the Coefficient of Consolidation**

Drainage effect of fines is one of the factors affecting the measured excess pore pressure and the cone penetration resistance (Thevanayagam and Ecemis, 2008). First, it is required to substantiate the effects of fines and relative density (D_r) on the coefficient of consolidation (c_h) of the sands with fines. This section focuses on sandy soils containing 0-30% non/low plastic fines by weight.

Relative density or density index is the ratio of the difference between the void ratios of a cohesionless soil in its loosest state and in existing natural state to the difference between its void ratio in the loosest and densest states.

$$D_r = \frac{e_{max} - e}{e_{max} - e_{min}} \tag{5.1}$$

Where;

e_{max} = void ratio of coarse grained soil in its loosest state,

e_{min} = void ratio of coarse grained soil in its densest state.

e = void ratio of coarse grained soil in its natural existing state in the field.

In the laboratory studies, the maximum and minimum void ratio tests were performed as mentioned in Chapter 4, section 4.3.4. However, it was not possible to define void ratio of soils in their natural existing state in the field due to obtaining disturbed samples for testing in laboratory. Because of this reason, the relative density values were estimated from the measured cone penetration resistance by using the empirical relationship given by Lunne, Robertson and Powell (1997);

$$D_r = -98 + 66 \log_{10}\left(\frac{q_c}{\sqrt{\sigma_{vo}'}}\right) \tag{5.2}$$

Where; D_r is the relative density in percentage and σ_{vo}' is the effective vertical stress in the same units as, q_c.

In this study, the measurements from the direct push permeability tests and dissipation tests are used to find the hydraulic conductivity at each depth. To define the hydraulic conductivity, Eq. 3.8 given by Lee et al. (2008) is used for clean sand soil

samples, whose volumetric flow rate, (Q) data is taken from direct push permeability test (DPPT) and equation 5.3 given below which is suggested by Parez and Fauriel (1988) for silty and clayey sand soil samples whose t_{50} data taken from pore pressure dissipation tests (PPDT).

$$k_h = \frac{1}{(251\, t_{50})^{1.25}} \tag{5.3}$$

where;

k_h = hydraulic conductivity (cm/sec),

t_{50} = the times for 50% consolidation (sec).

It is known that the coefficient of consolidation is influenced by a number of different factors, such as the effects of penetration process, stress level, void ratio, stress history, and anisotropy. Therefore, an appropriate method is needed to determine the coefficient of consolidation of the soil. In this part, the coefficient of consolidation of soils throughout the depths is determined by using the equation given below (Robertson et al, 1998).

$$c_h = \frac{k_h}{m_v\ \gamma_w} \tag{5.4}$$

Where;

k_h = hydraulic conductivity,

γ_w = the unit weight of water and

m_v = the compressibility of the soil estimated from the CPTu tests based on the correlation proposed by Robertson (2009):

$$m_v = \frac{1}{\alpha_M (q_t - \sigma_{vo})} \tag{5.5}$$

Where;

σ_{vo}=in-situ total vertical stress,

q_t=corrected total cone resistance,

α_M; If $I_c > 2.2$ and $q_{c1N} < 14$ use $\alpha_M = q_{c1N}$.

If $I_c > 2.2$ and $q_{c1N} > 14$ use $\alpha_M = 14$.

If $I_c < 2.2$ use $\alpha_M = 0.03[10^{(0.55I_c + 1.68)}]$. .

Where; I_c = soil behavior index (see Eq 2.11, 2.12, 2.13)

All relative density, fines content, hydraulic conductivity and coefficient of consolidation values were calculated according to the equations given above and listed in Appendix C. Variations of the coefficient of consolidation with fines content for different ranges of relative densities were plotted in Figure. 5.1. Figure. 5.1 a-d illustrates the variation of the coefficient of consolidation with fines content for four individual ranges of relative densities.

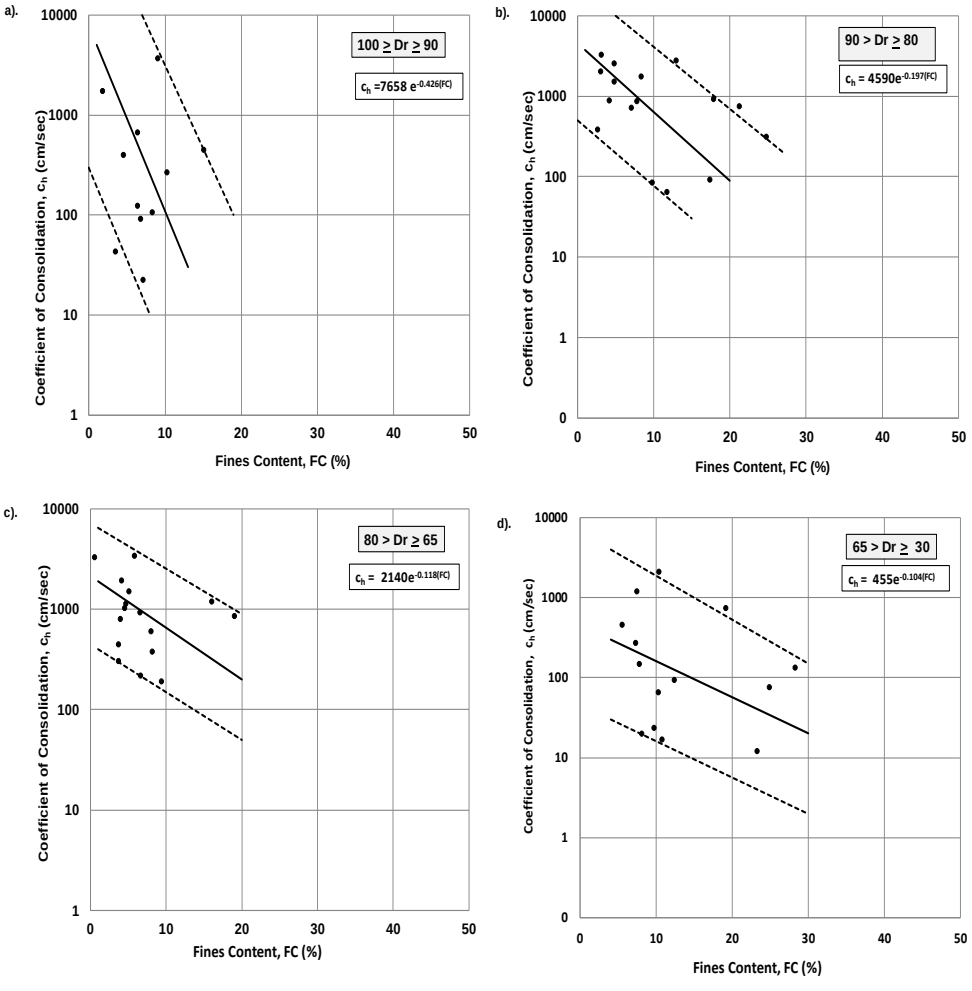

Figure 5.1. The changes of the coefficient of consolidation with fines content (FC≤30%) at the relative density ranges between (a) 90-100%, (b) 90-80%, (c) 65-80% and (d) 30-65%.

The relationships between coefficient of consolidation and fines content are so scattered, the reason of that; the coefficient of consolidation values were found from field tests and they have not a clear distribution to plot a trend clearly. Therefore, the relationship between c_h and FC are ploted with different relative densities range and the corresponding limit values of Dr are given with different dotted lines as upper and lower limits. The average relative densities of 95%, 85%, 78% and 48% are represented by the solid lines.In Figure 5.1, at the same relative density, the coefficient of consolidation decreases steadily with an increase in fines content (FC) up to 30%. An increase in fines content significantly reduces the hydraulic conductivity and constrained modulus ($M=1/m_v$), which decreases the coefficient of consolidation. It is apparent that, there is a major difference in the coefficient of consolidation between clean sands and sands with fines, even if it is compared at the same relative density (D_r). In order to compare the effect of different relative density to the relationship between the coefficient of consolidation (c_h) and fines content, the variation of c_h with FC for an average D_r, obtained from the above mentioned figures is plotted together in Figure. 5.2.

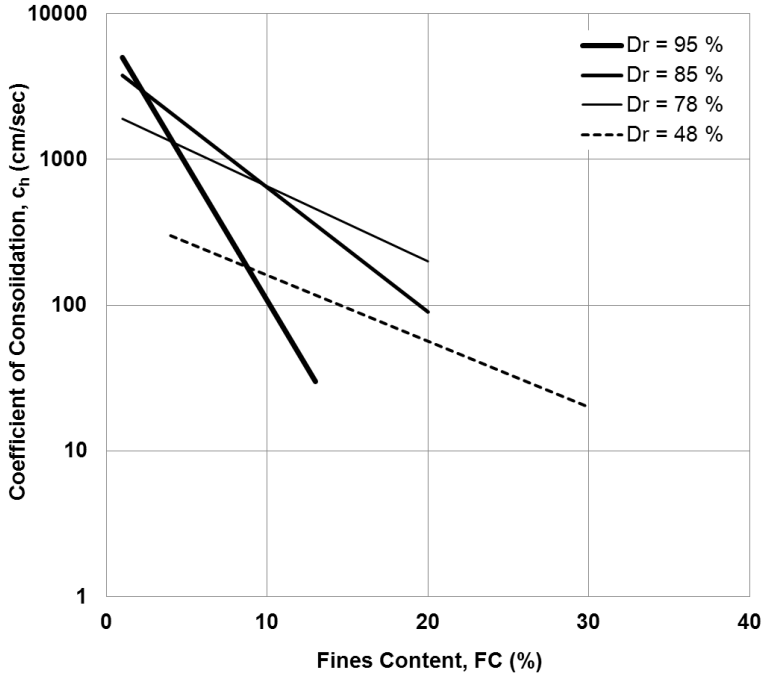

Figure 5.2. Summary of the effects of fines content on the coefficient of consolidation at different relative density

With an increase in fines content, the linear declinations of the coefficient of consolidation for stiff/dense soils are determined to be greater than that for the medium dense and loose soils. The above combined observations indicate that, both the fines content and the relative density affect the coefficient of consolidation of the soils.

5.3. **Effects of Consolidation Characteristics and Relative Density on Cone Penetration Resistance**

It is necessary to understand the effects of coefficient of consolidation on cone penetration resistance, in order to interpret the effects of consolidation characteristics of soil on liquefaction resistance based on the cone penetration. It is known that, if coefficient of consolidation of soils has low value, dissipation of excess pore pressures has a slow rate. Thevanayagam and Ecemis (2008), suggested that low coefficient of consolidation values can cause lower effective stress near the penetration tip of a cone in sands with fines, than in clean sand at the same contact density. Also numerous researchers have suggested that the measured cone penetration resistance and the excess pore water pressure during penetration of the cone in soils depend on the rate of penetration (v), the coefficient of consolidation (c_h), and the diameter of the cone (d) (Finnie and Randolph 1994, House et al. 2001, Randolph and Hope 2004, Chung et al. 2006, Kim et al. 2008, Thevanayagam and Ecemis 2008). A non-dimensional parameter, normalized penetration rate (V) was proposed by Finnie and Randolph (1994) as a function of v, d, and c_h. and is expressed as:

$$V = \frac{v\,d}{c_h} \tag{5.6}$$

Where;

v = penetration velocity,

c_h = the coefficient of consolidation,

d = and the diameter of the cone.

In this study as mentioned before CPTu tests were performed with constant penetration velocity which was 2 cm/sec and the cone with 3.57cm diameter was used

for penetration. Because of the constant v and d parameters, the normalized penetration rate, V value depends on the coefficient of consolidation. All V values for each known c_h value of soil samples were calculated and listed in Table 5.1. Normalized penetration resistance is also known from Chapter 3 and is calculated using by Eq 3.3.

Table 5.1. Calculated ormalized penetration rate and normalized cone penetration resistance data for each relative density and fines content

D_r	FC	c_h	V (vd/c_h)	q_{c1N}	D_r	FC	c_h	V (vd/c_h)	q_{c1N}
%	%	cm^2/sec	-	-	%	%	cm^2/sec	-	-
	0	7658	0,00094	107		0	455,1	0,01582	22,50
	5	910,056	0,00791	95		5	270,5663	0,02661	21,50
	10	108,14859	0,06658	87		10	160,85723	0,04476	21,00
	15	12,852086	0,56022	81		15	95,632926	0,07529	20,00
95	20	1,5273071	4,71418	75	55	20	56,85574	0,12664	19,50
	25	0,181501	39,6692	70		25	33,801905	0,21301	18,00
	30	0,0215691	333,811	66		30	20,095927	0,35828	17,00
	35	0,0025632	2808,97	63		35	11,947442	0,60264	15,20
	40	0,0003046	23637,1			40	7,1029996	1,01366	15,00
	0	4590	0,00157	69		0	455,05	0,01582	13,00
	5	1714,0861	0,00420	62		5	270,53658	0,02661	12,50
	10	640,10697	0,01125	57		10	160,83955	0,04477	12,20
	15	239,04105	0,03012	54		15	95,622419	0,07530	12,00
85	20	89,267306	0,08066	51	38	20	56,849493	0,12665	11,80
	25	33,335914	0,21598	49		25	33,798192	0,21303	11,50
	30	12,448938	0,57836	47		30	20,093719	0,35832	11,30
	35	4,6489217	1,54875	45		35	11,946129	0,60271	11,00
	40	1,7360897	4,14725	43		40	7,1022192	1,01377	11,00
	0	21398	0,00034	50,00		0	200	0,03600	6,29
	5	11861,495	0,00061	47,00		5	167,8914	0,04288	6,28
	10	6575,1504	0,00110	44,00		10	140,93762	0,05109	6,26
	15	3644,7853	0,00198	41,00		15	118,31107	0,06086	6,25
78	20	2020,4039	0,00356	39,00	15	20	99,317061	0,07250	6,24
	25	1119,965	0,00643	37,00		25	83,372404	0,08636	6,23
	30	620,82717	0,01160	36,00		30	69,98755	0,10288	6,22
	35	344,14144	0,02092	35,00		35	58,75154	0,12255	6,20
	40	190,76699	0,03774	34,00		40	49,319393	0,14599	6,19

To see the relationship between the normalized penetration resistance and coefficient of consolidation, the curves of cone penetration resistance versus log normalized penetration ratio were plotted in Figure 5.3. Figures 5.3 a-f illustrate the variation of normalized cone penetration resistance with normalized penetration rate for six distinct ranges of relative densities.

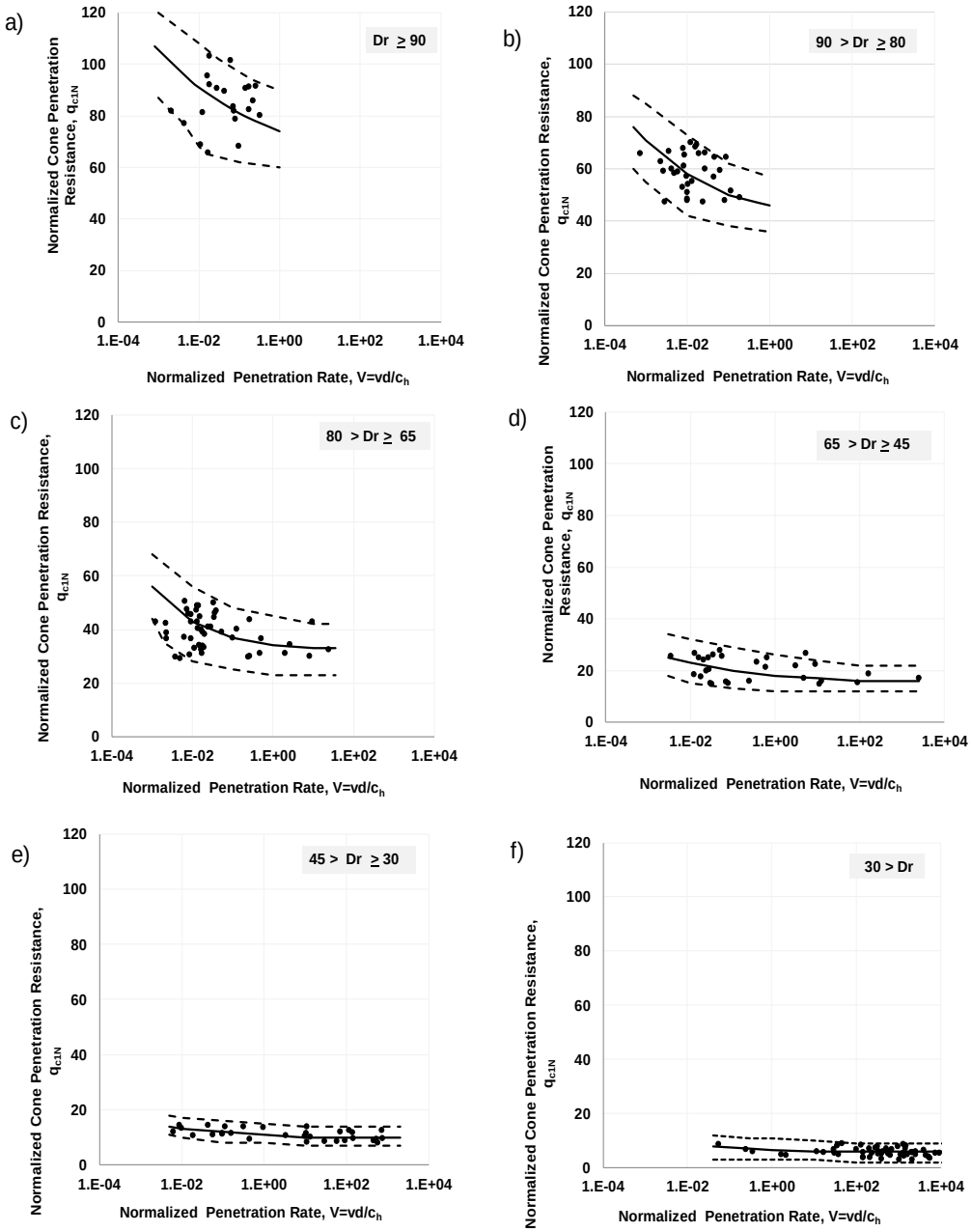

Figure 5. 3 The change of normalized cone penetration resistance, q_{c1N} with normalized penetration rate, V at relative density ranges between (a) 100-90%, (b) 80-90%, (c) 65-80 %, (d) 45-65%, (e) 30-45% and (f) 0-30%.

Upper and lower limit values of D_r are displayed with different dotted lines and the average relative densities (95%, 85%, 78%, 55%, 38%, and 15%) are represented by the solid lines in each figure. For Figure 5.3, it can be said that; Figure 5.3 a,b,c which illustrates the relationship between normalized cone penetration resistance and normalized penetration rate for relative density range of between 65% and 100% are scattered. The reason of that, the data which were found from CPTu insitu tests have not

so clear distribution. On the other hand the relationship between qc1N and V are more clear for relative density less than 65% as seen in Figure 5.3 d,e,f.

It can be observed from the Figure 5.3 that for dense soils which have high D_r values of more than about 80% and non/low plastic fines content of less than 30%, it is not possible to measure low coefficient of consolidation. Hereby, at dense soils the change of normalized penetration rate is investigated from about 10^{-3} to 1. At medium dense soils, where the relative density ranges from 80% to 45%, the change of normalized penetration rate is investigated from about 10^{-3} to 10^{3}. At loose soils, where the relative density is smaller than 45%, the change of normalized penetration rate is investigated from about $5x10^{-3}$ to 10^{4}. In order to compare the results, the variation of q_{c1N} with normalized penetration rate for different average relative densities obtained from the Figure 5.3 is also plotted together in Figure 5.4. Figure 5.4 shows the change of normalized cone penetration resistance, q_{c1N} with normalized penetration rate, V at average relative densities as 95%, 85%, 78%, 55%, 38%, and 15%.

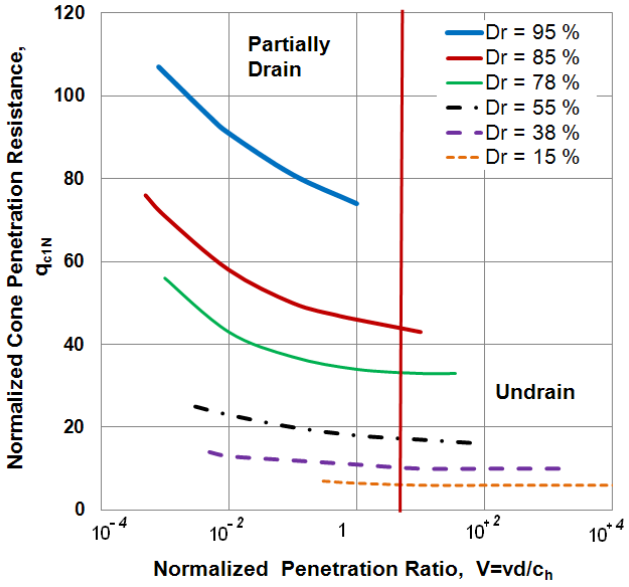

Figure 5.4. Effects of normalized penetration rate and relative density on normalized cone penetration resistance

According to the Figure 5.4, it can be said that, the normalized cone resistance decreased significantly with an increase normalized penetration rate. Fines in soils can cause partially drained conditions during penetration in fine grained soils and lead to a decrease in cone resistance, compared to clean sand. For dense to medium dense soils,

above normalized penetration rate of 10 cm/sec there is not much alteration observed in CPT penetration resistance with an increase in V. This shows that, the transition value of normalized penetration rate from partially drained to undrained response is determined as 10.

On the other hand, for loose soils, the normalized cone resistance is not significantly changed with an increase in normalized penetration ratio, from partially drained to undrained conditions. It is apparent that, both normalized penetration ratio and relative density of the dense to medium dense soils indicate a significant influence on the measured CPT penetration resistance around the probe. However, for loose soils only the relative density indicates a significant influence on the measured CPT penetration resistance around the probe.

These suggested transition values of normalized penetration rate from partially drained to undrained conditions almost align with the related research conducted by Finnie and Randolph (1994), House et al. (2001), Randolph and Hope (2004), Chung et al. (2006), Kim et al. (2008) and Ecemis (2008). The results of tests conducted on circular foundations reported by Finnie and Randolph (1994) have suggested that the undrained limit for V to be around 30. A cylindrical T-bar penetrometer test analysis reported by House et al. (2001) have suggested the undrained limit for V to be around 10. Similarly, Randolph and Hope (2004) observed that undrained penetration occurs at V of approximately 30 to 100. According to Chung et al. (2006) and Kim et al. (2008) the transition from fully undrained to partially drained conditions was approximately around 10. Similarly, based on the recent numerical simulations by Ecemis (2008), the undrained limit for V was in the range of about 5 to 10.

5.4. **Effects of Fines Content and Relative Density on Cone Penetration Resistance**

The correlations suggested above show that, the use of the coefficient of consolidation has significant impact on the quality of the penetration resistance and relative density relationship. Therefore, to investigate the effects of fines and relative density on the normalized cone penetration resistance, the coefficient of consolidation values were obtained for each relative density and fines content from Figure 5.3 and Figure 5.4. For this purpose, curves which show the variation of the normalized

penetration resistance against the relative density for different fines contents were plotted (Figure 5.6). In Figure 5.5, The method of getting data from Figure 5.3 and 5.4 is briefly described to plot a chart illustrating a relationship normalized penetration resistance between the relative density between as plotted in Figure 5.6. In Figure 5.3, there are relationship between c_h and FC for average D_r values and each lines can be defined by a linear equation. Therefore, for each average relative density, any c_h value can be found that for any FC value. According to this knowlage c_h values were derived from graph shown in Figure 5.3 against to each FC percentage of 0, 5, 10, 15, 20, 25, 30 and for each average D_r values as shown in Figure 5.5.a. Normalized penetration rates were calculated according to Eq. 5.6 for each value of c_h and q_{c1N} which are against the V values were found in Figure 5.4 as shown in Figure 5.5.b for each average D_r value. At least according to the relationship between c_h and FC as shown in Figure 5.3 and relationships between c_h and q_{c1N} for different average relative densities as shown in Figure 5.4, relationships between q_{c1N} and D_r were plotted for different FC in Figure 5.6 which is described schematically in Figure 5.5.c.

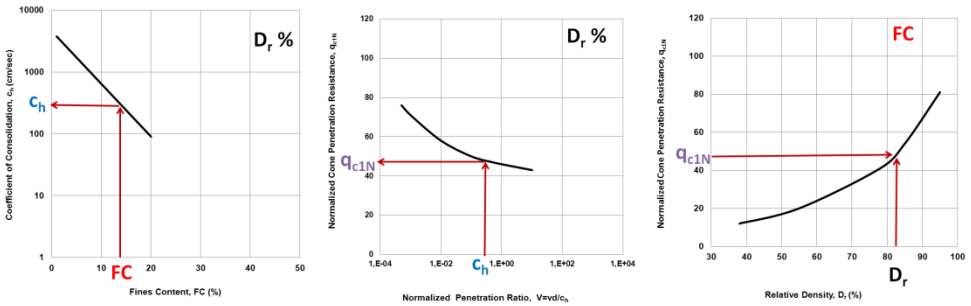

(a) (b) (c)

Figure 5.5. Schematic illustration of plotting (c) q_{c1N} against D_r chart according to the (a) c_h-FC and (b) q_{c1N}-c_h charts.

Figure 5.6 illustrates the effects of fines on the relationship between the normalized penetration resistances and relative density for fines content of 0%, 5%, 10%, 15%, 20%, 25%, 30%.

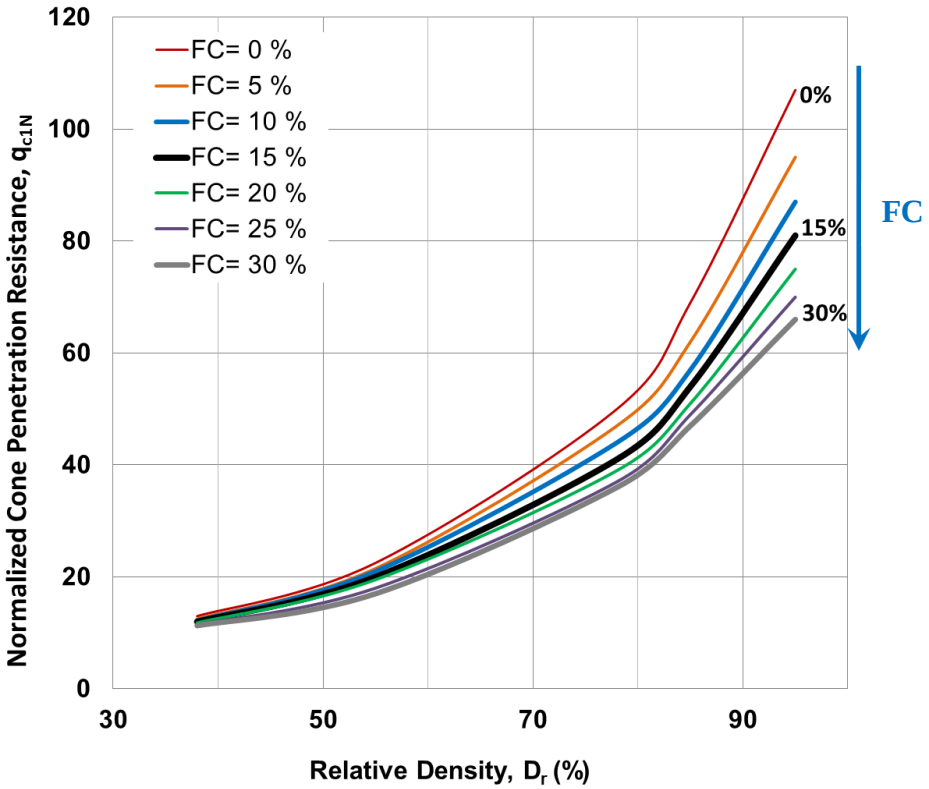

Figure 5.6. The relationship between the normalized cone penetration resistance and relative density of clean sands and sands with different fines content

It can be observed in Figure 5.6 that the penetration resistance significantly decreases with an increase in fines content at a given relative density. It meas that the fines content has a significant influence on the cone penetration resistance. The change in normalized cone penetration resistance according to a change in relative density from 40% to 80% for clean sand is 1.5 times bigger than the same change for sand, containing 30% fines. The increase in CPT resistance of clean sand determined in this study is also compatible with the estimated increase in CPT resistance by Idriss and Boulanger (2008).

5.5. **Effects of Fines Content and Relative Density on Liquefaction Resistance**

Liquefaction screening methods requires determining the cyclic resistance ratio (CRR) as explained in detail in Chapter 2. $(CRR)_{7.5}$ corresponds to the 7.5 magnitude earthquakes which is about 15 cycles (Liu et al. 2001; Green and Terri 2005) and

$(CRR)_{7.5}$ can also be approximated and expressed as the Eq 2.17a and Eq. 2.18b. by Robertson and Wride, 1998. $(CRR)_{7.5}$ values were computed according to the liquefaction assessment method, based on cone penetration test by using equations given in section 2.5.1 (see section 2.5.1). Also all q_{c1N}, calculated $(q_{c1N})_{cs}$, and calculated CSR data for each D_r and FC value are given in Table 5.2.

Table 5.2. Calculated $(q_{c1N})_{cs}$, and CSR data for each D_r and FC values

FC	Dr	(qc1N)	(qc1N)cs	CSR	FC	Dr	(qc1N)	(qc1N)cs	CSR
%	%	-	-	-	%	%	-	-	-
	38	13,0	13,0	0,061		38	11,8	20,6	0,067
	55	22,5	22,5	0,069		55	19,5	34,0	0,078
0	78	50,0	50,0	0,092	20	78	39,0	67,9	0,109
	85	69,0	69,0	0,111		85	51,0	88,9	0,145
	95	107,0	107,0	0,194		95	75,0	130,7	0,288
	38	12,5	12,5	0,060		38	11,5	25,0	0,071
	55	21,5	21,5	0,068		55	18,0	39,1	0,083
5	78	47,0	47,0	0,089	25	78	37,0	80,5	0,128
	85	62,0	62,0	0,102		85	49,0	106,5	0,192
	95	95,0	95,0	0,160		95	70,0	152,2	0,408
	38	12,2	14,3	0,062		38	11,3	30,4	0,075
	55	21,0	24,6	0,071		55	17,0	45,8	0,088
10	78	44,0	51,6	0,093	30	78	36,0	96,9	0,165
	85	57,0	66,9	0,108		85	47,0	126,5	0,268
	95	87,0	102,1	0,179		95	66,0	177,7	0,602
	38	12,0	16,9	0,064		38	11,0	36,1	0,080
	55	20,0	28,2	0,073		55	15,2	49,9	0,092
15	78	41,0	57,7	0,098	35	78	35,0	114,9	0,221
	85	54,0	76,0	0,121		85	45,0	147,7	0,380
	95	81,0	114,0	0,218		95	63,0	206,8	0,902

Over the past decade, many researchers used different density measures such as; void ratio, relative density and equivalent contact density, as a reference for comparison of liquefaction resistance of clean sands and sands containing fines. In this study, to quantify the effect of fines on liquefaction resistance, the curves which show the variation of the cyclic resistance ratio $(CRR)_{7.5}$ against the relative density at different fines contents were plotted. (Figure 5.7) Figure 5.7 illustrates this proposed relationship the changing in undrained cyclic resistance ratio $(CRR)_{7.5}$ of the sands and sands with fines in terms of the relative density. The solid lines shown in the figure are for seven different fines content of 0%, 5%, 10%, 15%, 20%, 25% and 30%.

Figure 5.7. shows that, for the same relative density of up to about 50%, cyclic resistance of clean sands is almost similar to the sands containing fines. An increase in fines content above 50% relative density, distinctly increases the liquefaction resistance. For medium dense soil, as FC increased from 0% to 15%, the $(CRR)_{7.5}$ slightly

increased by a factor of 1.1, whereas fines content increasing from 15% to 30%, $(CRR)_{7.5}$ increased by a factor of 1.7. For stiff/dense soil, as FC has increased from 0% to 15%, the $(CRR)_{7.5}$ has slightly increased by a factor of 1.3, whereas $(CRR)_{7.5}$ has increased by a factor of 2.4 with an increase in fines content from 15% to 30%. In summary, above 50% relative density, the increase in liquefaction resistance from 0% to 15% is greater than the increase in liquefaction resistance from 15% to 30%.

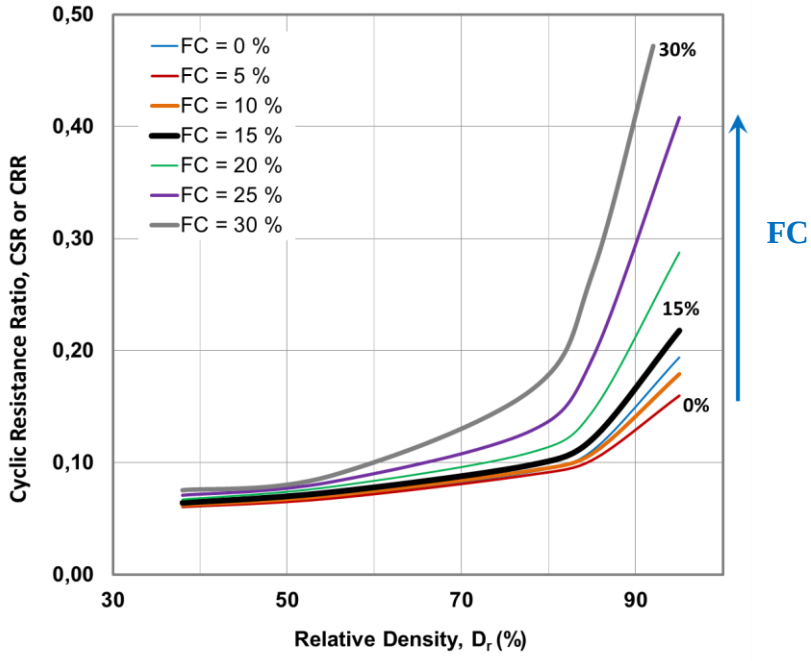

Figure 5.7. The relationship between the cyclic stress ratio at about 15 cycles (estimated from the CPT based criteria for liquefaction assessment of Robertson and Wride, 1998 curves) and relative density of clean sands and sands with different fines content

Clearly, the increase of CRR in the CPT based liquefaction assessment (Figure 2.13) with an increase in fines content is caused by both decrease in the cone penetration resistance and increase in the liquefaction resistance. These suggested trends are compared with the laboratory based correlations obtained by several researchers in the literature (e.g. Chien et al. 2002, Kokusho et al. 2005, and Cubrinowski et al. 2010). Kokusho et al. (2005) found a single correlation between the liquefaction resistance and the cone penetration resistance despite the large differences in relative density or fines content. Chien et al. (2002) and Cubrinowski et al. (2010) reported that the liquefaction

resistance decreases with an increase in fines content at the same relative density. The discrepancy of findings in the literature may occur due to the determination methods of relative densities in the laboratory. The relative densities in these studies were determined from the limiting void ratios. Although there are some standard testing procedures to obtain limiting void ratios of sands with fines content up to 30% in the laboratory, it is still not clear whether these methods are reliable or not. Hence, the exceptions to these trends which show the decrease in liquefaction resistance with an increase in fines content can be possible (Cubrinowski et al. 2010).

CHAPTER 6

CONCLUSIONS

6.1. **Summary of Findings**

In this study, a number of field and laboratory studies were carried out to investigate the effects of fines content on consolidation characteristics and the effects of coefficient of consolidation on liquefaction resistance and cone penetration resistance.

According to the results of experimental studies, first, the effects of the fines content and densities of soil on coefficient of consolidation are examined and it is established that;

- Both the fines content and the relative density affect the coefficient of consolidation of the sands and silty sands.

Second, the changes in cone penetration resistance due to the change in consolidation characteristics are investigated for different range of relative density.

- The transition value of normalized penetration ratio as a function of coefficient of consolidation from partially drained to undrained condition is determined about 10 which align with related research findings in literature.
- The coefficient of consolidation indicates a significant influence on the measured penetration resistance during insertion of the CPT cone to the soil having different relative density.
- For stiff-dense to medium dense soil, the decrease of normalized cone resistance is observed due to the change in drainage characteristics of fines or coefficient of consolidation of the sands containing fines.
- For loose soils only the relative density indicates a significant influence on the measured CPT penetration resistance around the probe.

Last, CPT based criteria for liquefaction assessment suggested by Robertson and Wride, 1998 are re-interpreted and presented in a form allowing direct evaluation of the influence of fines on the liquefaction resistance.

- Cyclic resistance of sands containing fines is determined almost similar to the clean sand for the same relative density up to about 50%.
- A pronounced increase in liquefaction resistance is observed with an increase in fines content above 50% relative density.
- The above mentioned manipulations indicate that increase of liquefaction resistance at the current method is caused by an increase of $(CRR)_{7.5}$ and decrease of penetration resistance due to effect of fines.

6.2. **Suggestions for Future Research**

The effects of soil density index as relative density or void ratio on liquefaction potential does not significantly come to light yet, hence, relative density of soils found by derivative methods from field test should be compared with labroratory standart methods to overcome the uncertainties of related studies. Also, performed field and laboratory studies provide to observe the effects soil consolidation characterstics and fines content on liquefaction resistance with using by other liquefaction potential screening methods based on SPT and shear wave velocity tests.

REFERENCES

Ambraseys, N.N. (1988). *Engineering seismology: Part II.* Earthquake engineering & structural dynamics, 17(1), 51-105.

Andrews, D.C.A., Martin, G.R. (2000). *Criteria for liquefaction of silty soils.* 12th World Conference of earthquake Engineering, New Zealand.

Andrus, R.D., Stokoe, K.H. (1997). *Liquefaction resistance Based on shear Wave Velocity.* Proceedings NCEER Workshop on Evulation of Liquefaction resistance of soils. Netional Center for Earthquake Engineering, State University of New York at buffalo, USA, 89-128.

Arulmoli, K., Arulanandan, K., Seed, H.B. (1985). *New method for evaluating liquefaction potential.* Journal of Geotechnical Engineering, 111(1), 95-114.

Bray, J., Sancio, R. (2006). *Assessment of the liquefaction susceptibility of fine-grained soils.* Journal of Geotechnical and Geoenvironmental Engineering, ASCE, Vol. 132(9), 1165–1177.

Campanella, R.G., Stewart, W.P. (1992). *Seismic cone analysis using digital signal processing for dynamic site characterization.* Canadian Geotechnical Journal, Vol.29, No.3, June 1992, 477-486.

Carraro, J.A.H., Bandini, P., Salgado, R. (2003). *Liquefaction resistance of clean and nonplastic silty sands based on cone penetration resistance.* Journal of Geotechnical and Geoenvironmental Engineering, ASCE, Vol. 129(11), 965-976.

Casagrande, A. (1936). *Characterstics of cohesionless soils affecting the stability of slopes and earth fills.* Journal of Boston society of Civil Engineers.

Chien, L.K., Oh, Y.N., Chang, C.H. (2002). *Effects of fines content on liquefaction strength and dynamic settlement of reclaimed soiL.* Canadian Geotechnical Journal, Vol. 39, 254-265.

Chung, S.F., Randolph, M.F., Schneider, J. A. (2006). *Effect of penetration rate on penetrometer resistance in clay*. Journal of Geotechnical and Geoenvironmental Engineering, ASCE, Vol.132(9), 1188-1196.

Cubrinovski, M., Rees, S., Bowman. E. (2010). *Effects of non-plastic fines on liquefaction resistance of sands soils*. Earthquake Engineering in Europe, Geotechnical, Geological and Earthquake Engineering. 125-144.

Dobry, R., Ladd, R.S., Felix, Y., Riley, M., Powell, D. (1982). *Prediction of pore water pressure buildup and liquefaction of sands during earthquakes by the cyclic strain method* (Vol. 138): US Department of Commerce, National Bureau of Standards.

Ecemis, N. (2008). *Effects of permeability and compressibility on liquefaction screening using cone penetration resistance.* Ph.D. Dissertation Department of Civil Structural and Environmental Engineering; State University of New York at Buffalo, 282.

Ecemis, N. (2013). *Effects of consolidation characteristics on CPT cone resistance and liquefaction resistance in silty soil.,* The Scientific and Technological Research Council of Turkey-TUBITAK, Project No: 110M602, Ankara, Turkey.

Ecemis, N. (2014). *Effects of permeability and compressibility on liquefaction assessment of silty soils using cone penetration resistance.* European Union 7th framework program Marie Curie fellowship, (Grant No: PIRG05-GA-2009-248218.

Finnie, I. M. S., Randolph, M. F. (1994). *Punch-through and liquefaction induced failure of shallow foundations on calcareous sediments*. Proc. Int. Conf. on Behaviour of Offshore Structures, Boston, 217-230.

Green, R.A., Terri, G.A. (2005). *Number of equivalent cycles concept for liquefaction evaluations.* Revisited, Journal of Geotechnical and Geoenvironmental Engineering, ASCE, Vol. 131(4), 477-488.

House, A.R., Oliveira, J.R.M.S., Randolph, M.F. (2001). *Evaluating the coefficient of consolidation using penetration tests.* Int. J. of Physical Modelling in Geotechnics,, Vol.1, No.3, 17-25.

Huang, A.B., Huang, Y.T., Ho, F.J., (2005). *Assessment of liquefaction potential for a silty sand in Central Western Taiwan.* 16th ICSMGE ,2653-2657**.**

Idriss, I.M., Boulanger, R.W. (2006). *Semi-empirical procedures for evaluating liquefaction potential during earthquakes.* Soil Dynamics and Earthquake Engineering, 26, 115–130**.**

Idriss, I.M., Boulanger, R.W. (2008). *Soil liquefaction during earthquakes*. Earthquake Engineering Research Institute, MNO-12.

Ishihara, K. (1996). *Soil Behaviour in Earthquake Geotechnics*. Oxford University Press.

Ishihara, K. (1985). *Stability of Natural Deposits During Earthquakes*. Proceedings of the 11th International Conference on soil Mechanics San Frasisco, Vol.1. 321-376.

Jamiolkowski M., Balid, G. Bellotti, R., Ghionna V., Pasqualini E. (1985). *Penetration Resistance and Liquefaction of sands.* Proceedings of 11th ICSMFE, 4;1891-1896.

Kayen, R.E., Mitchell, J. K., Seed, R. B., Lodge, A., Nishio, S., Coutinho, R. (1992). *Evaluation of SPT-, CPT-, and shear wave-based methods for liquefaction potential assessment using Loma Prieta data*.Proc., 4th Japan-U.S. Workshop on Earthquake Resistant Des. of Life-line Fac. and Countermeasures for Soil Liquefaction, Tech. Rep.NCEER-92-0019.

Kayen, R.E., Mitchell, J.K. (1997). *Assessment of Liquefaction Potential During Earthquakes by Arias Intensity.* Journal of Geotechnical and Geoenvironmental Engineering , December. 1162-1174.

Kim, K., Prezzi, M., Salgado, R. Lee, W. (2008). *Effect of penetration rate on cone penetration resistance in saturated clayey soils*. Journal of Geotechnical and Geoenvironmental Engineering, Vol.134(8), 1142-1153.

Kokusho, T., Hara, T., Murahata, K., (2005). *Liquefaction strength of fines containing sands compared with cone resistance in triaxial specimens.* Pre-Workshop Proc. 2nd Japan-US Workshop on Testing, Modelling, and Simulation in Geomechanics, Kyoto, Japan, 280-296.

Kramer, S.L., Seed, H.B. (1988). *Initiation of soil liquefaction under static loading conditions.* Journal of Geotechnical Engineering, 114(4), 412-430.

Kramer, S.L. (1996). *Geotechnical earthquake engineering.* Prentice-Hall Civil Engineering and Engineering Mechanics Series, Upper Saddle River, NJ: Prentice Hall,| c1996, 1.

Kuribayashi, E., Tatsuoka,F. (1975), *Brief review of liquefaction during earthquakes in Japan.* Soils and Foundations, Vol.15, No.4, pp.81-92.

Law, K.T., Cao, Y. L., He, G.N. (1990). *An energy approach for assessing seismic liquefaction potential.* Canadian Geotechnical Engineering, ASCE,120(9), 1554,1569.

Lee, D.S., Elsworth, D., Hryciw, R. (2008). *Hydraulic conductivity measurement from on-the-fly uCPT sounding and from VicCPT*. Journal of Geotechnical and Geoenvironmental Engineering, ASC), 1720-1729.

Lee, K.L., and Seed, H.B. (1967). *Cyclic Stress conditions causing Liquefaction of Sand.* Jo. Of the Soil Mechanics and foundations Divition, ASCE, Vol.93 No. SM1. 47-70.

Liao, S.C., Whitman, R.V. (1986). *Overburden correction factors for SPT in sand.* ASCE Journal of Geotechnical Engineering 112(3):373-377.

Liu, A.H., Stewart, J.P., Abrahamson, N.A., Moriwaki, Y. (2001). *Equivalent number of uniform stress cycles for soils liquefaction analysis.* Journal of Geotechnical and Geoenvironmental Engineering, ASCE, Vol. 127(12), 1017-1026.

Lunne, T., Robertson, P.K., Powell, J.J.M. (1997). *Cone penetration testing.* Geotechnical Practice.

Mitchell, J.K., Tseng, D.J., (1990). *Assessment of Liquefaction Potential by Cone Penetration Resistance.* Proceedings from the H. Bolton Seed Memorial Symposium Duncan, J. M. BiTech, Vancouver, B. C., 335-350

Parez, L., Fauriel, L. (1988). *Le piezocone ameliorations apportees a la reconnaissance de sols*. Revue Francaise de Geotech. Vol. 44, 13-27.

RADIUS Project. (1999), *Izmir deprem senaryosu ve master plani,* http://www.izmirbld.gov.tr/izmirdeprem/izmirrapor.htm

Randolph, M.F., Hope, S. (2004). *Effect of cone velocity on cone resistance and excess pore pressures.* Proc. Int. Sym. on Eng. Practice and Performance of Soft Deposits, Osaka,147-152.

Robertson, P.K., Campanella, R.G. (1985). *Liquefaction Potential of Sands Using the Cone Penetration Test.* Journal of Geotech. Div., ASCE, Vol. 111, No. 3, 384-407 (U.B.C. Soil Mechanics Series No. 64).

Robertson, P.K., Woeller, D.J. Finn, W.D.L. (1992). *Seismic cone penetration test for evaluating liquefaction potential under cyclic loading.* Canadian Geotechnical Journal, Vol. 29, No. 4. 686-695.

Robertson, P.K., Wride C.E. (1998). *Evaluating cyclic liquefaction potential using the cone penetration test.* Canadian Geotechnical Journal, Vol. 35(3), 442-459.

Seed, H.B., Idriss, I.M., Arango, I. (1983). *Evaluation of Liquefaction Potential using Field Performance data.* Journal of Geotechnical Engg, ASCE, 109(3); 458-482.

Seed, H.B., De Alba, P., (1986). *Use of SPT and CPT tests for evaluating the liquefaction resistance of sands.* Use of in situ tests in geotechnical engineering, Geotech. Spec. Publ. No. 6 , ASCE, New York, 1249–1273.

Seed, R.B., Tokimatsu, K., Harder, L.F., and Chung, R.M. (1985). *Influence of SPT Procedures in Soil Liquefaction resistance Evulations.* Journal of Geotechnical Engineering, ASCE Vol.111. 1425-1445.

Seed, R.B., Cetin, KO, Moss, RES, Kammerer, AM, Wu, J., Pestana, JM, & Riemer, MF. (2001). *Recent advances in soil liquefaction engineering and seismic site response evaluation*: NISEEE.

Silver, M.L., Seed, H.B. (1971). *Volume changes in sands during cyclic loading.* Journal of Soil Mechanics & Foundations Div.

Shibata, T., Teparaska, W. (1988). *Evaluation of Liquefaction Potential of Soils Using Cone Penetration Testing.* Soils and Foundations, Journal of the Japanese Society of Soil Mechanics and Foundation Engineering, 28(2), 49-60

Stark, T.D., Olson, S.M. (1995). *Liquefaction resistance using CPT and field case histories.* Journal of Geotechnical Engineering, ASCE, (1995), Vol. 121(12), 856-869.

Suzuki, Y., Tokimatsu, K., Koyamada, K., Taya, Y., Kubota, Y. (1995). *Field correlation of soil liquefaction based on CPT data.* Proc. Int. Symp. On Cone Penetration Testing, Vol. 2, Linköping, Sweden, October, 583-588.

Tezcan, S.S., Özdemir, Z., (2004). *Liquefaction risk analysis and mapping techniques.* Higher Education Research Foundation.

Thevanayagam, S., Ecemis, N. (2008). *Effects of permeability on liquefaction resistance and cone resistance.* Geotechnical Earthquake Engineering and Soil Dynamics IV, ASCE.

Tokimatsu, K., Uchida A. (1990). *Correlation between Liquefaction Resistance and Shear Wave Velocity.* Soils and Foundations, 30, 2, 33-42.

Turkey-US Geotechnical Reconnaissance Team Report of Adapazari Earthquake, 1999.

Wang, W. (1979). *Some Findings in Soil Liquefaction.* Report Water Conservancy and Hydro-electric Power Scientific Research Institute, Beijing, China, 1-17.

Wang, W. (1981). *Foundation Problems in Aseismatic Design of Hydraulic Structures.* In Proceedings of the Joint US – PRC Microzonation Workshop, 11-16 September, Harbin, PRC.

Youd, T. L., et al. (2001) *Liquefaction resistance of soils: Summary report from the 1996 NCEER and 1998 NCEER/NSF workshops on evaluation of liquefaction resistance of soils.* Journal of Geotechnical and Geoenvironmental Engineering, Vol. 127(10), 817–833.

Youd, T.L., Hoose, S.N. (1977). *Liquefaction susceptibility and geologic setting.* Paper presented at the Proc., 6th World Conf. on Earthquake Engineering.

Youd, T.L. (1991). *Mapping of earthquake-induced liquefaction for seismic zonation.* Paper presented at the International Conference on Seismic Zonation, 4th, August.

Zlatovic, S., Ishihara, K. (1997). *Normalized behavior of very loose non-plastic soils: Effects of fabric.* Soils and Found., Tokyo, Vol. 37(4), 47-56.

APPENDIX A

BORING LOGS

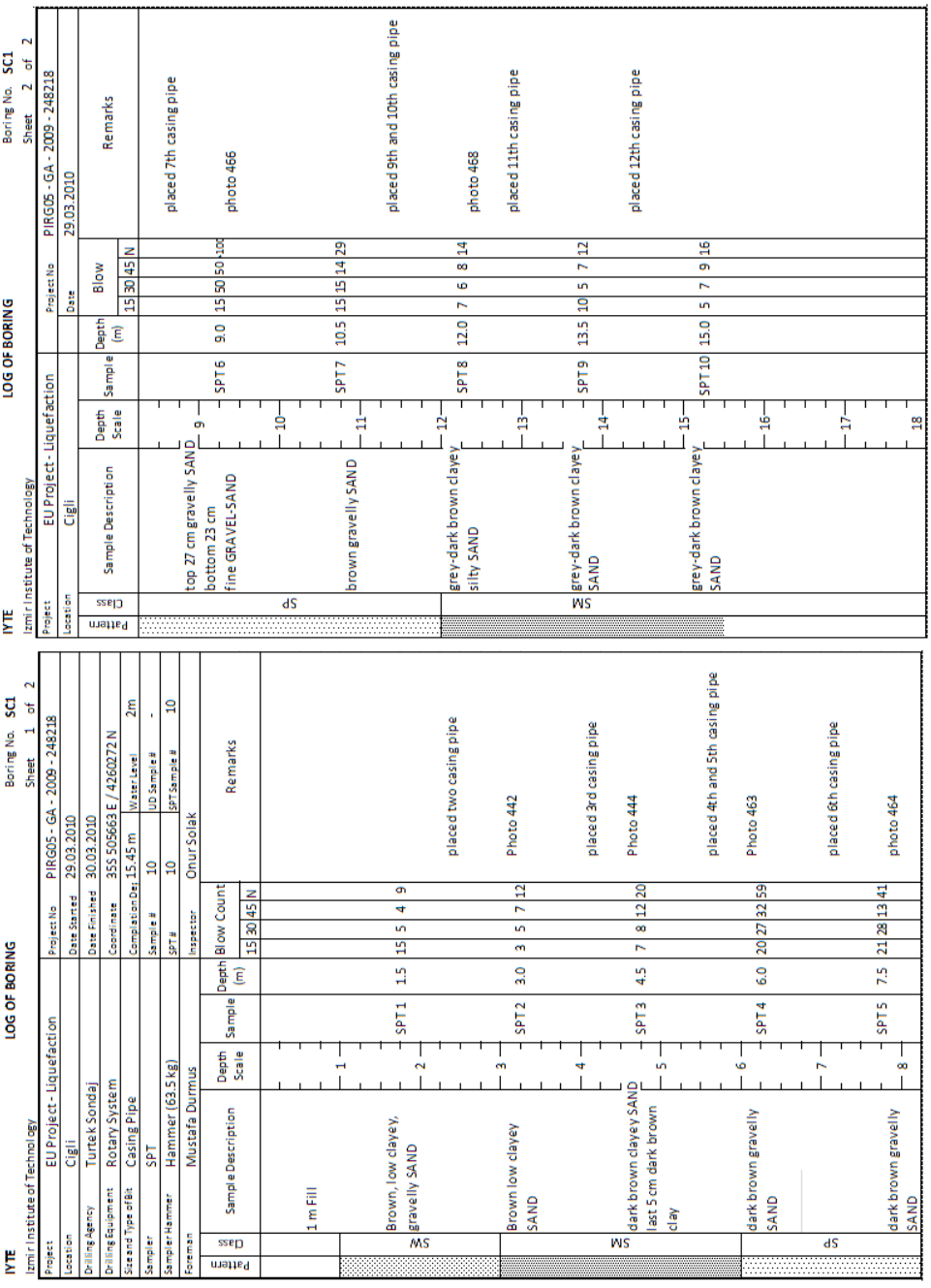

Figure A.1. Boring logs of SPT insitu tests

(Cont. on next page)

Figure A.1. (cont.)

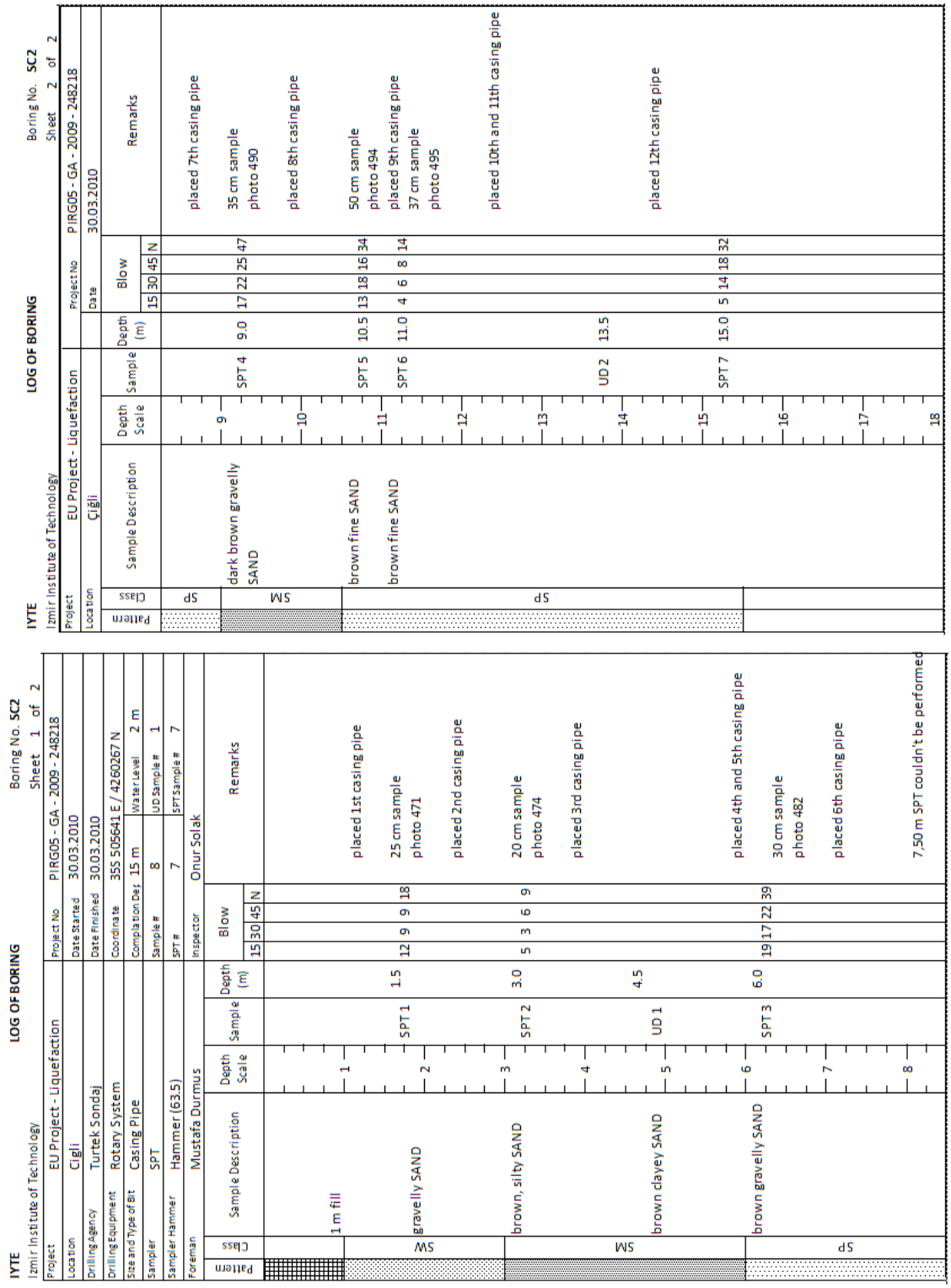

(Cont. on next page)

Figure A.1. (cont.)

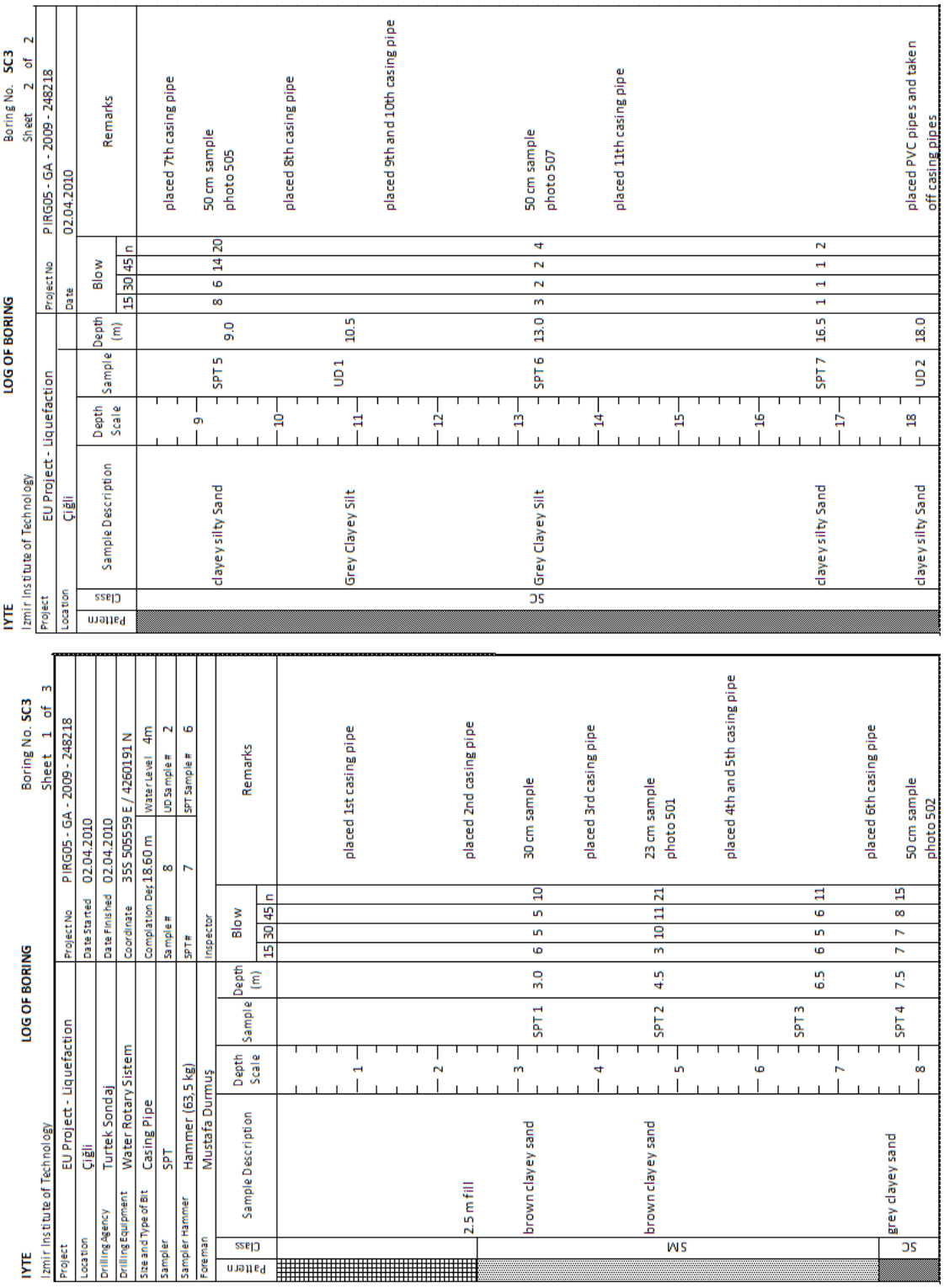

(Cont. on next page)

Figure A.1. (cont.)

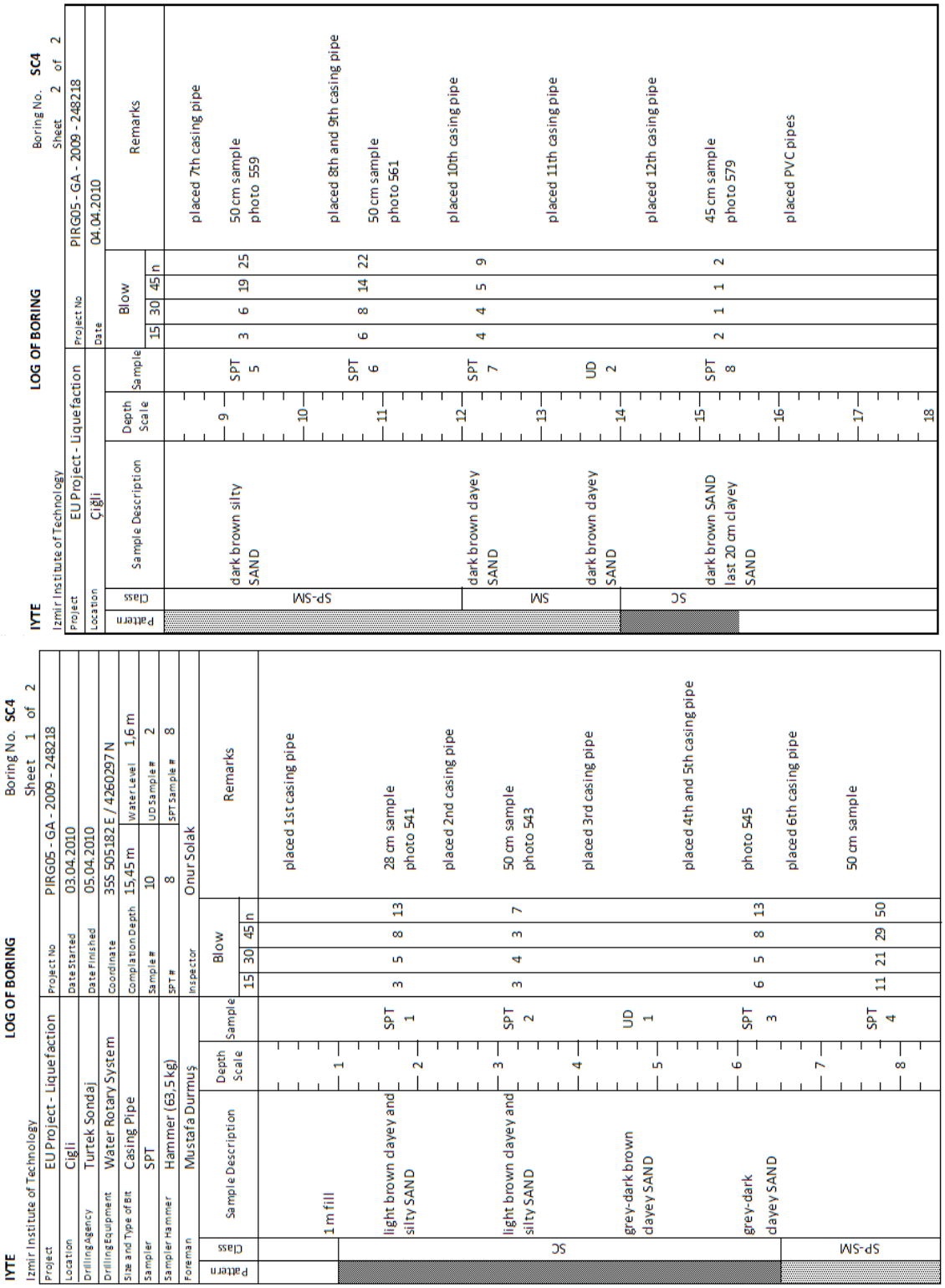

(Cont. on next page)

Figure A.1. (cont.)

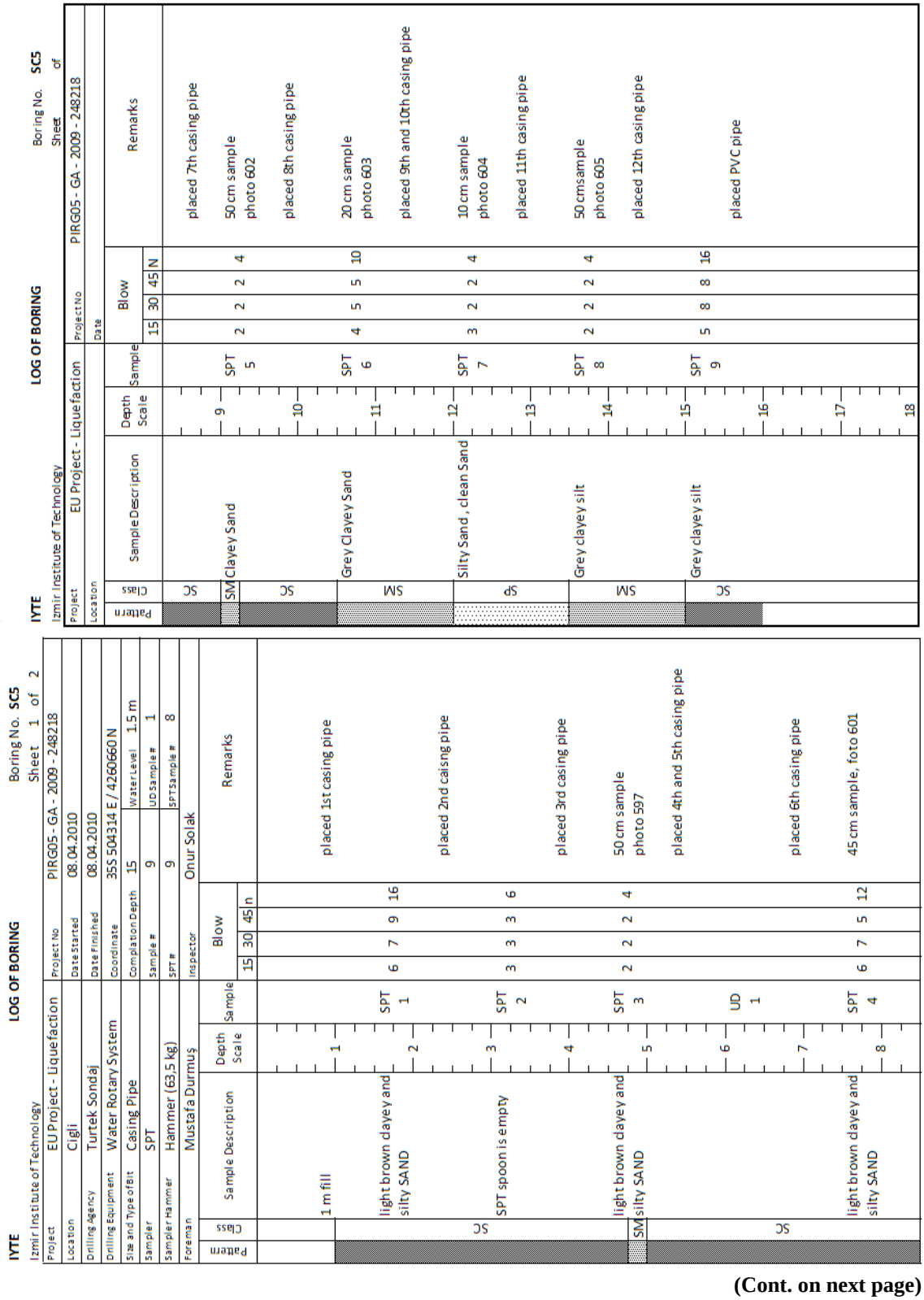

(Cont. on next page)

Figure A.1. (cont.)

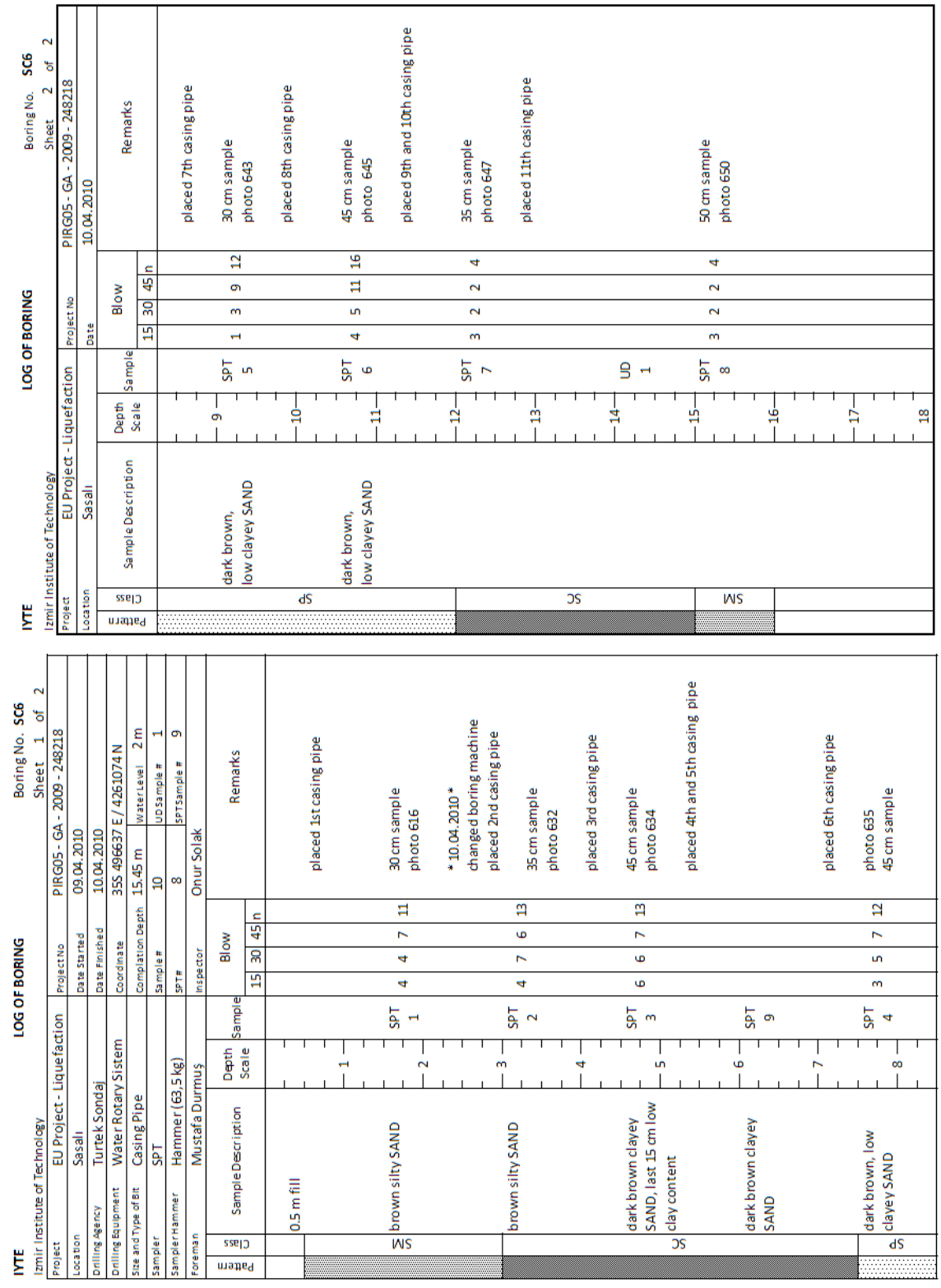

(Cont. on next page)

Figure A.1. (cont.)

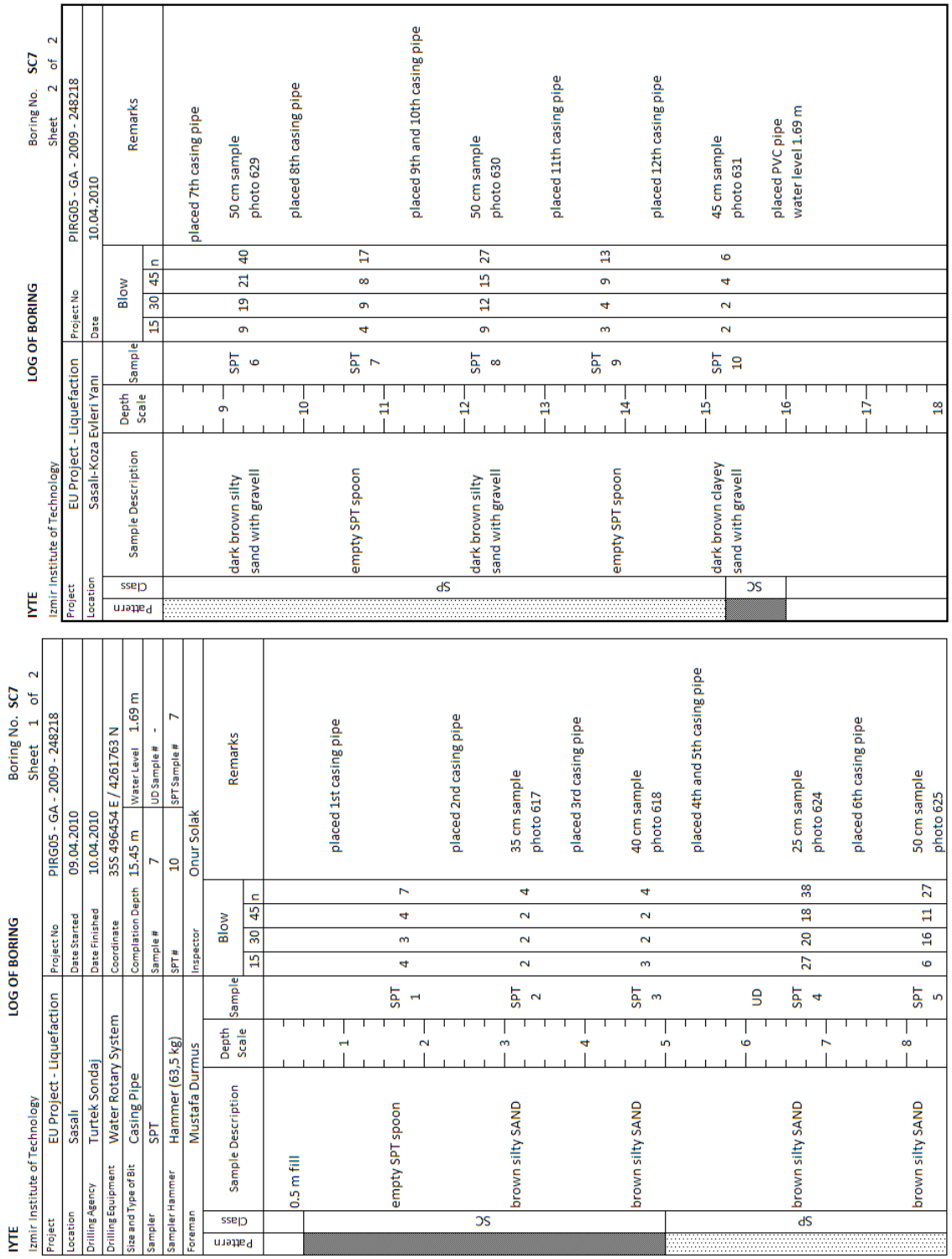

(Cont. on next page)

Figure A.1. (cont.)

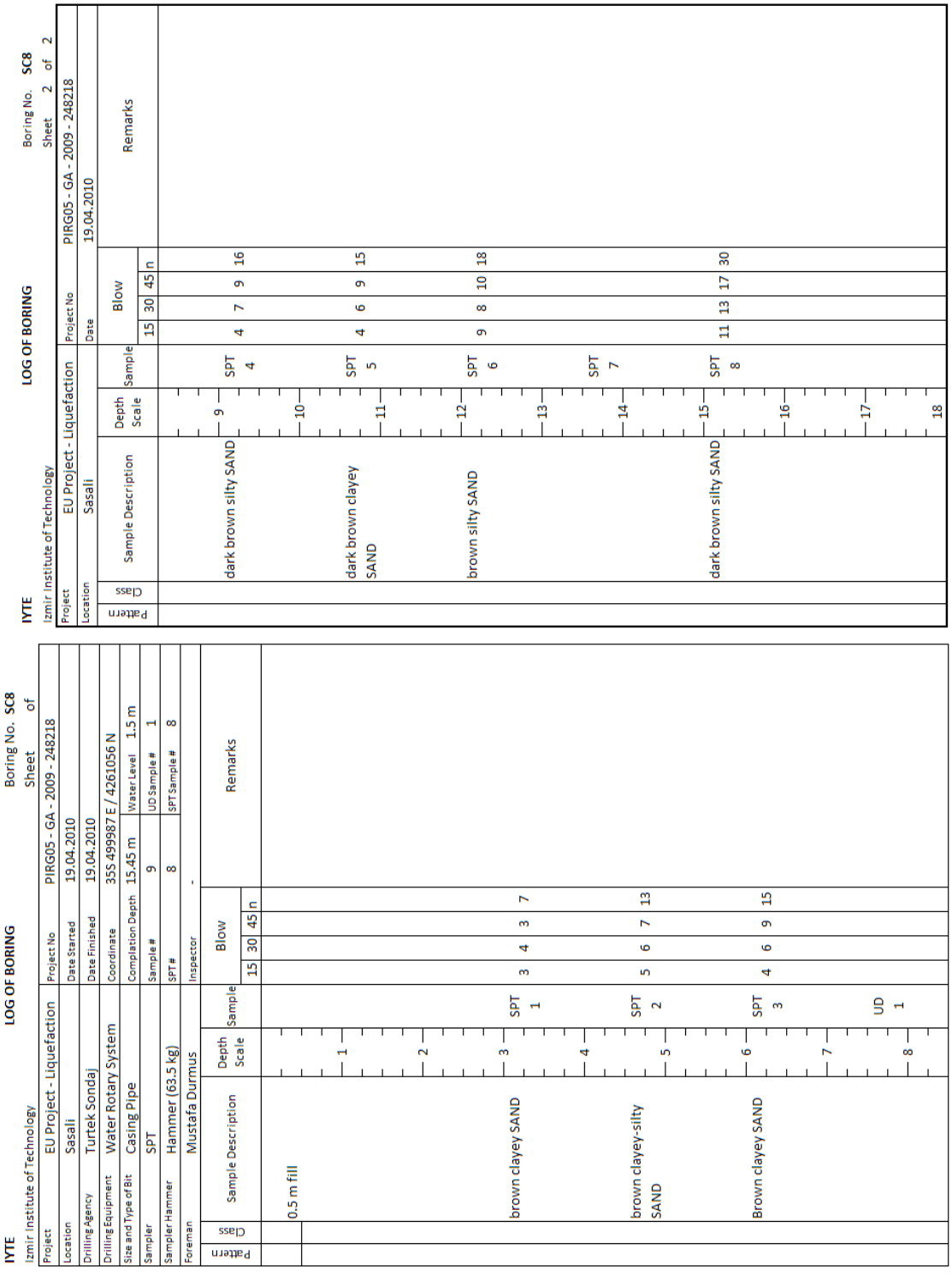

(Cont. on next page)

Figure A.1. (cont.)

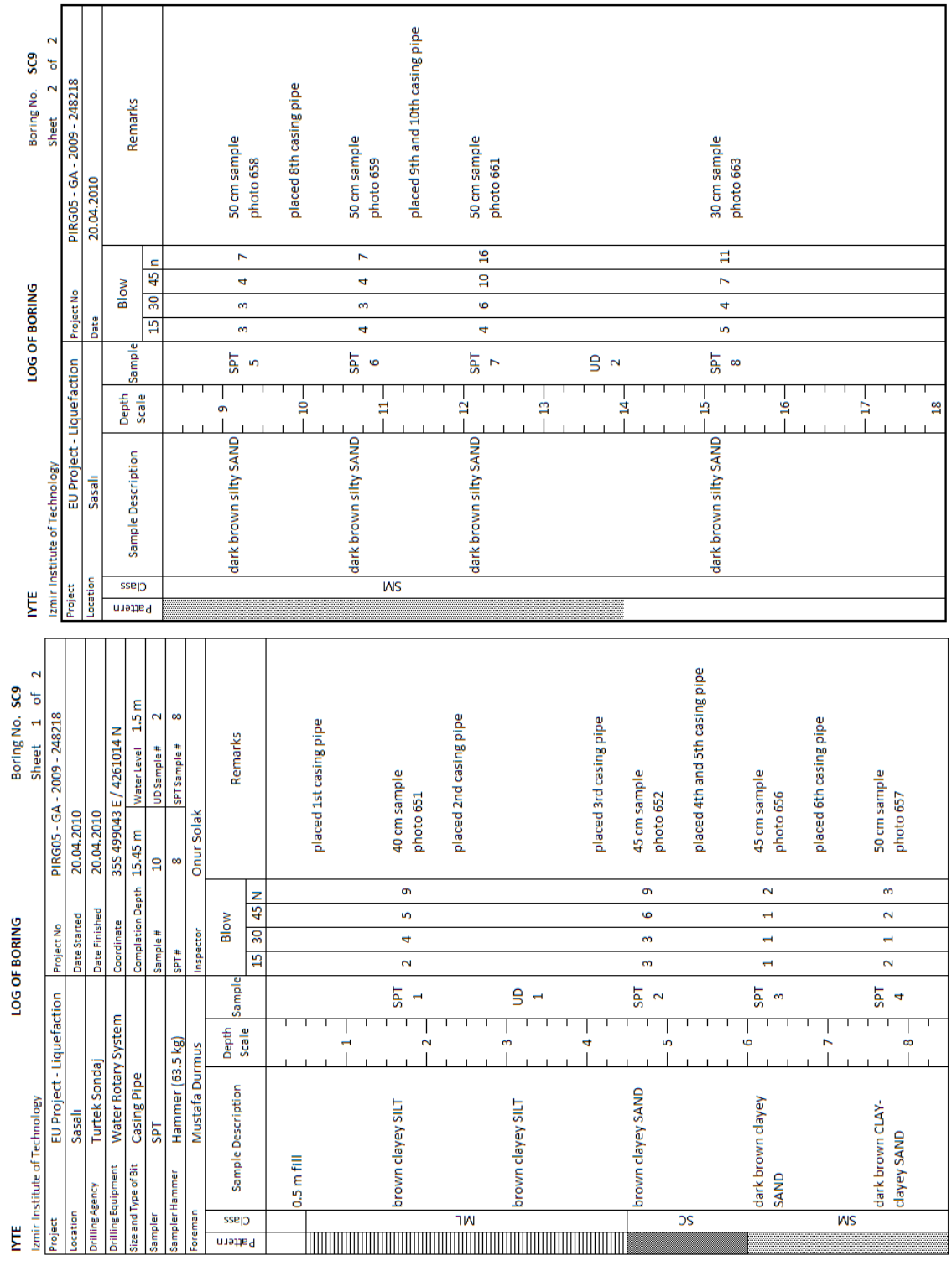

(Cont. on next page)

Figure A.1. (cont.)

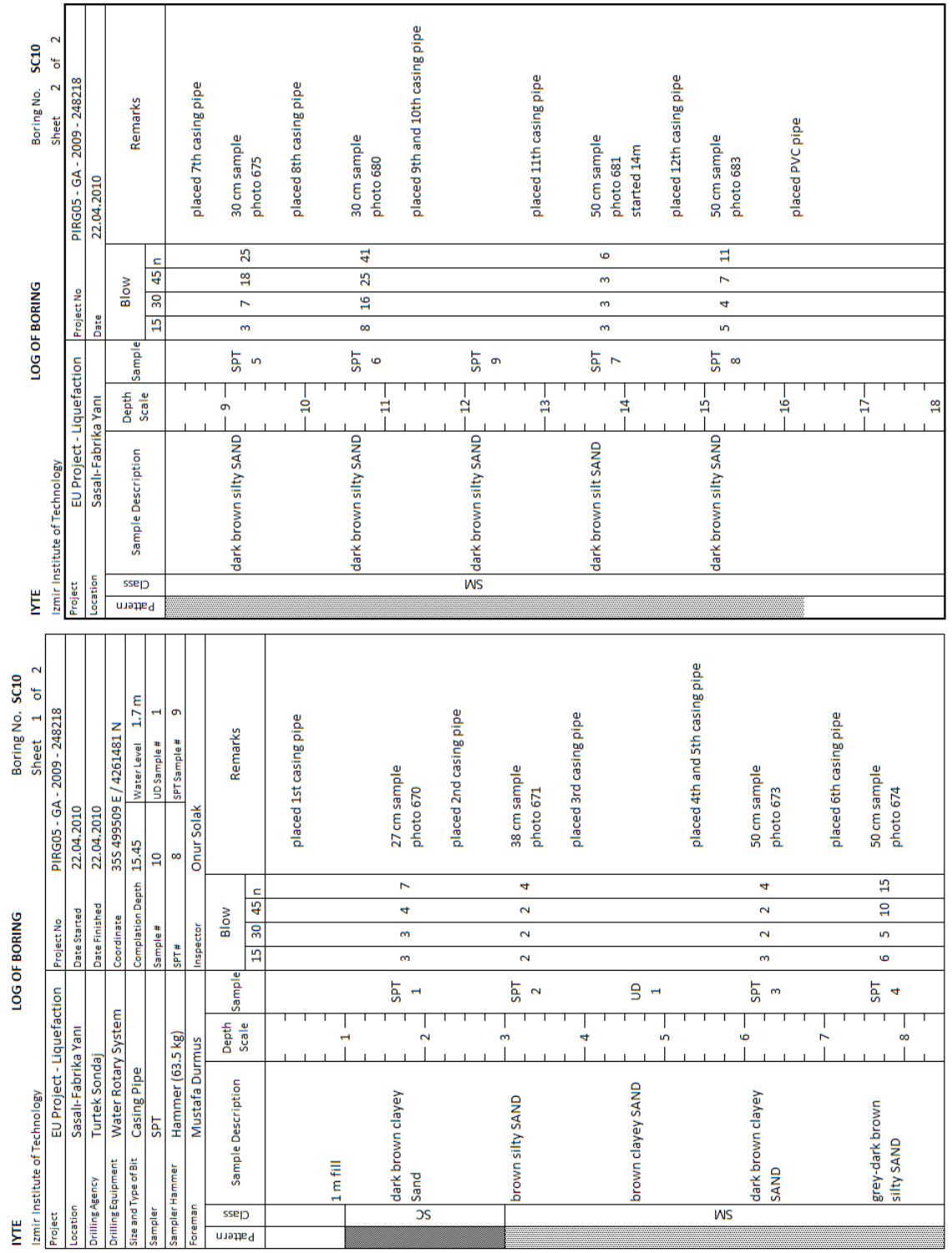

(Cont. on next page)

Figure A.1. (cont.)

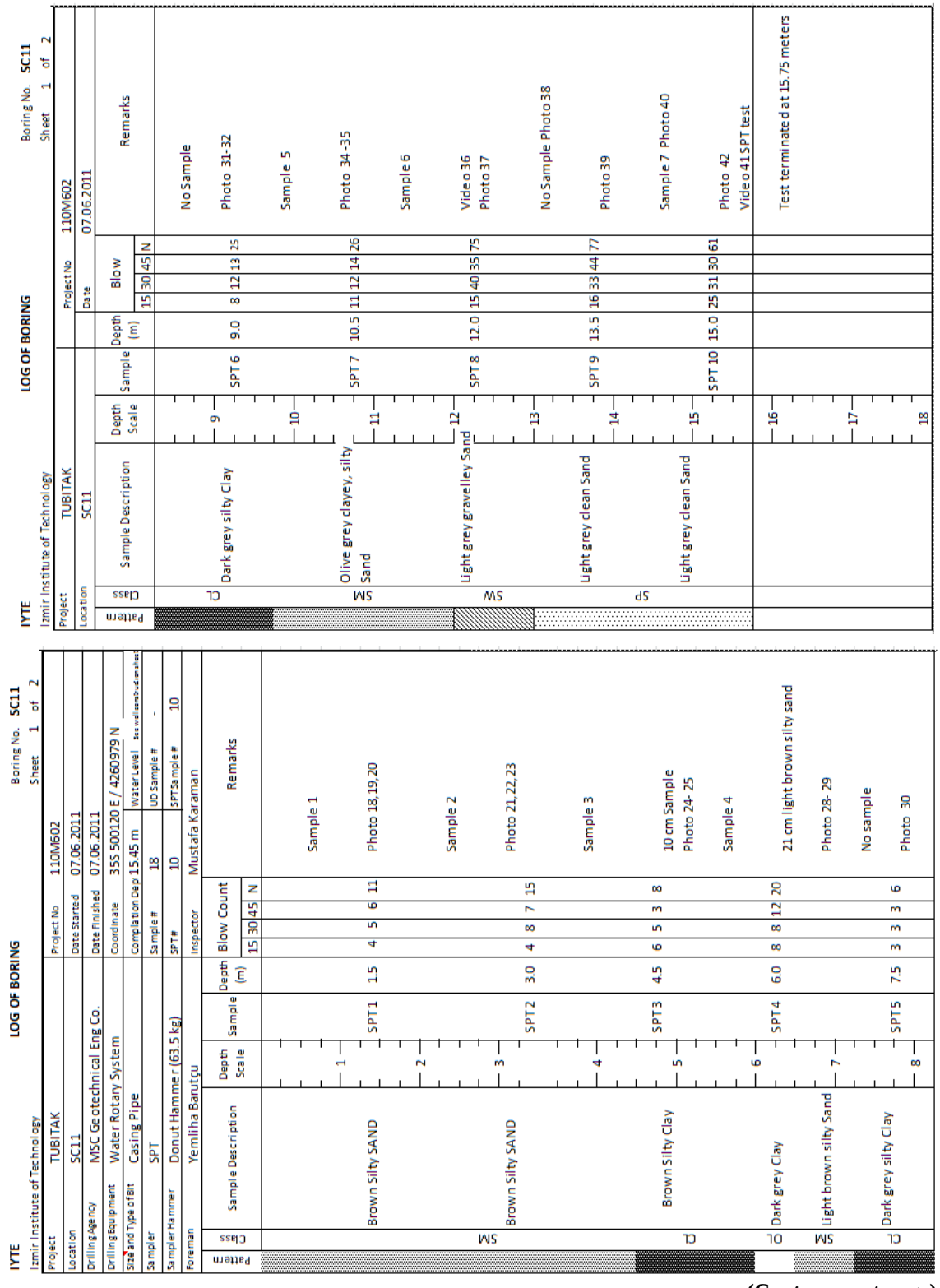

(Cont. on next page)

Figure A.1. (cont.)

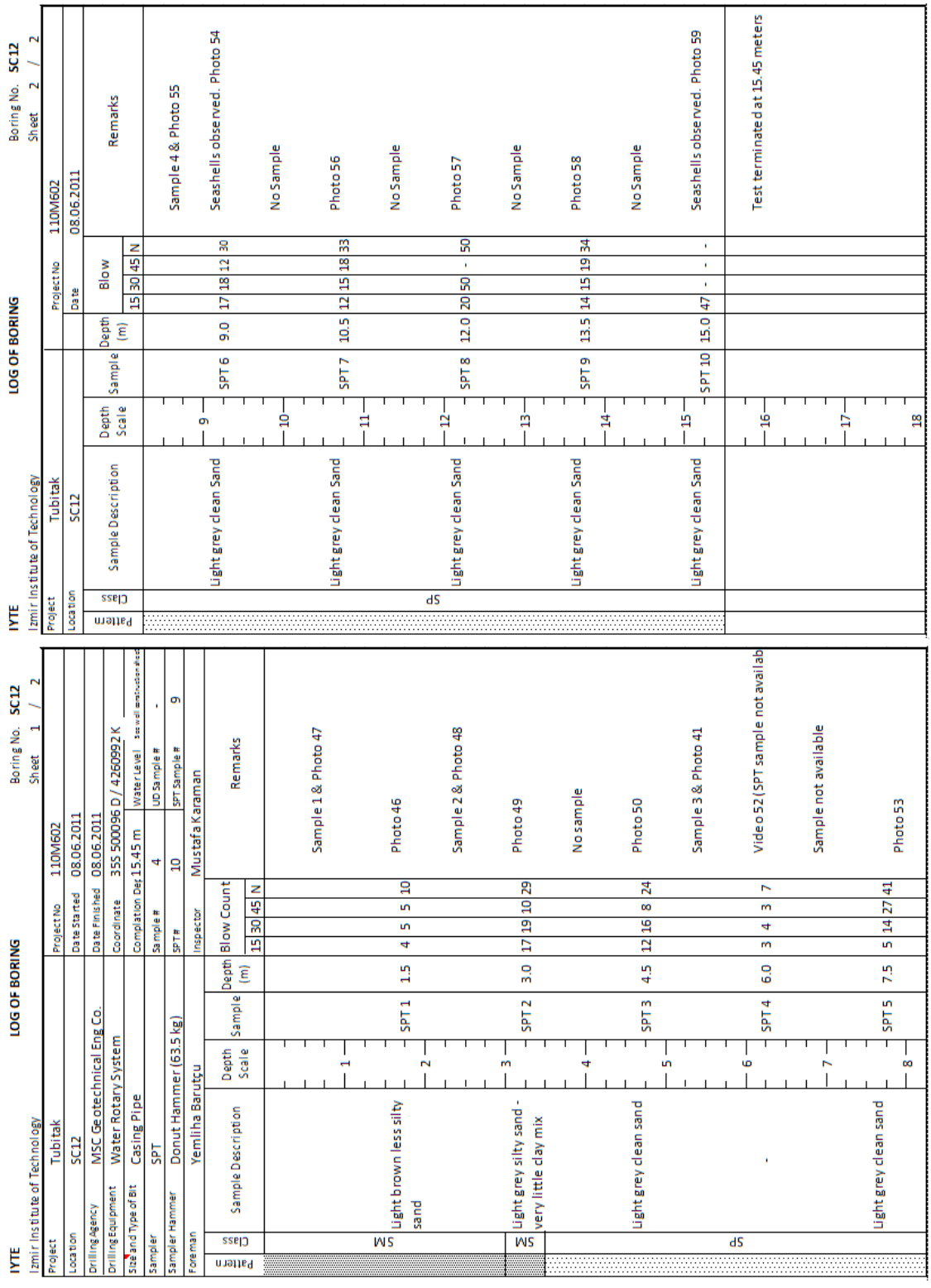

(Cont. on next page)

Figure A.1. (cont.)

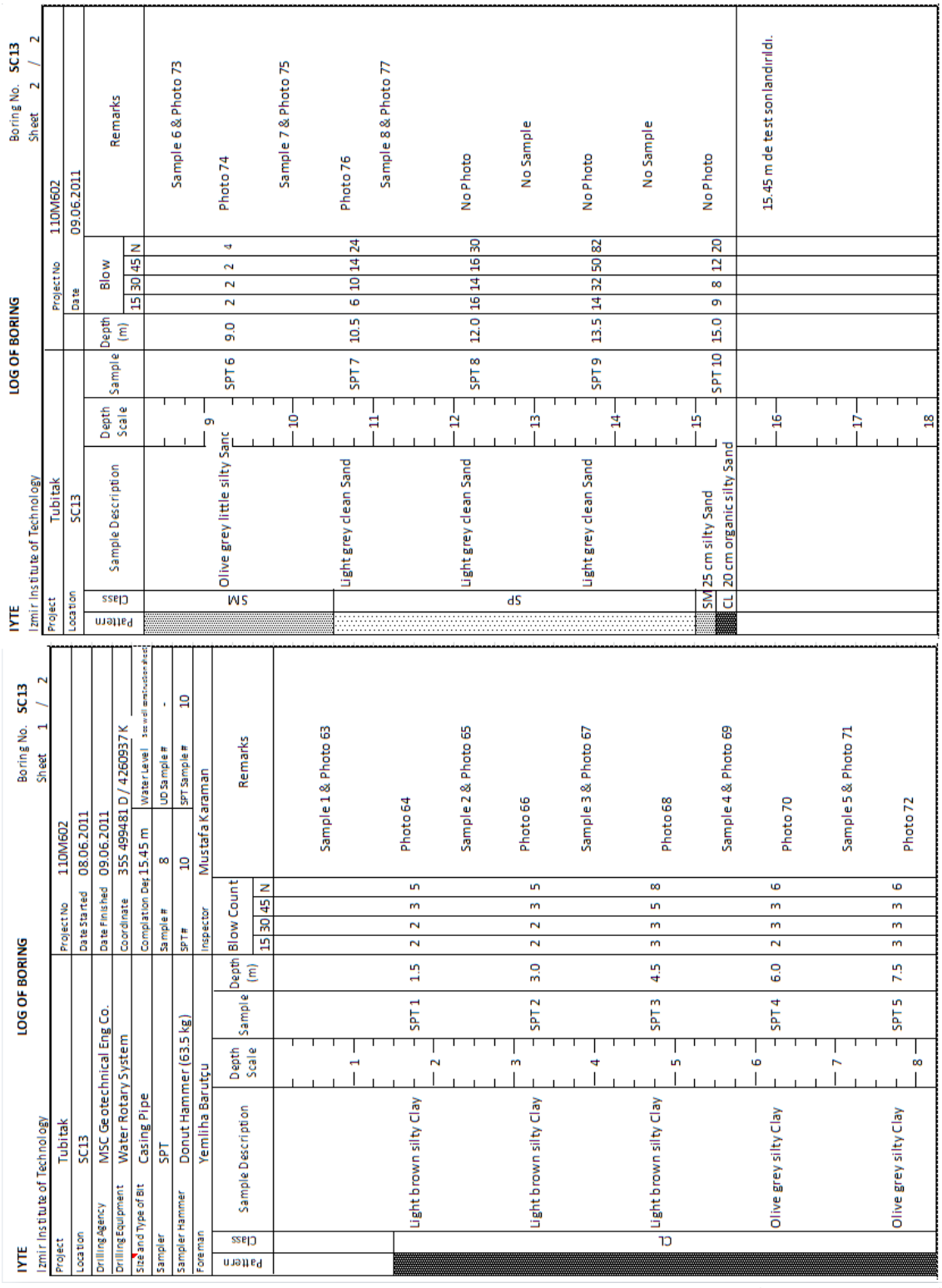

(Cont. on next page)

Figure A.1. (cont.)

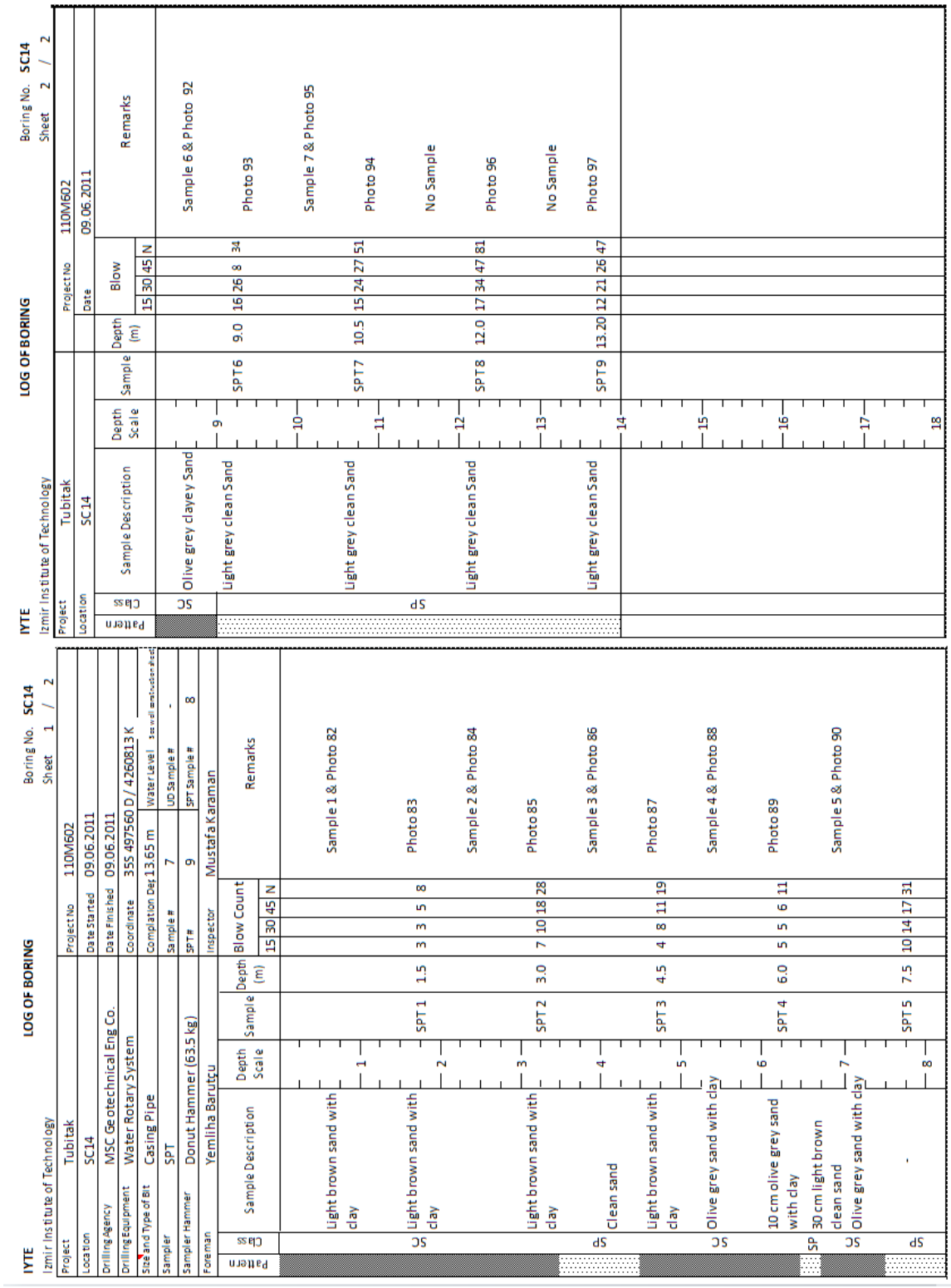

(Cont. on next page)

Figure A.1. (cont.)

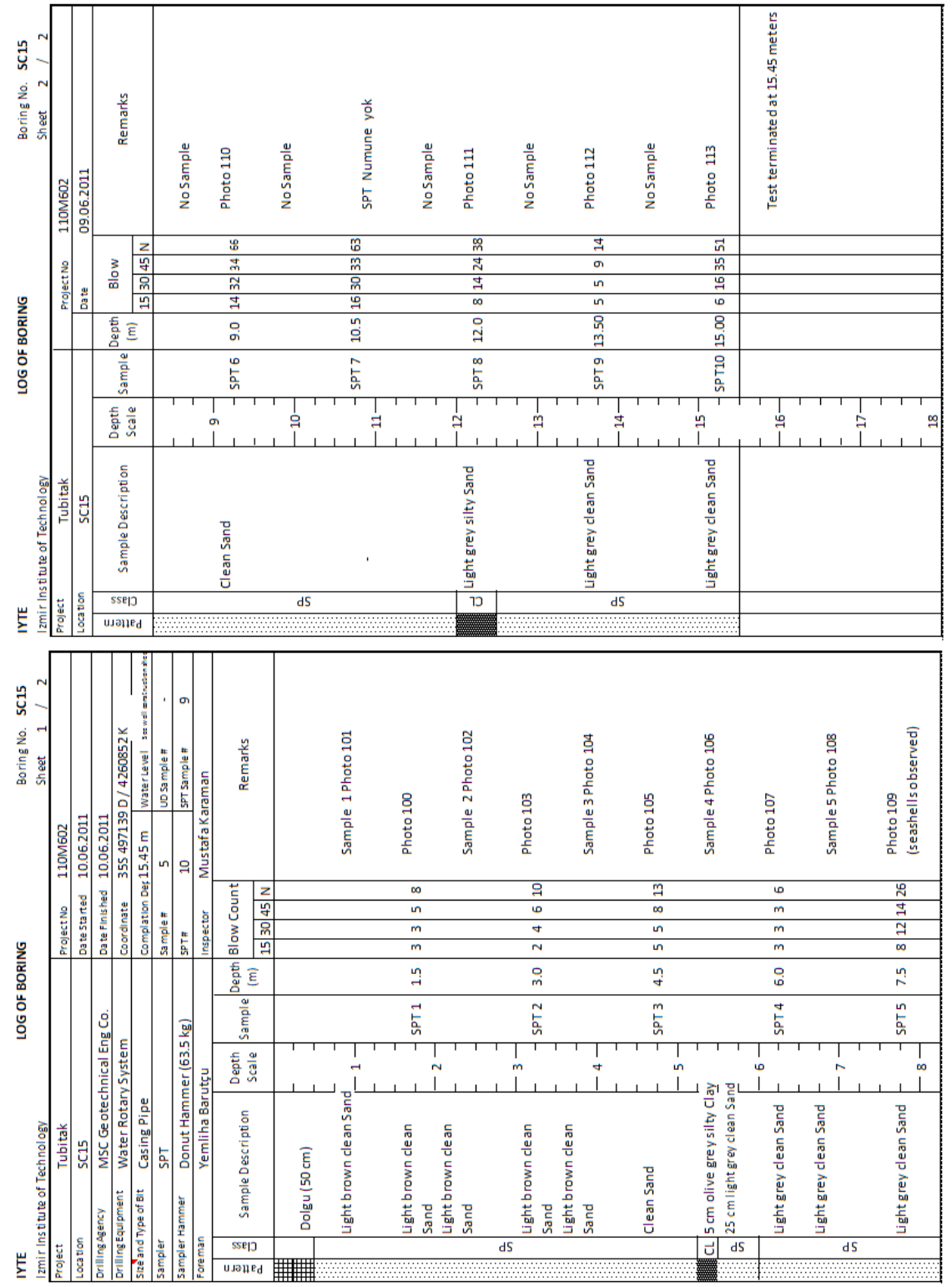

(Cont. on next page)

Figure A.1. (cont.)

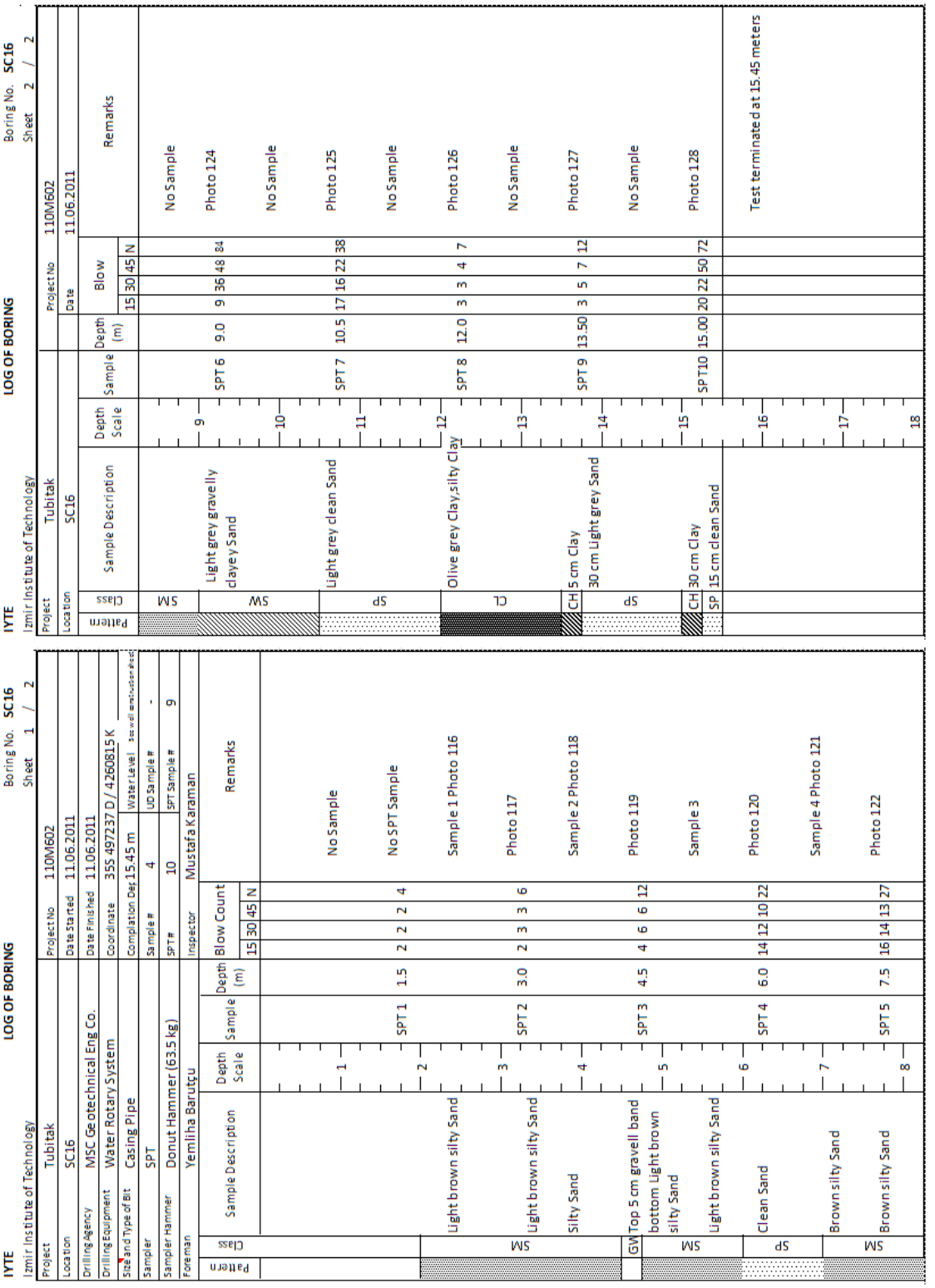

(Cont. on next page)

Figure A.1. (cont.)

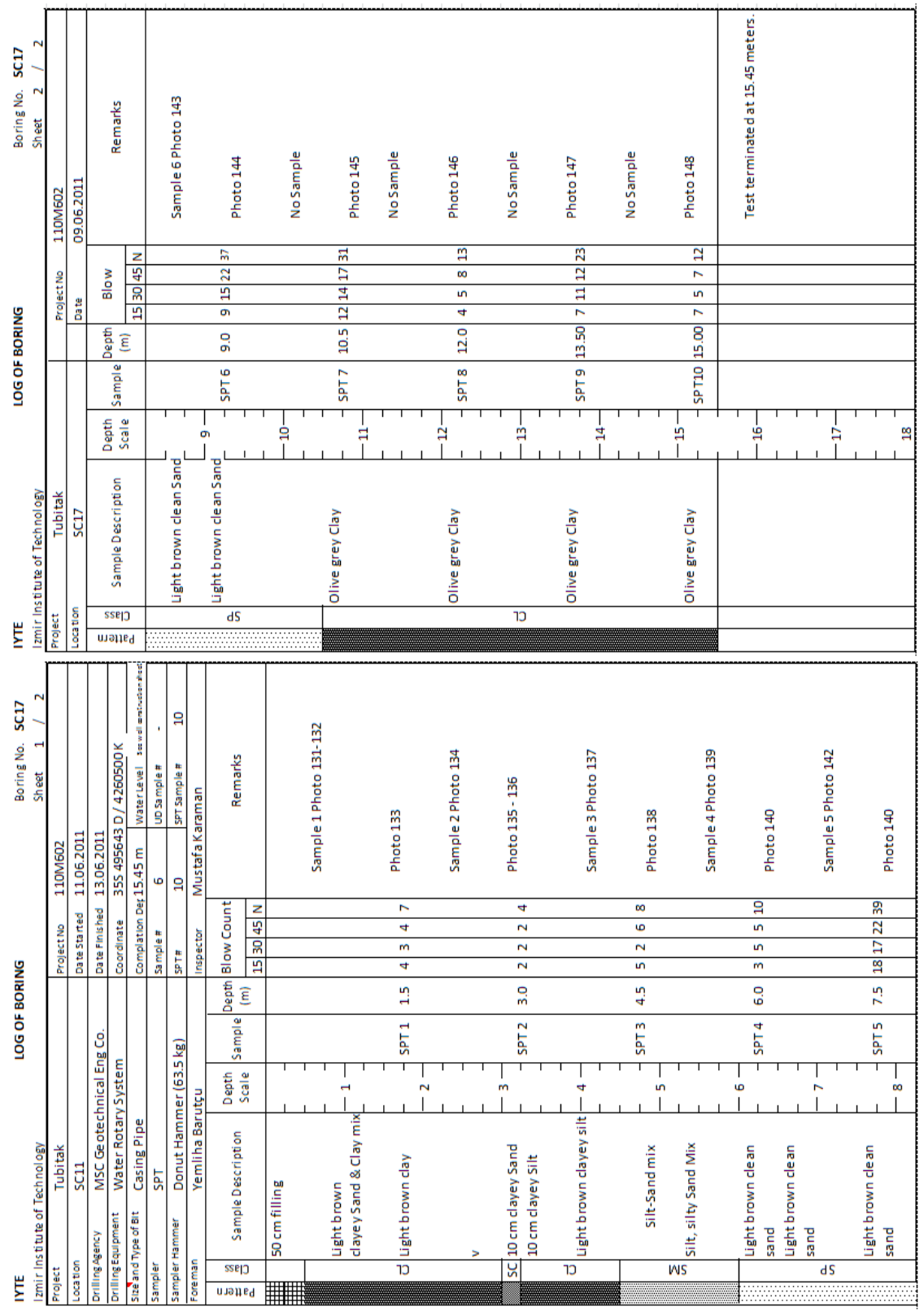

(Cont. on next page)

Figure A.1. (cont.)

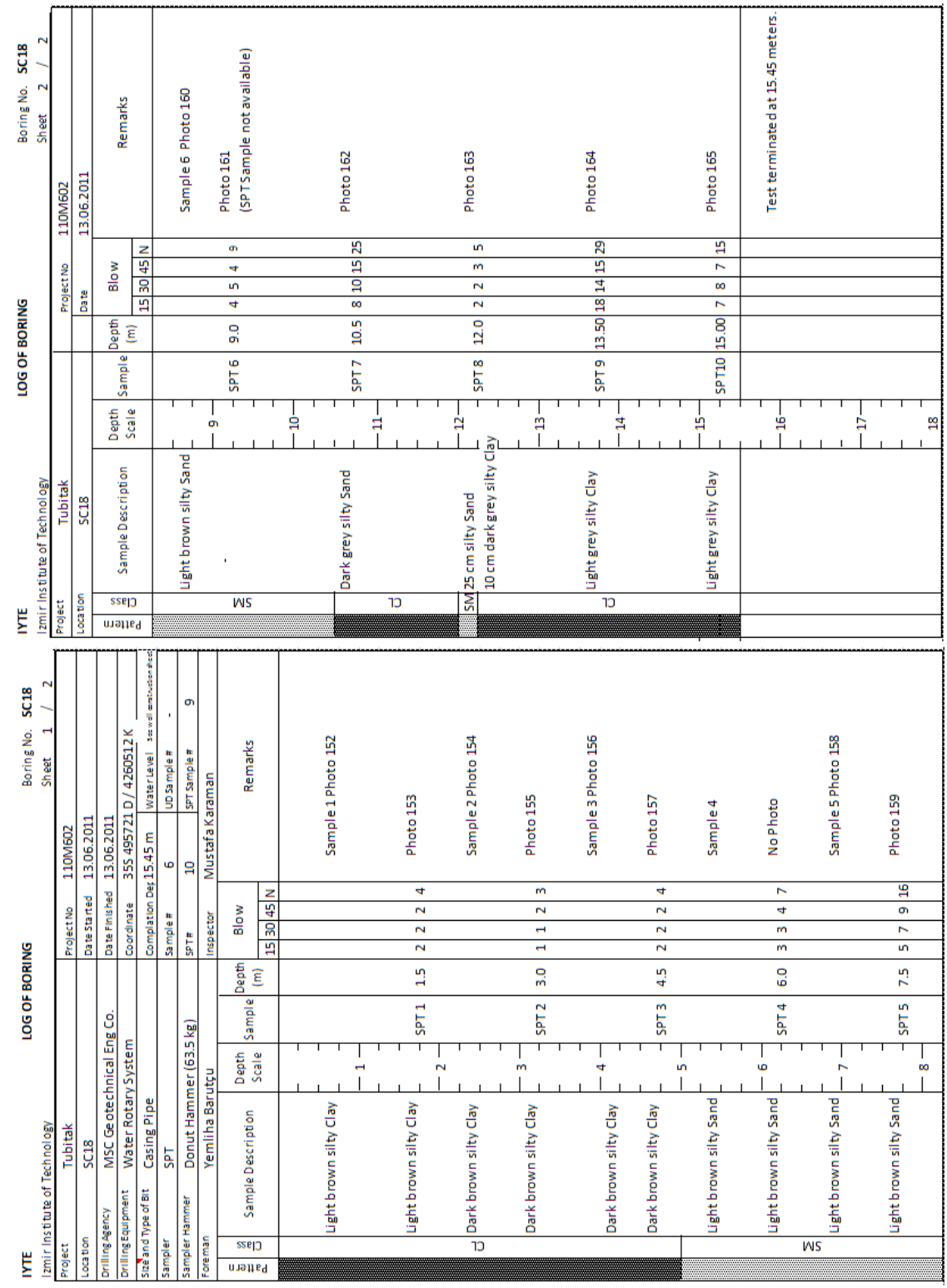

(Cont. on next page)

Figure A.1. (cont.)

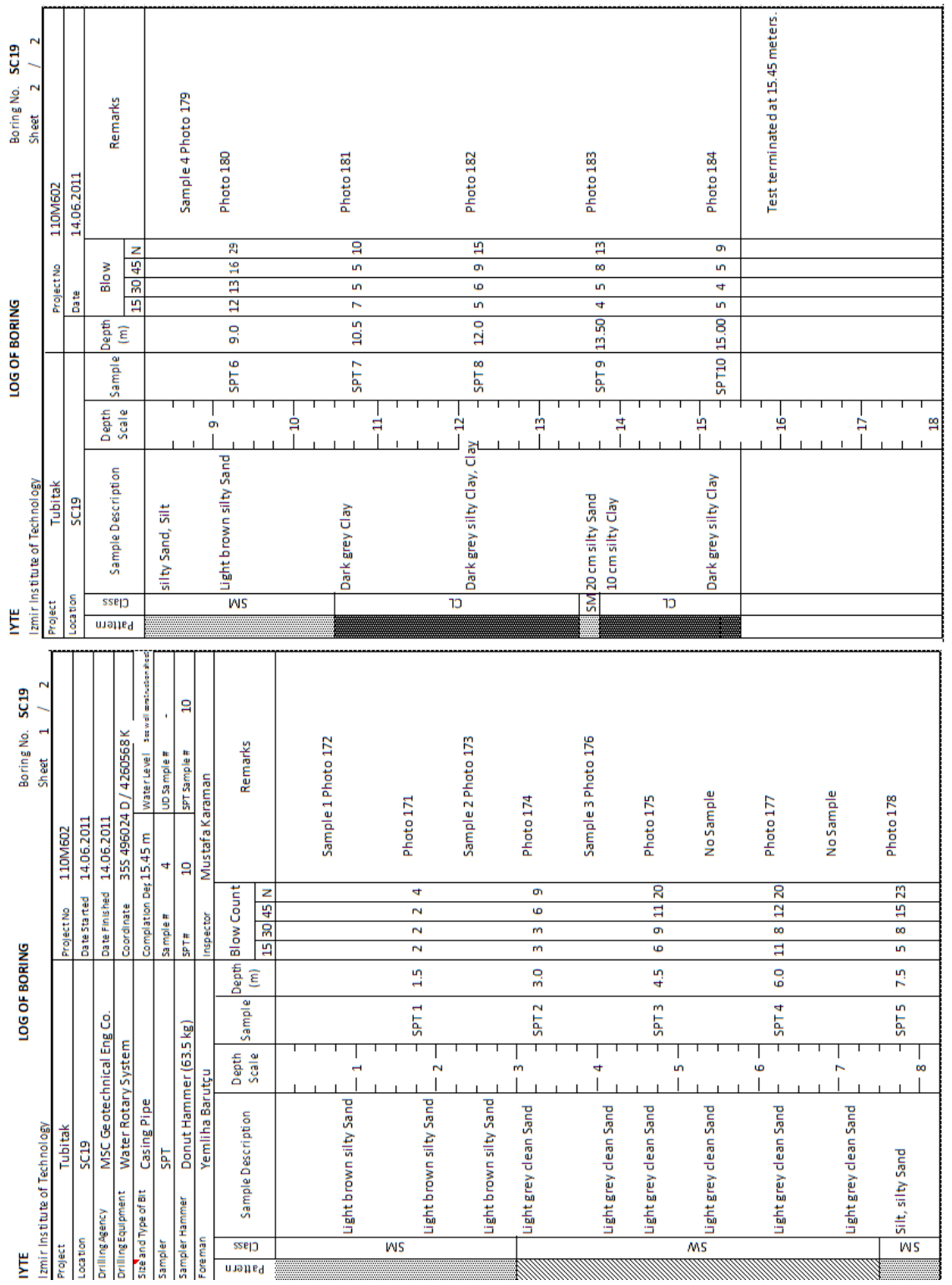

(Cont. on next page)

Figure A.1. (cont.)

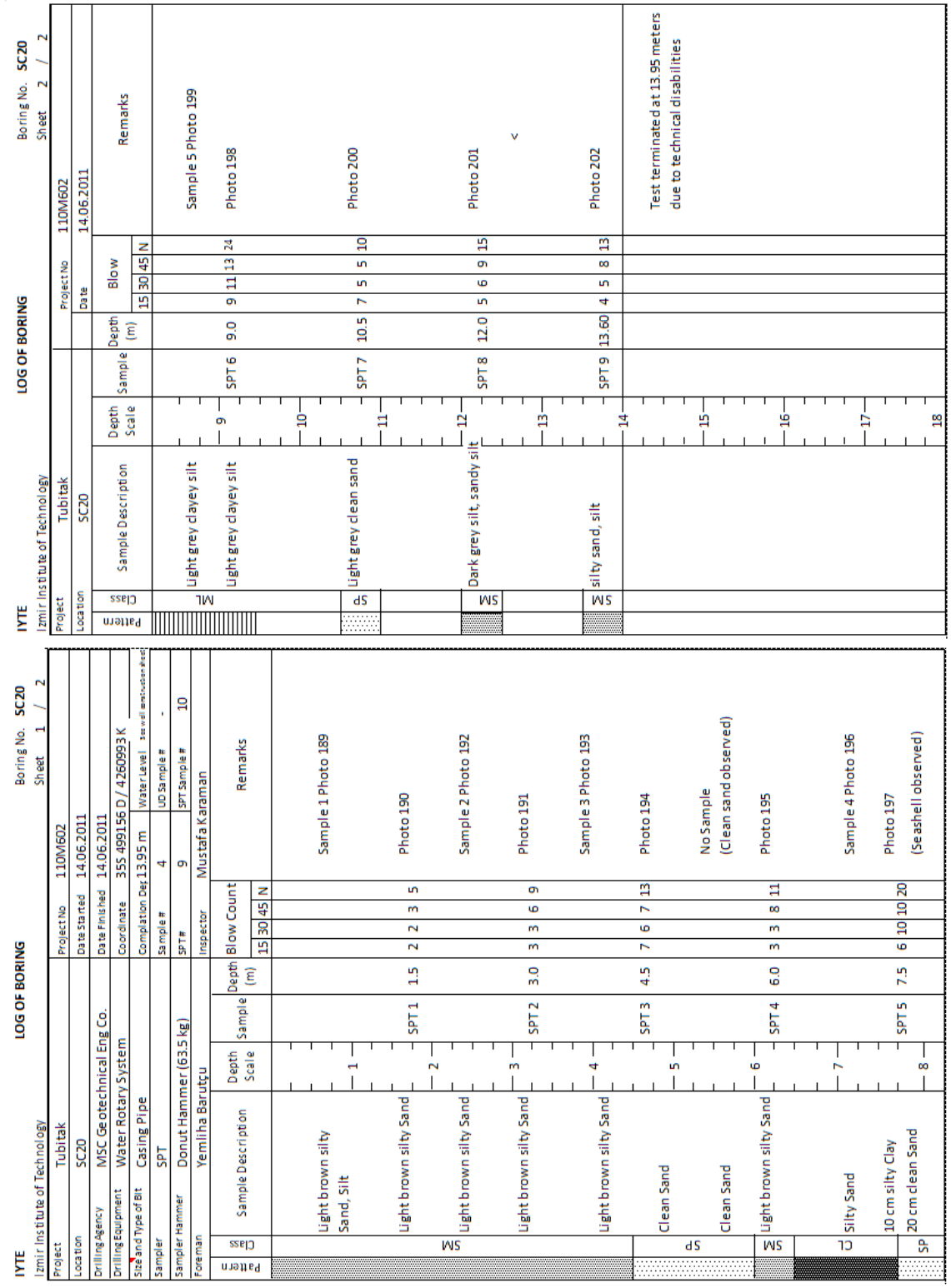

APPENDIX B

CPTu TEST RESULTS GRAPHICS

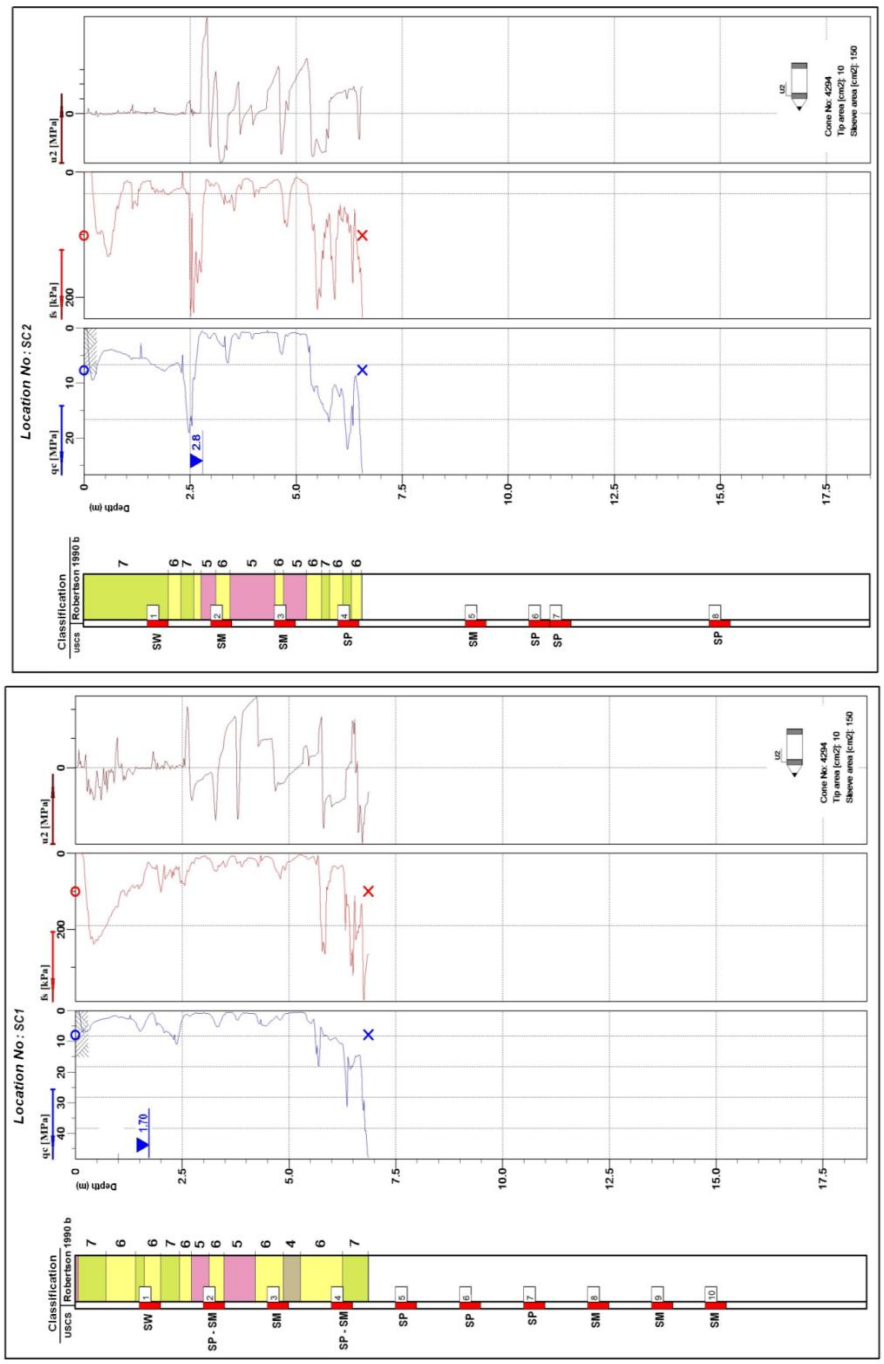

Figure B.1. CPTu insitu tests results

(Cont. on next page)

Figure B.1. (cont.)

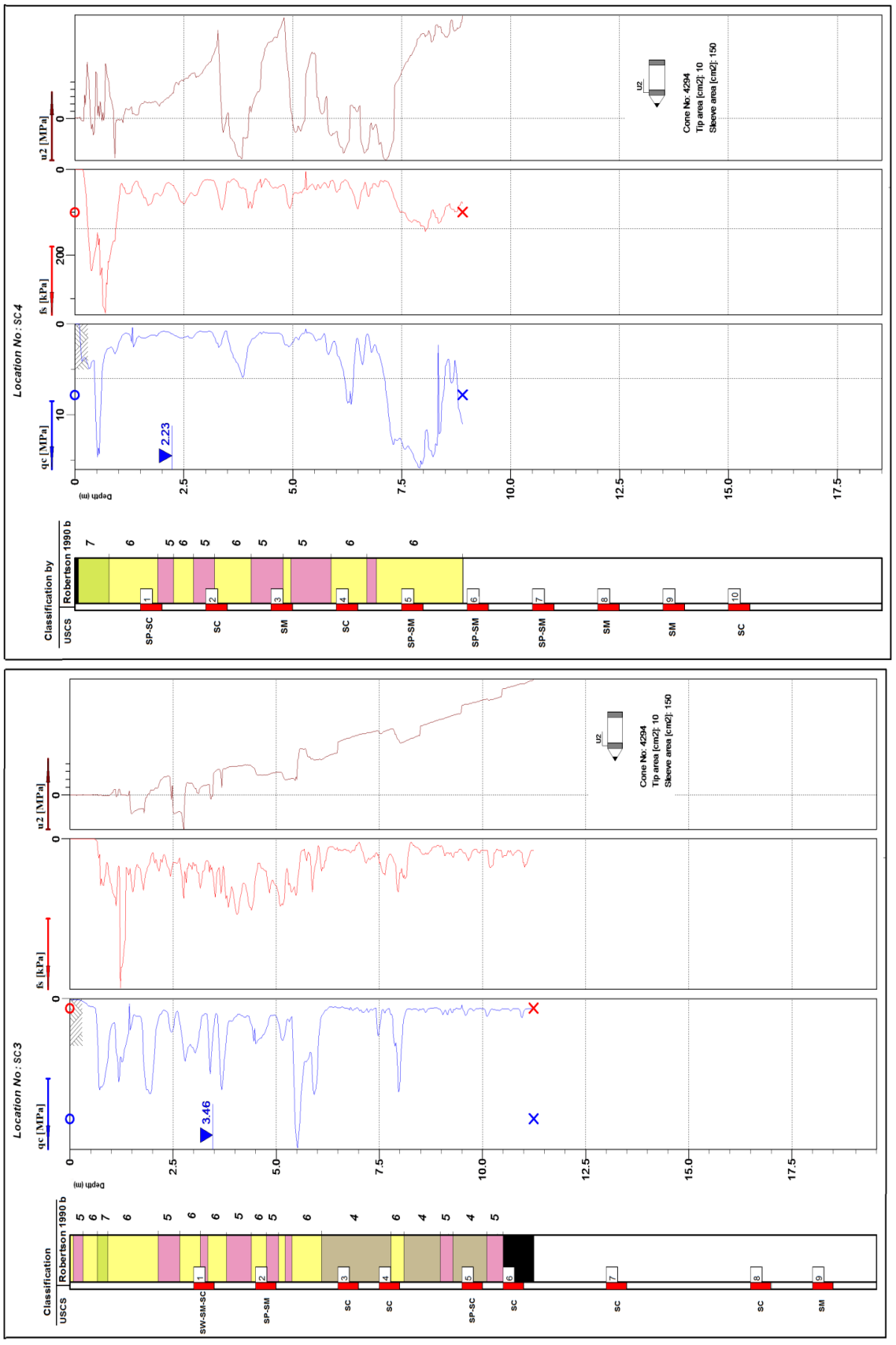

(Cont. on next page)

Figure B.1. (cont.)

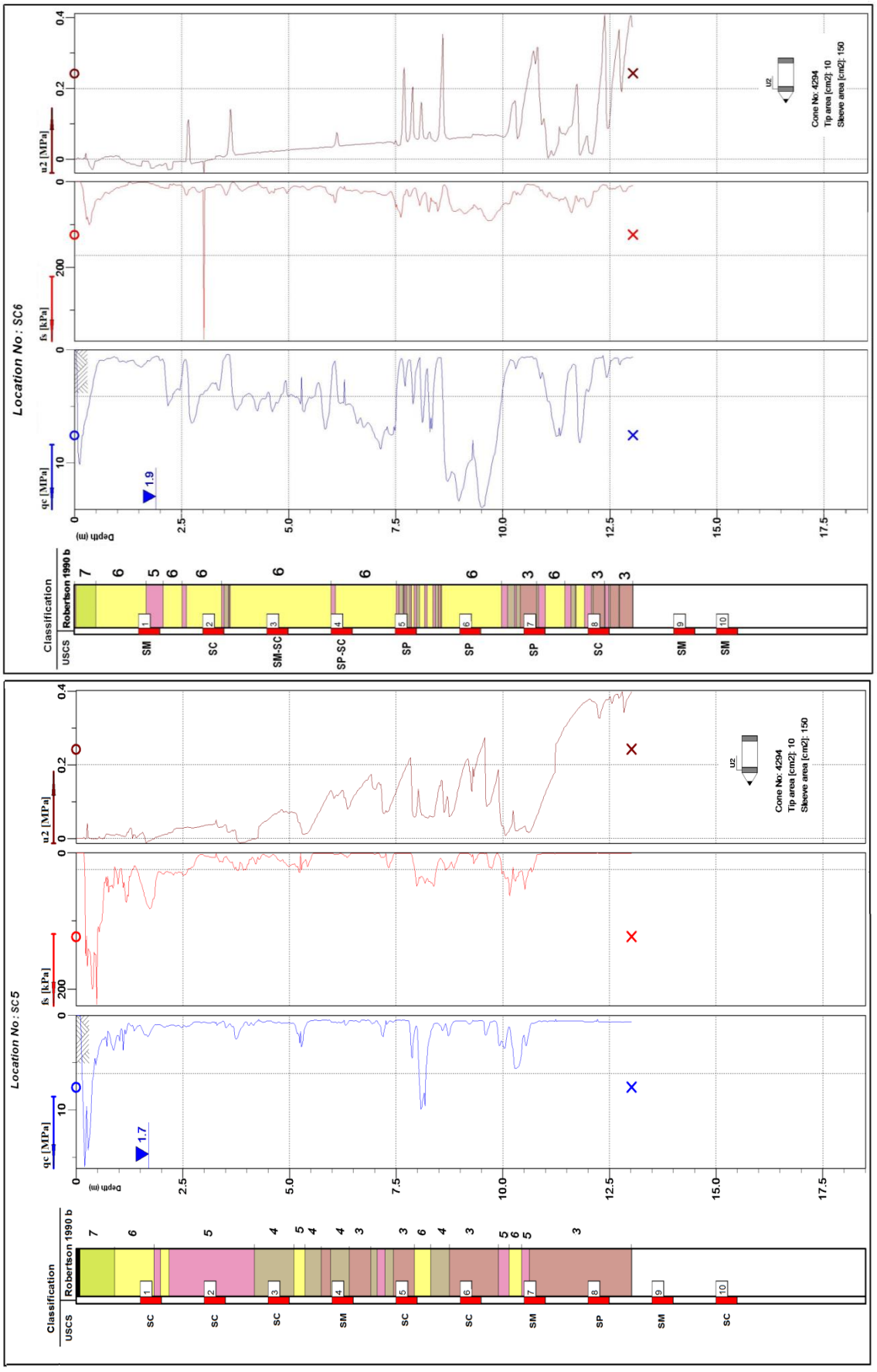

(Cont. on next page)

Figure B.1. (cont.)

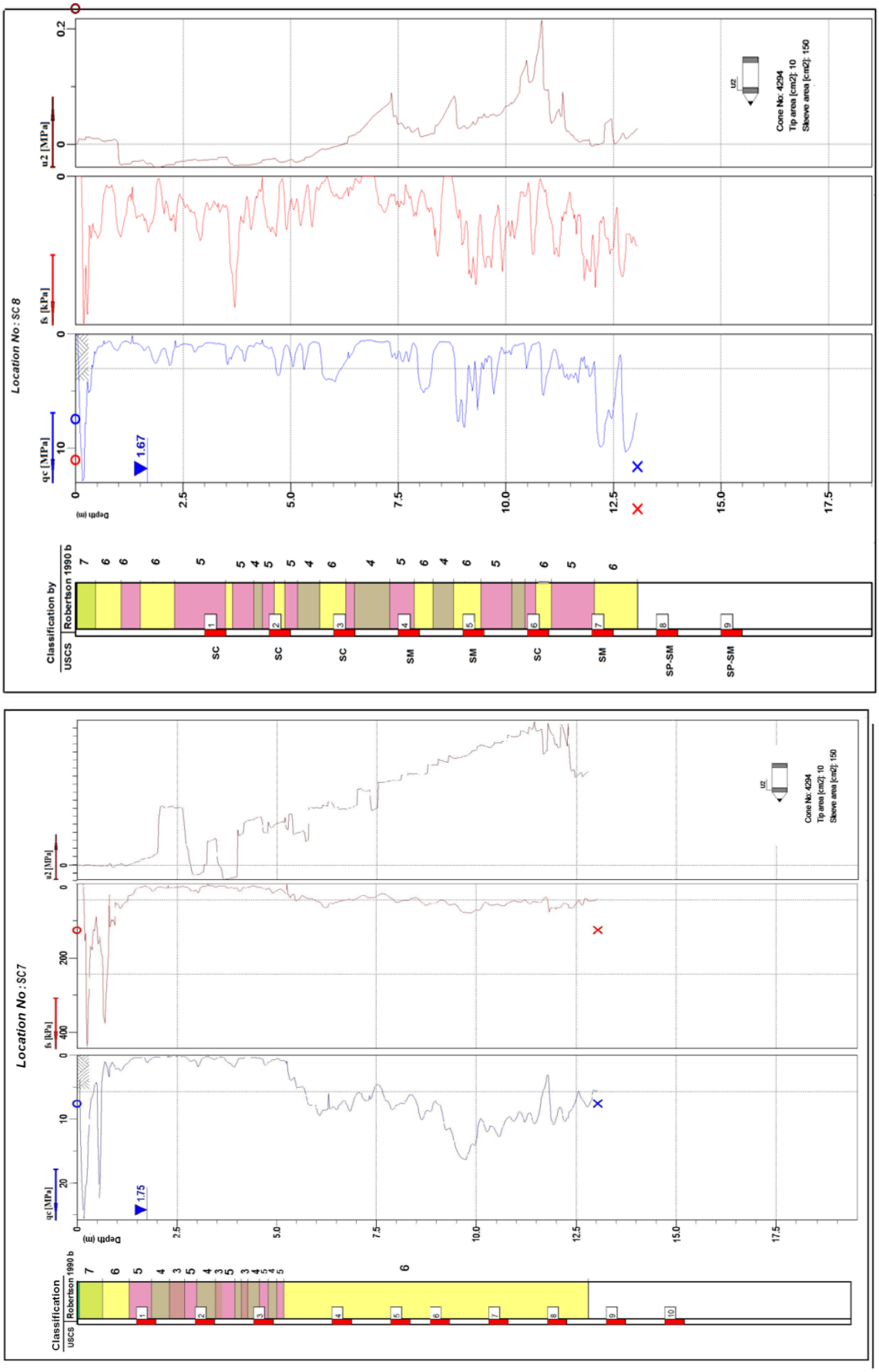

(Cont. on next page)

Figure B.1. (cont.)

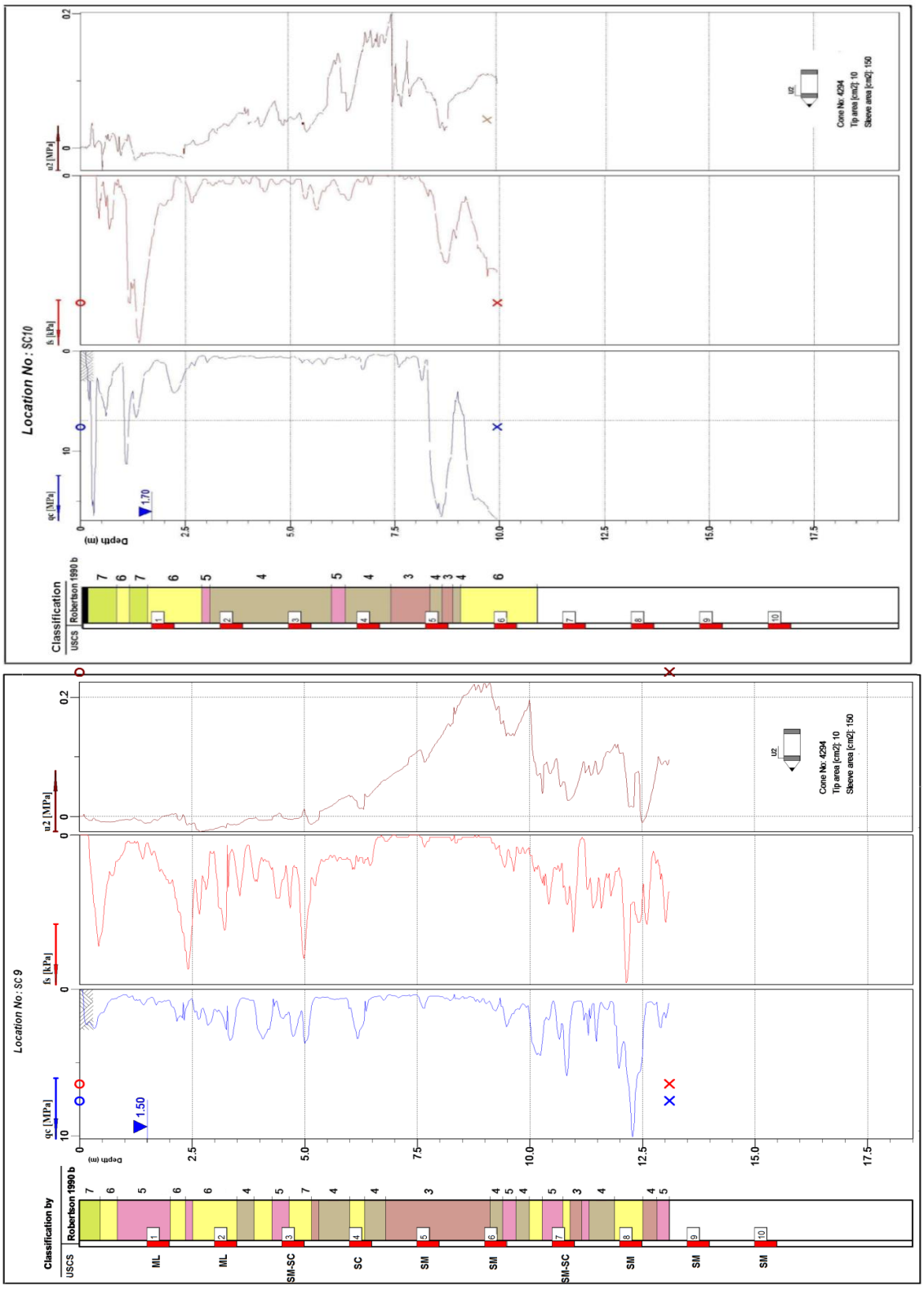

(Cont. on next page)

Figure B.1. (cont.)

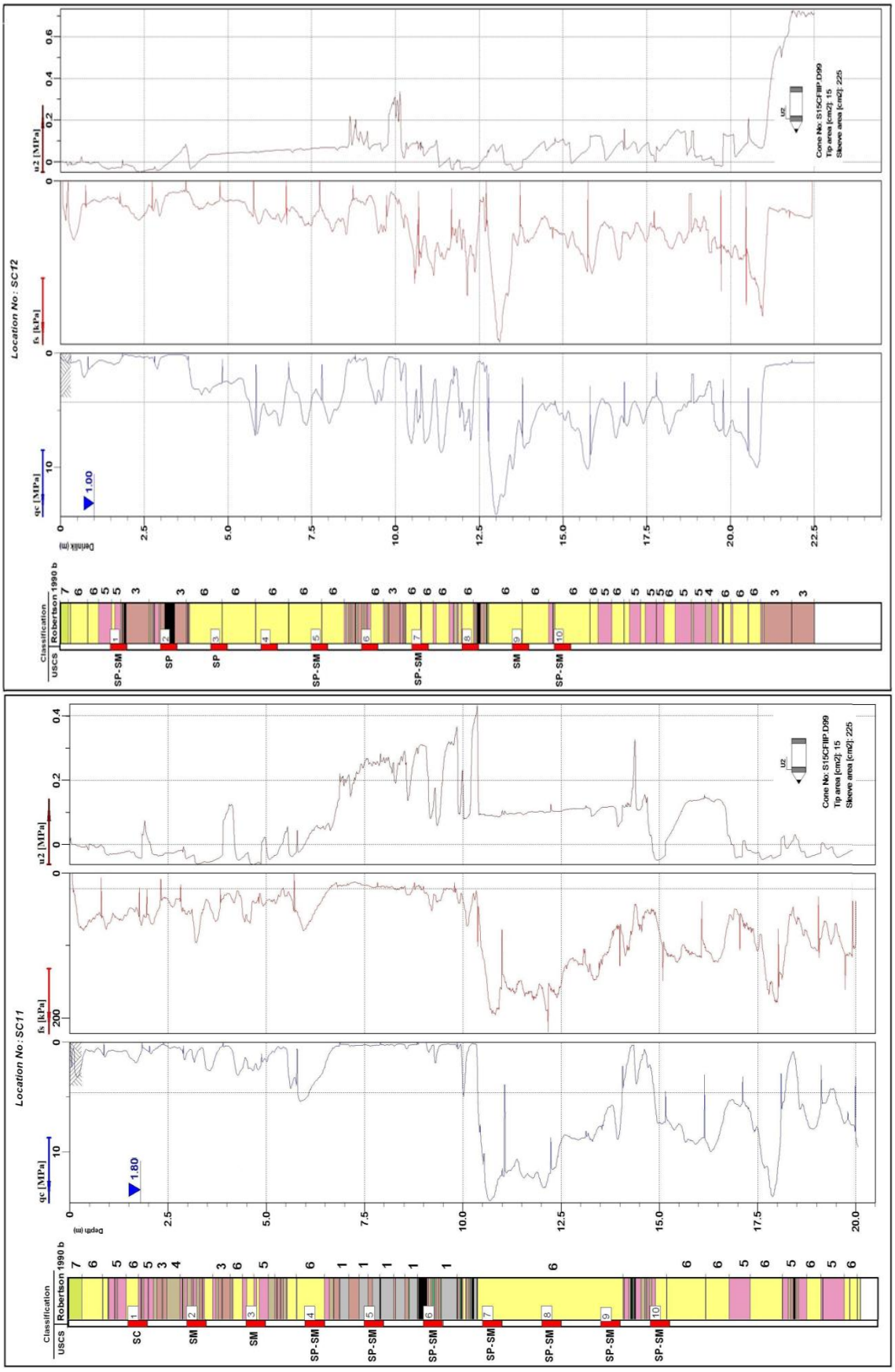

(Cont. on next page)

Figure B.1. (cont.)

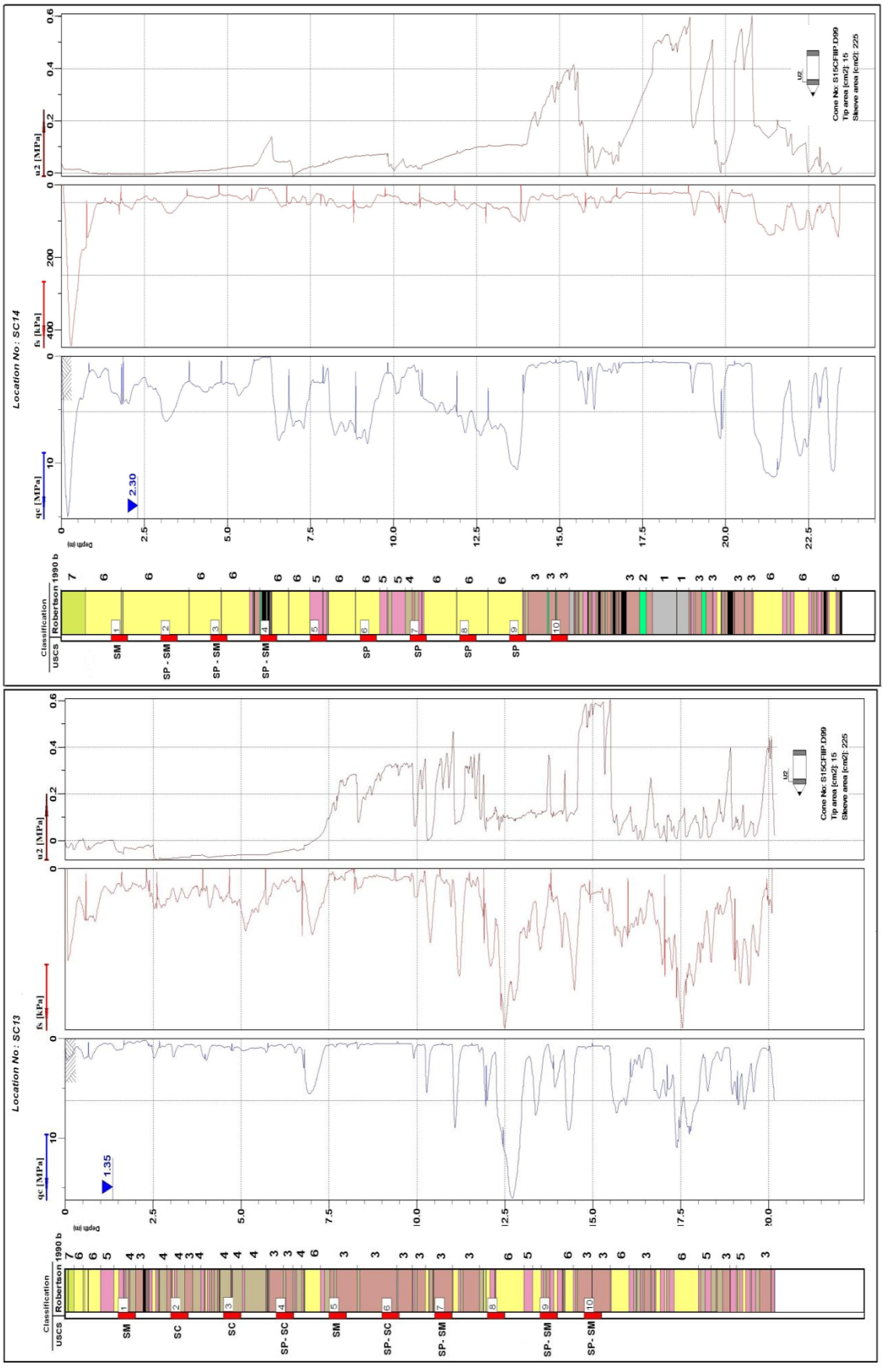

(Cont. on next page)

Figure B.1. (cont.)

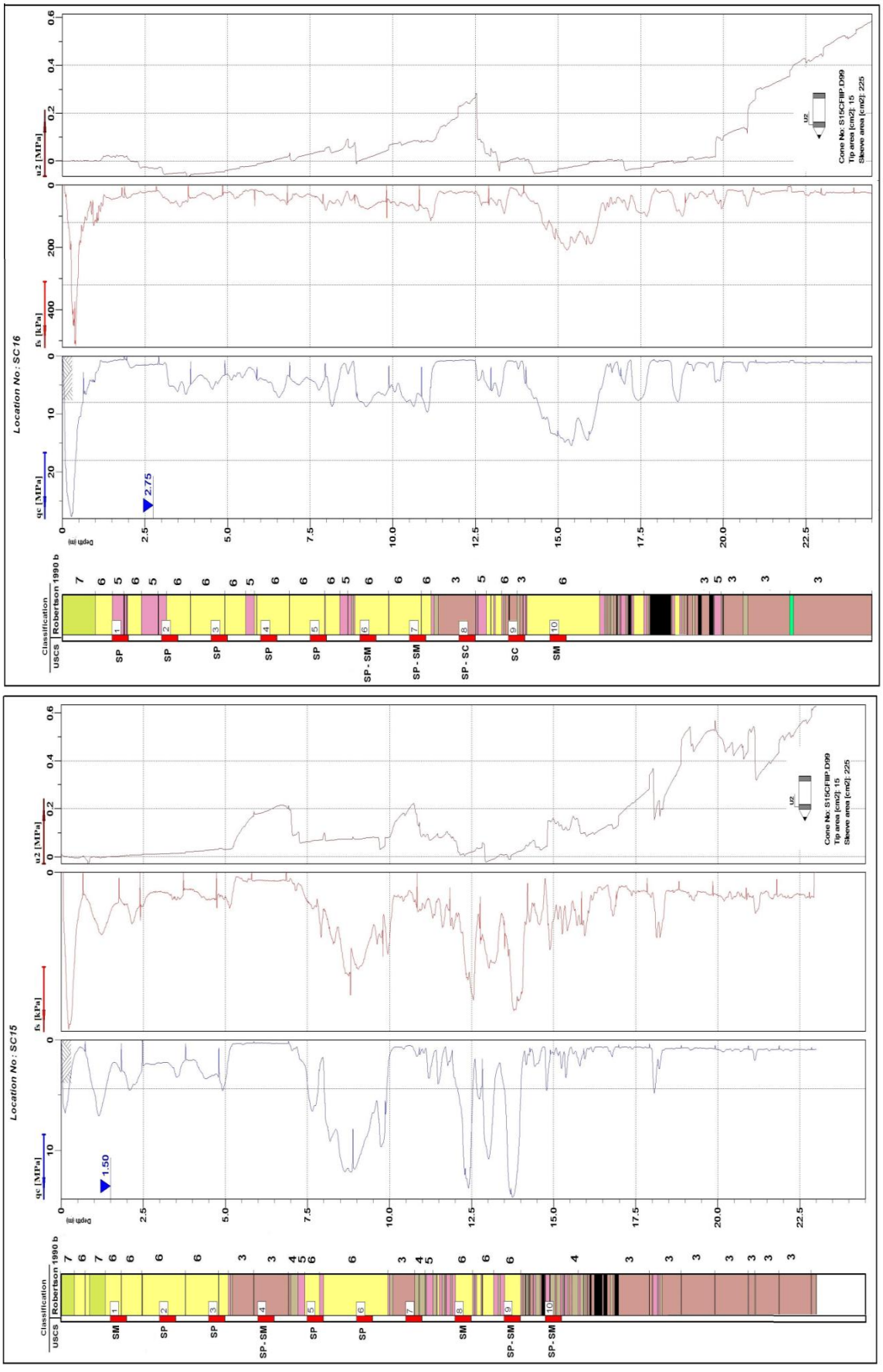

(Cont. on next page)

Figure B.1. (cont.)

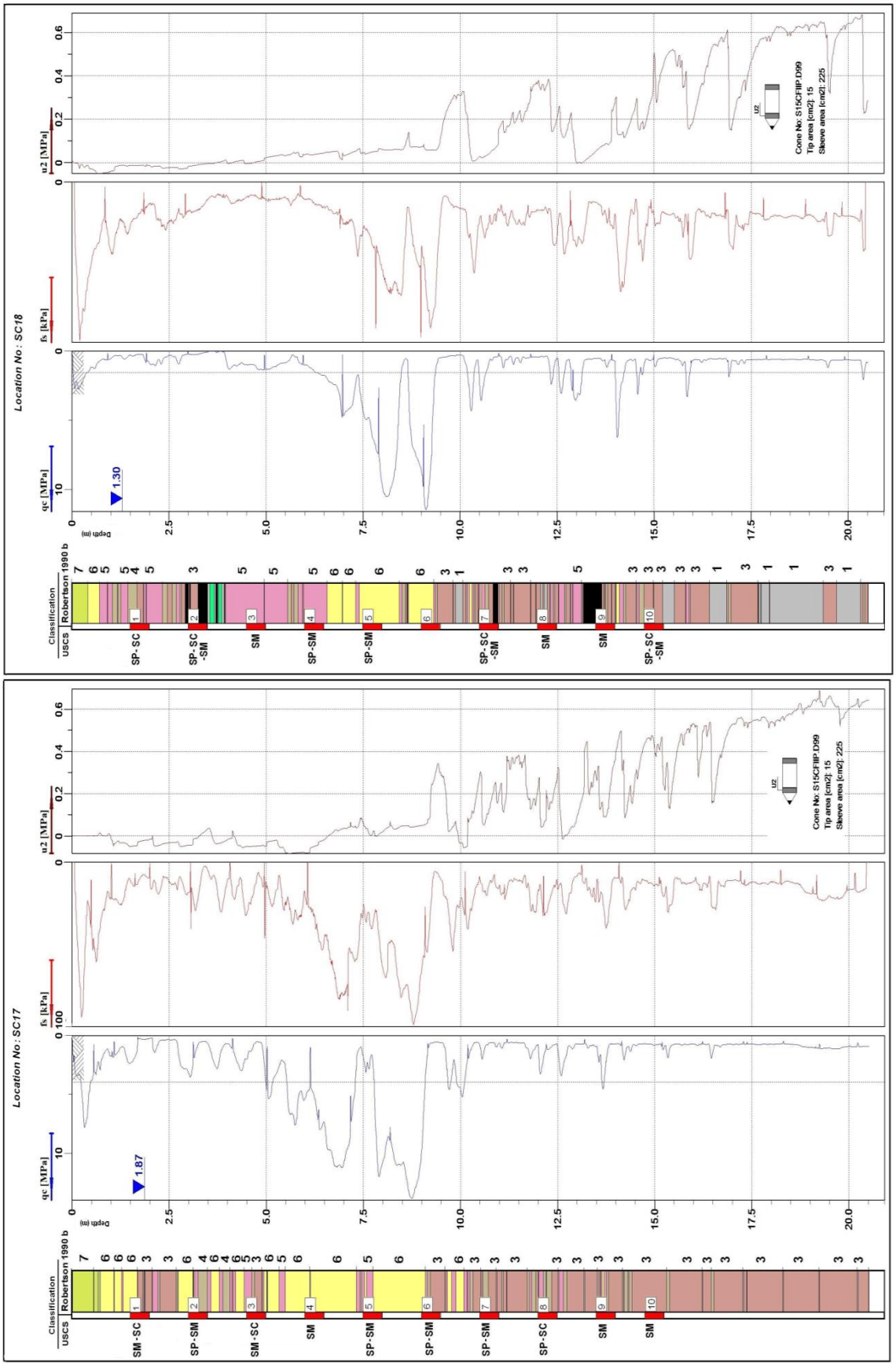

(Cont. on next page)

Figure B.1. (cont.)

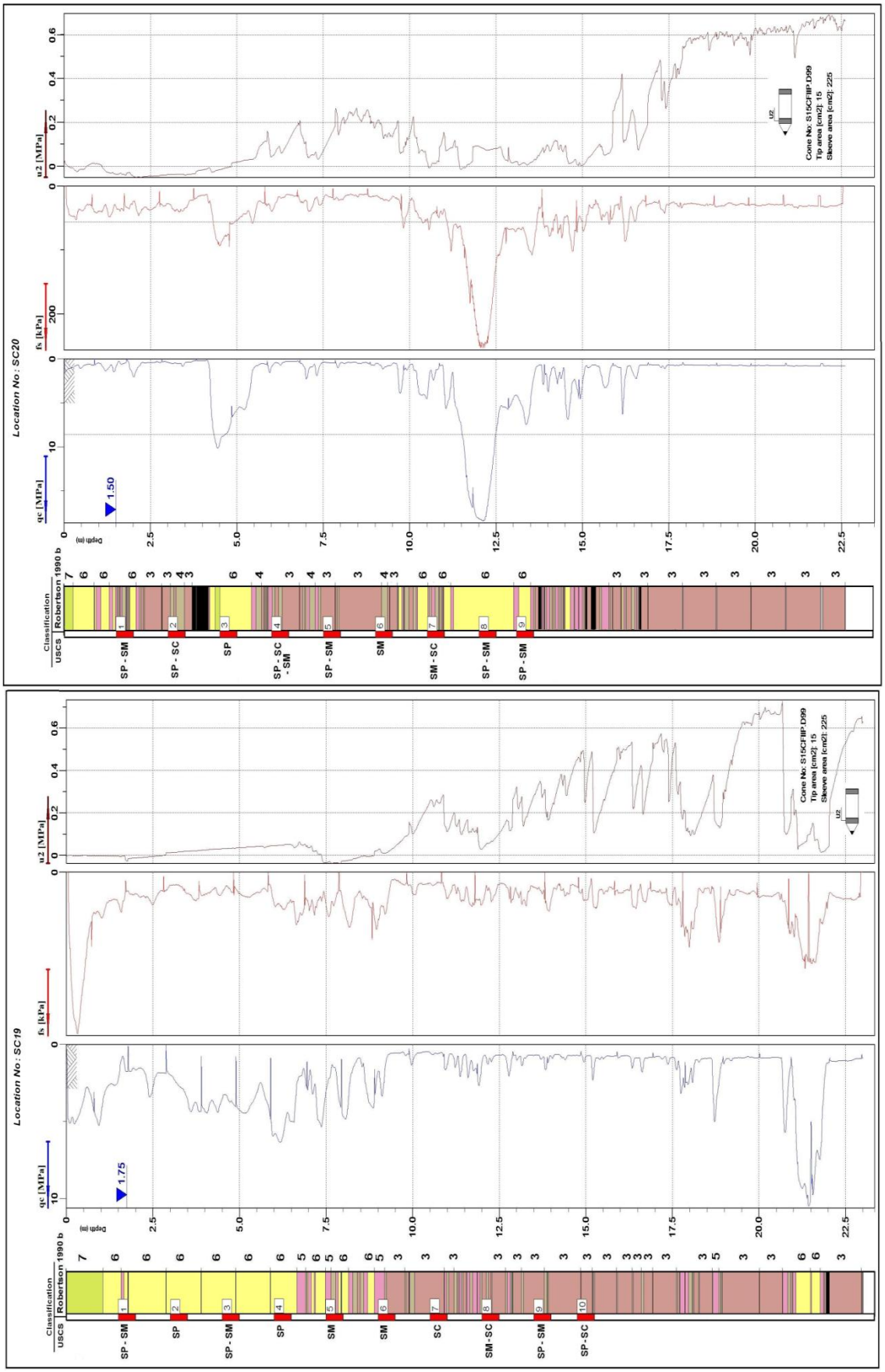

APPENDIX C

TABLE OF DATA FROM FIELD TESTS

Table C.1. Data from field tests and Fines Contents

			Piezocone Penetration Test (CPTu)				Dissipation / Hydraulic Conductivity Test		
Location	Sample No.	Depth	q_c	Δu_2	D_r	CPTu-based soil type	k	c_h	FC
-	-	*m*	*MPa*	*kPa*	%	-	*cm/sec*	*cm/sec*	%
L1	S1	3,0	0,7	-17,6	31	5	1,88E-04	1,69E+01	11
	S2	3,5	1,2	6,8	45	6	1,51E-03	2,35E+02	-
	S3	4,5	4,6	-6,4	83	6	1,51E-03	7,54E+02	21
L2	S1	3,0	1,5	-15,1	55	6	1,31E-03	2,73E+02	7
	S2	3,5	1,5	-2,9	54	5	1,49E-03	3,11E+02	-
	S3	4,0	1,1	-21,5	44	5	1,18E-03	1,75E+02	-
	S4	4,5	0,9	26,5	37	5	7,88E-04	7,71E+01	25
	S5	5,0	0,9	20,0	38	5	4,69E-04	4,80E+01	-
L3	S1	4,2	1,2	14,9	44	4	1,54E-04 *	2,37E+01	10
	S2	5,2	2,3	-5,4	61	5	3,74E-05	1,16E+01	-
	S3	5,7	3,8	13,5	75	6	5,41E-04	2,58E+02	-
	S4	7,2	0,6	10,9	21	4	9,36E-06	6,61E-05	-
	S5	8,4	0,6	-3,8	20	4	2,03E-07 *	6,61E-05	-
L4	S1	3,5	1,0	-9,6	42	6	5,85E-03	7,55E+02	19
	S2	4,0	2,1	-11,9	64	5	2,01E-03	5,93E+02	-
	S3	4,8	0,7	22,2	30	6	2,24E-03	1,36E+02	28
	S4	5,5	1,6	0,0	52	5	2,90E-03	6,19E+02	-
	S5	6,0	2,8	-42,5	67	6	2,31E-03	8,70E+02	19
	S6	7,0	4,1	-58,1	77	6	8,02E-03	6,25E+03	-
L5	S1	4,8	0,7	42,0	32	4	6,86E-07	5,24E-02	-
	S2	6,0	0,7	-29,7	30	4	1,33E-06	8,14E-02	-
	S3	7,0	0,8	-38,8	30	5	1,76E-06	1,27E-01	-
	S4	8,3	2,9	-8,0	66	4	2,40E-06	9,43E-01	-
	S5	9,5	0,6	-51,9	18	3	1,56E-06	3,19E-02	-
	S6	10,8	0,8	-38,5	26	3	1,09E-06	3,78E-02	-
	S7	11,5	0,6	-65,2	17	3	1,31E-06	2,31E-02	-
L6	S1	1,8	1,0	-13,4	47	5	1,35E-04	3,00E+01	-
	S2	2,3	4,4	-28,4	89	6	3,97E-04	1,67E+02	-
	S3	3,0	3,9	-13,6	82	6	1,70E-04	9,30E+01	17
	S4	3,8	5,2	-3,4	88	6	2,32E-04	1,20E+02	-
	S5	4,3	5,4	-0,6	87	6	5,07E-04	2,82E+02	-
	S6	5,3	4,6	-0,7	80	6	1,18E-03	7,37E+02	-
	S7	6,3	4,7	-0,9	79	6	2,79E-04	1,95E+02	9
	S8	6,8	6,9	-1,4	90	6	5,45E-04	4,73E+02	-
	S9	7,3	7,1	-2,5	90	6	4,52E-04	4,41E+02	-
	S10	7,8	1,7	-4,0	48	4	2,72E-06 *	6,04E-01	-
	S11	8,3	3,5	11,2	68	6	2,31E-05	3,08E-01	-
	S12	9,5	13,9	-2,7	105	6	3,89E-04	6,04E+02	3
	S13	10,3	1,1	79,6	31	3	9,51E-06	6,87E-01	-
	S14	12,3	0,7	101,9	17	3	1,77E-04 *	3,43E+00	-
L7	S1	2,8	0,5	-6,7	29	4	2,72E-06 *	1,66E-01	-
	S2	3,3	0,2	-28,7	5	4	4,39E-06 *	3,58E-02	-
	S3	3,8	1,0	-22,5	44	5	6,34E-03	8,71E+02	-
	S4	4,0	1,1	-24,6	45	4	4,69E-06 *	6,79E-01	-
	S5	4,8	1,3	-13,2	50	4	8,83E-06 *	1,58E+00	-
	S6	5,3	0,9	5,3	36	5	1,27E-03	1,31E+02	-
	S7	6,3	8,4	-2,3	100	6	2,32E-04	2,67E+02	10
	S8	6,8	7,8	-3,1	96	6	4,22E-05	4,31E+01	-
	S9	7,5	4,7	-10,3	81	6	4,47E-05	3,94E+01	-
	S10	8,0	7,8	-5,7	95	6	1,99E-05	2,27E+01	7
	S11	8,8	8,6	-3,9	96	6	2,69E-05	3,41E+01	-
	S12	11,3	9,7	-7,2	97	6	2,13E-05	2,91E+01	-
	S13	11,8	3,3	-20,4	66	6	6,42E-05	2,85E+01	-
	S14	12,3	9,9	-17,3	96	6	2,94E-05	4,32E+01	3

(Cont. on next page)

Table C.1. (cont.)

			Piezocone Penetration Test (CPTu)				Dissipation / Hydraulic Conductivity Test		
Location	Sample No.	Depth	q_c	Δu_2	D_r	CPTu-based soil type	k	c_h	FC
-	-	*m*	*MPa*	*kPa*	%	-	*cm/sec*	*cm/sec*	%
L8	S1	3,0	0,9	-20,6	42	5	6,86E-05	7,79E+00	-
	S2	4,0	1,2	-59,1	51	5	2,51E-03	4,19E+02	-
	S3	5,0	1,9	-59,2	60	5	1,43E-03	3,68E+02	-
	S4	6,0	4,1	-47,6	81	5	5,64E-04	3,17E+02	25
	S5	8,0	4,3	-47,2	79	6	3,30E-04	2,11E+02	-
	S6	9,5	2,6	-23,8	62	5	6,35E-04	2,20E+02	-
	S7	10,0	1,5	-15,7	46	5	1,35E-03	2,52E+02	-
	S8	11,5	3,5	-78,7	69	5	9,93E-04	6,79E+02	-
	S9	12,0	3,4	-104,4	67	5	3,55E-05	1,61E+01	12
L9	S1	2,0	0,8	-1,7	43	5	1,85E-03	6,41E-02	-
	S2	2,5	0,7	-21,4	37	5	4,55E-03	3,95E+02	-
	S3	3,3	2,8	-35,8	76	6	6,16E-03	3,73E+02	-
	S4	4,0	3,0	-30,0	76	6	9,05E-04	4,27E+02	-
	S5	4,8	3,2	-35,4	75	6	2,68E-04	1,40E+02	-
	S6	5,5	0,5	-24,7	23	4	3,24E-07 *	1,09E-02	-
	S7	6,3	2,6	-31,8	66	6	6,15E-05	3,12E+01	-
	S8	7,0	0,4	19,1	14	3	4,38E-07 *	6,69E-03	-
	S9	7,8	0,5	39,1	16	3	7,51E-07 *	1,30E-02	-
	S10	8,5	0,5	129,8	15	3	3,84E-07 *	6,26E-03	-
	S11	9,3	1,4	102,4	44	4	3,94E-06 *	6,98E-01	-
	S12	10,5	-	-9,4	30	4	4,12E-06 *	2,18E-01	-
	S13	11,5	2,4	-20,7	58	4	2,63E-06 *	8,42E-01	-
	S14	12,3	9,7	-87,1	96	5	4,19E-05	5,19E+01	-
L10	S1	2,8	1,0	-26,9	46	5	2,16E-03	1,05E+02	-
	S2	3,3	0,5	-30,7	28	4	9,02E-08 *	5,88E-03	-
	S3	4,0	0,5	-28,0	22	4	1,78E-07 *	5,26E-03	-
	S4	4,8	0,6	-24,6	24	4	2,43E-07 *	2,73E-02	-
	S5	5,8	1,1	-19,1	41	4	7,63E-08 *	1,06E-02	-
	S6	6,3	0,7	-19,7	29	4	1,68E-03	5,93E-02	-
L11	S1	2,5	0,4	-33,2	17	3	1,40E-06 *	5,28E-02	-
	S2	4,5	1,7	-53,1	56	5	5,41E-05	1,23E+01	23
	S3	5,5	0,9	14,0	36	4	2,23E-05 *	2,20E+00	-
	S4	6,5	2,1	3,2	59	6	7,25E-05	2,02E+01	8
	S5	7,4	0,3	191,8	0	1	1,82E-06 *	7,40E-03	-
	S6	10,5	10,5	8,3	100	6	7,44E-05	1,25E+02	6
	S7	12,5	9,0	-1,1	94	6	5,40E-05	1,07E+02	8
	S8	13,3	8,7	-21,1	92	6	7,71E-05	9,28E+01	7
	S9	15,5	7,5	-47,4	86	6	8,39E-05	8,62E+01	10
	S10	16,5	7,8	-3,4	86	5	1,38E-04	2,77E+02	-
	S11	17,5	7,8	-177,1	85	6	1,56E-04	1,66E+02	-
	S12	19,5	5,2	-210,8	73	5	8,50E-05	5,88E+01	-
L12	S1	1,0	0,9	-2,2	56	6	7,47E-04	9,49E+01	12
	S2	2,0	0,2	-14,1	9	3	1,69E-06 *	1,90E-02	-
	S3	3,0	0,4	-30,0	22	3	7,48E-07 *	2,21E-02	-
	S4	4,0	3,1	-48,6	79	6	6,16E-03	3,44E+03	6
	S5	5,0	2,5	2,6	70	6	8,29E-04	4,48E+02	4
	S6	6,0	4,9	1,3	87	6	9,26E-04	7,75E+02	3
	S7	7,0	3,4	-1,6	74	6	4,36E-03	3,25E+03	-
	S8	8,0	6,1	0,3	89	6	8,66E-04	8,81E+02	8
	S9	9,0	0,7	19,6	24	3	2,52E-06 *	7,45E-02	-
	S10	11,0	7,2	-35,6	90	6	4,30E-04	6,28E+02	10
	S11	12,0	5,2	-137,9	79	6	8,14E-04	5,75E+02	-
	S12	14,0	7,5	-95,5	88	5	6,35E-04	9,39E+02	18
	S13	15,0	5,4	-28,9	78	6	8,23E-04	6,06E+02	8
	S14	16,0	5,4	-22,5	77	5	1,12E-03	8,12E+02	-
	S15	17,0	5,2	-83,0	75	5	8,21E-04	5,73E+02	-
	S16	17,5	5,0	-72,5	73	5	8,34E-04	5,54E+02	-
	S17	18,0	5,5	-85,5	76	6	6,69E-04	4,98E+02	-
	S18	18,5	5,0	-29,6	73	5	6,77E-04	4,53E+02	-
	S19	19,0	4,0	-151,8	66	5	8,18E-04	4,30E+02	-
	S20	19,5	4,5	-169,3	68	5	8,75E-04	5,11E+02	-
	S21	20,0	6,2	-60,2	78	6	6,32E-04	5,30E+02	-

(Cont. on next page)

Table C.1. (cont.)

			Piezocone Penetration Test (CPTu)				Dissipation / Hydraulic Conductivity Test		
Location	Sample No.	Depth	q_c	Δu_2	D_r	CPTu-based soil type	k	c_h	FC
-	-	*m*	*MPa*	*kPa*	%	-	*cm/sec*	*cm/sec*	%
L13	S1	2,8	0,7	-24,9	39	4	1,13E-06 *	1,07E-01	-
	S2	3,8	0,7	-36,1	37	4	7,53E-06 *	7,21E-01	-
	S3	4,8	1,2	-43,9	49	4	1,79E-08 *	2,95E-03	-
	S4	5,7	1,2	-48,1	46	3	5,39E-07 *	8,42E-02	-
	S5	6,8	2,3	-56,0	63	4	2,75E-06 *	1,39E+00	-
	S6	7,8	0,5	133,6	19	3	7,45E-07 *	1,77E-02	-
	S7	8,8	0,5	157,7	17	3	4,33E-08 *	8,30E-04	-
	S8	10,8	0,6	166,2	18	3	9,77E-07 *	1,90E-02	-
	S9	13,8	1,1	231,0	32	3	4,12E-06 *	2,54E-01	-
	S10	14,8	0,8	432,9	23	3	1,02E-07 *	2,99E-03	-
	S11	15,7	6,5	-113,5	82	6	4,00E-04	5,77E+02	-
	S12	16,8	5,2	-86,1	75	3	4,13E-07 *	7,86E-01	-
	S13	17,7	9,7	-114,5	92	6	3,16E-04	6,01E+02	-
L14	S1	2,3	2,7	-4,8	74	6	2,01E-04	7,55E+01	-
	S2	3,3	5,7	-6,0	94	6	6,65E-04	6,78E+02	6
	S3	4,0	2,7	-7,8	70	6	1,01E-03	3,81E+02	8
	S4	4,8	2,5	-10,3	66	6	3,71E-03	1,52E+03	5
	S5	5,3	3,0	-5,5	70	6	1,03E-03	4,22E+02	-
	S6	5,8	1,0	-4,7	39	5	1,05E-02	1,22E+03	7
	S7	6,8	6,3	-1,5	89	6	9,26E-03	1,04E+04	-
	S8	7,3	6,4	-35,4	89	6	4,02E-04	3,88E+02	3
	S9	7,8	2,5	-25,2	61	5	8,56E-04	2,82E+02	-
	S10	8,5	6,7	-1,0	89	6	1,68E-03	2,07E+03	3
	S11	9,2	7,9	1,3	93	6	1,31E-03	1,77E+03	2
	S12	11,5	4,7	-31,0	75	6	1,28E-03	8,21E+02	-
	S13	12,3	5,6	-6,9	80	6	1,49E-03	1,15E+03	5
	S14	13,0	6,7	-0,1	84	6	8,58E-04	1,26E+03	-
	S15	14,0	1,3	-2,6	37	3	1,06E-05 *	7,79E-01	-
	S16	15,0	0,6	206,0	11	3	7,34E-06 *	5,15E-02	-
L15	S1	3,3	2,0	-3,4	67	6	6,89E-03	1,96E+03	4
	S2	4,0	1,8	-1,9	62	6	1,90E-03	4,67E+02	5
	S3	4,8	3,3	-0,6	77	3	4,79E-04 *	3,08E+02	4
	S4	5,5	0,4	81,9	17	3	7,26E-08 *	1,26E-03	-
	S5	6,3	0,3	144,8	4	3	5,54E-07 *	2,83E-03	-
	S6	7,0	0,7	130,0	30	3	1,11E-06	5,97E-02	-
	S7	7,8	5,9	7,5	88	6	3,39E-03	3,31E+03	3
	S8	9,2	9,1	2,2	99	6	2,60E-04	4,03E+02	5
	S9	12,3	10,1	-92,1	98	6	2,73E-04	4,54E+02	15
	S10	15,0	1,1	16,0	33	4	2,94E-07 *	1,63E-02	-
	S11	16,0	0,8	-53,6	17	4	6,78E-08 *	1,02E-03	-
	S12	17,0	0,7	23,3	69	3	2,59E-07 *	2,98E-03	-
L16	S1	3,3	5,2	-57,3	89	6	9,88E-04	9,04E+02	4
	S2	4,0	4,1	-67,2	81	6	9,12E-04	7,40E+02	31
	S3	4,8	4,2	-66,1	80	6	3,13E-03	2,59E+03	5
	S4	5,5	3,3	-51,0	72	6	4,78E-03	3,31E+03	1
	S5	6,3	4,5	-36,4	80	6	1,22E-03	1,05E+03	4
	S6	7,0	4,4	-38,7	79	6	1,05E-03	9,35E+02	7
	S7	7,8	5,8	-9,4	85	6	1,42E-03	1,54E+03	5
	S8	8,5	1,4	-2,9	44	5	4,09E-04	6,57E+01	10
	S9	9,2	8,5	-49,6	94	6	2,46E-03	3,69E+03	9
	S10	10,0	5,6	0,7	82	6	7,69E-04	9,66E+02	-
	S11	10,7	6,5	5,9	85	6	1,98E-03	1,77E+03	8
	S12	11,5	0,9	59,8	26	3	4,38E-07 *	1,50E-02	-
	S13	12,3	0,7	150,4	21	3	1,66E-07 *	3,69E-03	-
	S14	13,8	1,2	-95,2	34	3	2,13E-07 *	1,40E-02	-
	S15	14,5	10,2	-164,5	95	6	8,94E-05	1,77E+02	-
	S16	16,0	12,0	-132,9	98	6	1,52E-04	4,10E+02	-

(Cont. on next page)

Table C.1. (cont.)

			Piezocone Penetration Test (CPTu)				Dissipation / Hydraulic Conductivity Test		
Location	Sample No.	Depth	q_c	Δu_2	D_r	CPTu-based soil type	k	c_h	FC
-	-	*m*	*MPa*	*kPa*	%	-	*cm/sec*	*cm/sec*	%
L17	S1	3,2	0,8	-20,1	37	4	7,79E-04	7,83E+01	-
	S2	4,0	0,7	-37,8	32	4	1,42E-07 *	1,00E-02	-
	S3	5,5	3,2	-115,5	73	6	2,75E-03	1,22E+03	16
	S4	6,3	5,4	-91,8	87	6	2,78E-03	2,81E+03	13
	S5	7,8	2,6	-35,9	64	6	4,22E-04	1,51E+02	8
	S6	10,0	4,5	-114,7	77	6	7,07E-04	2,88E+01	-
	S7	12,2	1,2	47,3	36	3	7,00E-06 *	5,65E-01	-
	S8	13,7	2,2	-23,7	53	3	1,64E-07 *	4,69E-02	-
	S9	15,0	0,8	258,3	22	3	5,67E-07 *	1,34E-02	-
	S10	18,7	0,9	459,5	22	3	1,49E-07 *	3,57E-03	-
L18	S1	1,8	0,2	-11,9	10	3	9,45E-08 *	1,37E-03	-
	S2	7,0	4,6	-22,9	83	5	8,02E-05	6,53E+01	12
	S3	7,8	6,4	-12,8	91	6	7,27E-05	7,69E+01	6
	S4	9,3	8,0	-20,0	95	6	6,31E-05	9,97E+01	-
	S5	10,8	0,6	-49,1	21	3	1,01E-03	2,13E+01	-
	S6	11,3	0,5	68,7	15	3	3,54E-04	4,43E+00	-
	S7	12,3	0,5	275,4	15	3	8,86E-07 *	1,19E-02	-
	S8	13,7	1,0	-34,3	29	3	1,86E-07 *	7,85E-03	-
	S9	15,0	1,0	369,4	30	3	2,52E-07 *	1,29E-02	-
	S10	17,5	0,6	315,7	14	3	1,52E-07	1,47E-03	-
L19	S1	2,0	1,6	-13,4	63	6	9,56E-03	2,12E+03	10
	S2	3,3	2,7	2,9	74	6	1,65E-03	8,02E+02	4
	S3	4,0	4,4	4,6	86	6	1,08E-03	7,20E+02	7
	S4	4,8	3,7	5,9	79	6	3,38E-04	2,20E+02	7
	S5	5,5	3,1	5,9	73	6	4,70E-04	1,47E+01	-
	S6	6,3	6,0	5,8	90	6	4,63E-04	4,47E+02	4
	S7	7,0	2,3	-13,8	62	5	4,36E-04	1,36E+02	-
	S8	9,3	0,8	-58,8	29	3	1,17E-07 *	4,97E-03	-
	S9	10,0	1,2	23,0	40	3	5,10E-07 *	5,40E-02	-
	S10	10,7	0,6	160,3	18	3	1,49E-05 *	2,51E-01	-
	S11	12,2	0,9	-40,4	29	3	5,63E-07 *	2,38E-02	-
	S12	13,8	0,9	167,5	26	3	1,00E-03 *	3,16E+01	-
	S13	15,0	0,7	184,5	20	3	3,09E-07 *	5,75E-03	-
	S14	17,5	0,8	331,4	22	3	1,99E-05 *	4,43E-01	-
L20	S1	2,0	2,0	-29,8	70	3	8,73E-06 *	3,70E+00	-
	S2	2,7	0,4	-36,0	22	3	6,08E-08 *	1,91E-03	-
	S3	3,8	0,2	-25,6	0	-	5,09E-08 *	2,13E-04	-
	S4	5,7	0,5	63,1	22	3	8,13E-06 *	2,54E-01	-
	S5	6,8	0,3	135,3	0	3	8,88E-07 *	3,55E-03	-
	S6	7,8	0,4	92,1	14	3	1,44E-05 *	2,03E-01	-
	S7	8,7	0,4	181,4	9	3	6,04E-06 *	5,25E-02	-
	S8	9,8	3,5	-17,7	70	4	4,33E-06 *	2,93E+00	-
	S9	12,8	5,4	-78,6	80	6	3,07E-04	2,28E+02	-
	S10	15,8	2,7	-65,8	57	3	7,00E-06 *	2,43E+00	-
	S11	16,8	0,7	-16,0	18	3	3,87E-07 *	4,66E-03	-
	S12	17,8	0,7	286,6	17	3	1,09E-07 *	1,74E-03	-
	S13	18,8	0,7	409,4	16	3	4,42E-07 *	5,60E-03	-